Intracortical sensorimotor projections in the rodent: patterns of connectivity and functional dynamics within the vibrissa sensorimotor system.

by

Mary Rocco Donovan

A dissertation submitted to the Graduate Faculty in Psychology in partial fulfillment of the requirements for the degree of Doctor of Philosophy, The City University of New York

2008

INFORMATION TO USERS

The quality of this reproduction is dependent upon the quality of the copy submitted. Broken or indistinct print, colored or poor quality illustrations and photographs, print bleed-through, substandard margins, and improper alignment can adversely affect reproduction.

In the unlikely event that the author did not send a complete manuscript and there are missing pages, these will be noted. Also, if unauthorized copyright material had to be removed, a note will indicate the deletion.

ProQuest LLC
789 East Eisenhower Parkway
P.O. Box 1346
Ann Arbor, MI 48106-1346

This manuscript has been read and accepted for the Graduate Faculty in Psychology in satisfaction of the dissertation requirement for the degree of Doctor of Philosophy.

Joshua C. Brumberg, Ph.D.

August 29th, 2008
Date

Chair of Examining Committee

Maureen O'Connor, Ph.D.

August 29th, 2008
Date

Executive Officer

Jonathan Levitt, Ph.D.

William Farrell, Ph.D.

H. Philip Zeigler, Ph.D.

Alex Reyes, Ph.D.

Supervisory Committee

THE CITY UNIVERSITY OF NEW YORK

Abstract

Intracortical sensorimotor projections in the rodent: patterns of connectivity and functional dynamics within the vibrissa sensorimotor system.

by

Mary Rocco Donovan

Advisor: Joshua C. Brumberg, Ph.D.

The reciprocal connections between primary motor cortex (M1) and primary somatosensory cortex (S1) are hypothesized to play a crucial role in an animal's ability to update its motor plan in response to changes in the sensory periphery. These interactions provide the motor cortex with information about the sensory environment which in turn provides the sensory cortex with anticipatory knowledge of ongoing motor plans. In the mouse neocortex there are representations of the body surface within both M1 and S1. Utilizing physiologically targeted micro injections of biotinylated dextran amine into either the whisker representation of M1 or S1, we characterized the axonal pathways connecting these two areas and demonstrated that the homotopic areas of the two representations were preferentially connected to each other. We then used this data to determine a plane of section that contained both whisker M1 and whisker S1 and maintained a functional axonal pathway between these two areas. To examine the synaptic mechanism of the feedforward (S1 to M1) and feedback (M1 to S1) connections directly, we utilized whole-cell recordings within the *in vitro* sensorimotor slice. Our findings indicate that these regions are connected through a reciprocal axonal pathway that transverses the infragranular layers in both directions (FF and FB). Direct synaptic connections are observed

following stimulation of both pathways. Larger responses are observed in the feedforward direction, while the feedback responses occur at a shorter latency. The morphology as well as the intrinsic firing properties indicates that differences exist in the synaptic organization within each of these circuits. The results of these studies suggest that the sensorimotor slice is a valuable method for the investigation of sensorimotor processing.

Acknowledgements

Many people have contributed to the completion of this dissertation and I would like to say a few words to express my gratitude. This work would not have been completed without their guidance, support and encouragement and I am grateful to have had such a positive experience in this challenging endeavor.

I would like to start by thanking my advisor and friend, Dr. Joshua Brumberg, for his mentorship during my graduate career. Despite ever- mounting responsibilities and commitments, he has always remained available to me to answer questions and provide useful feedback. I thank him for always being a strong advocate for me and for having unrelenting faith in my work. His patience, optimism and determination have influenced me greatly both professionally and personally.

I am grateful to my entire committee, Drs. Jonathan Levitt, William Farrell, Phil Zeigler and Alex Reyes for sharing their expertise and insightful suggestions despite severe time constraints.

Many lab members contributed to the completion of this project, especially Dr. Raddy Ramos, Sandra Giraldo, Aileen Tlamsa and Eric Chen. They were always willing to help at a moment's notice. I am fortunate to have worked with such generous and dedicated lab mates. To my honorary lab mates, Drs. Lora Kasselman and Gad Klein-I cannot image having made it through all of the hurdles without you; I will always remember the fun times we shared.

To my undergraduate advisor, Dr. David Rivers, thank you for inspiring me to pursue a career in research. My experiences in the lab and your knowledgeable advice

most definitely changed the path of my life. Many thanks to my first lab partner, Dr. Anis Frayha, for making organic chemistry tolerable and entomology research fun- who knew that was even possible.

I would like to that my parents, Richard and Pat Rocco for their undying love and support. I would not have begun this journey without their encouragement. I thank them for giving me the educational opportunities that I needed to achieve this goal. To my dad- thank you for always encouraging me to aim high, and for believing that all of my goals were within reach. You have taught me that some things are worth fighting for and that most things worth having do not come easy. This was not easy, but it was certainly worth the fight. To my mom- I thank you for always being amazed by my accomplishments, no matter how small. You always know the right thing to say and your patience, kindness, and personal educational accomplishments continue to inspire me today. To my sister, Christina, thank you for reminding me not to take life too seriously and for loving me unconditionally. Thanks to my brother Rob, for providing some competitive academic spirit (on my end, of course). Who knows, I may never have tried so hard in high school if I didn't have to hang my report card next to yours on the fridge.

To my wonderful husband, Michael Donovan, I thank you for always putting me first. Your countless sacrifices have enabled me to follow my heart. Thank you for taking interest in my work and for sharing my passion. You are truly one of- a- kind, thanks for making it all worthwhile. Many thanks to my writing buddy, Murphy, you are a great listener.

This work is dedicated to the memory of my grandfather, Charles Rocco, for believing in the power of education.

"Do not go where the path may lead, go instead where there is no path and leave a trail."

-- **Ralph Waldo Emerson**

Table of Contents

List of Tables

List of Figures

General Introduction

Both sensory and motor cortices contain finely scaled topographic maps (Woolsey et al. 1952; Brooks et al. 1961; Buser et al.1959; Li and Waters, 1991). These maps allow both primary motor cortex (M1) and primary somatosensory cortex (S1) to have highly specialized responses to changes in the periphery, allowing for precise execution of motor tasks. S1 and M1 are reciprocally connected yet the functional influence of these interactions remains unknown. In primates S1 inactivation can result in disruption of chewing (Len et al. 1993, 1998; Hiraba et al. 2000), fine motor coordination, sustained muscle contraction, appropriate grip force and the ability to determine the weight of an object (Rothwell et al. 1982; Johansson and Westling 1984; Hikosaka et al. 1985; Brochier and Boudreau 1999). These results suggest that motor control can be strongly influenced by S1 inputs. Understanding the pathway between S1 and M1 is an important first step towards comprehending how sensorimotor computations are preformed.

Cortical Organization

The cerebral cortex is comprised of functionally and cytoarchitectually distinct regions that contain discrete systems for each modality. In general, sensory information is conveyed from the periphery to the spinal cord followed by the brain stem and then the thalamus. The thalamus sends afferents to the primary sensory cortices which are reciprocally connected to the thalamus and to other cortical and subcortical areas. The primary motor cortex contains neurons that project directly to the spinal cord to mediate voluntary movement. Secondary areas also exist for each of

the modalities. These areas refine the information received from the primary area and sends outputs to other association areas.

Lamination

The neocortex can be further divided into six horizontal layers based on cell types and densities (Brodmann 1909). In some cases these layers also include sublayers, which can be seen as variations in cell densities within a layer. The layers are in large part defined by the cell bodies that are present within them.

In homotypic cortex, layer I is known as the plexiform or molecular layer. This is largely a cellular layer comprised of axons and dendrites that often originate outside of the cortex. Layer II is a layer of small pyramidal cells, III is medium and large superficial pyramidals, IV is the granular layer made up of granule cells, V is comprised of large pyramids and layer VI, also called the multiform layer, is a heterogeneous layer made up of polymorphic or fusiform cells (White 1994). Layer depths vary across cortical regions based on functional requirements. For instance, in the primary somatosensory cortex layer 4 comprises the largest area of the cortical plate because it receives the majority of the thalamic afferents.

Classification of cells

There are essentially two categories of cells within the cortex: pyramidal and non-pyramidal. Pyramidal cells are identified by their pyramid (triangular) shaped cell body, a large apical dendrite that usually extends upward toward the pial surface and horizontally extending basal dendrites (White 1989). In addition to a large apical

dendrite, these cells also possess smaller diameter axon collaterals. These collaterals can extend for great distances beyond the cell body usually traveling within the supragranular layers (Gilbert and Wiesel 1979; Rockland et al. 1982). Additionally, these neurons can also target contralateral (callosal neurons) as well as subcortical (e.g. thalamus, striatum…) locations (rev. in Jones 1995; White 1989). Projection neurons are glutamatergic neurons characterized by a typical pyramidal morphology, and function to transmit information both between different regions of the cortex and to other regions of the brain (Elhanany and White 1990; Porter 1997) . Retrograde labeling studies have shown that both glutamate and aspartate are transported into the perikarya of pyramidal cells (Streit et al. 1979). These results indicate that pyramidal cell axons likely utilize these two excitatory neurotransmitters.

Nonpyramidal cells are more morphologically diverse than pyramidal cells. For this reason, there have been many attempts to create a unified method of classification for these types of cells. Feldman and Peters (1978) created a method for classification that is widely accepted and often utilized. According to their method, these cells are classified based on their dendritic tree (multipolar, bipolar or bitufted) and according to the concentration of spines on their dendrites (spiny, sparsely spiny or smooth/nonspiny). While some nonpyramidal cells can be characterized as excitatory, (i.e. spiny stellate cells) most are in fact inhibitory. The neurotransmitter most often released from a nonpyramidal cell is gamma-amino-butyric-acid (GABA).While GABAergic cell types typically participate in short range (<400μM) interactions, long-range interactions have also been described in certain morphological subtypes (Kisvardey 1987; McDonald and Burkhalter 1993).

Functional Properties: *Columnar Organization*

In addition to a horizontal laminar organization, there also exists a vertically aligned pattern of organization within the cortex. This finding was first made by Mountcastle while performing electrophysiological recordings of the somatosensory cortex of the cat (Mountcastle 1957; Powell and Mountcastle 1959). It was found that stimulating a specific part of the animal's skin caused a response in all of the neurons that the vertically penetrating electrode encountered. These findings led to the notion that cells that are within a vertical column share similar receptive field properties. This organization of the cortex into functional columns has been most extensively studied in the visual cortex (Hubel and Wiesel 1962) but these columns have also been identified in many other regions as well including the somatosensory cortex (Mountcastle 1957; Favorov et al. 1987) the auditory cortex (Abeles and Goldstein 1970) and the motor cortex (Asanuma and Rosen 1972).

Functional Properties: *Receptive Fields*

The receptive field of a neuron is the area of the periphery where, if stimulation is made, a change in cell firing is observed (Hartline 1940; Swadlow 1994). The size and patterns of receptive fields vary depending on cell type and the location of the cell within the cortex (White 1994). Receptive field properties have been extensively studied in the visual and somatosensory cortices. One method of classifying cells in the somatosensory cortex is based on what aspect of tactile stimulation they respond to. Cells that respond preferentially to a change in the

stimulus are known as rapidly adapting, those that respond continuously to a steady stimulus are known as slowly adapting (Mountcastle 1957). In the somatosensory cortex of the rodent (barrel cortex) most cells have a preferential response to movement of a single whisker; this whisker is referred to as the principal whisker (Simons 1978; Welker 1976). Cells with single whisker receptive fields are found predominantly in layer IV of the barrel cortex (Armstrong-James et al. 1992; Simons et al. 1992). Some cells within the barrel cortex can respond to movements other than that of their principal whisker. The cells are said to have multiple-whisker receptive fields and are often found in the region between barrels (known as the septal region) and in the layers above and below layer IV (Simons 1978). Studies of receptive field properties of layer IV barrel and septal neurons have shown that these cells function in parallel networks, but that local circuit dynamics regulate how these neurons integrate their thalamic inputs (Brumberg et al. 1999).

Cortical Maps

In addition to being both horizontally (laminae) and vertically organized (columns), many areas of the cortex are also somatotopically organized as well. Somatotopic organization implies that body part representations within the cortex are arranged based on their relative locations within the body itself. The somatotopic organization of the somatosensory and motor areas has been well studied in many species.

S1 Map

Information about tactile stimuli is relayed to the primary somatosensory cortex via the thalamus. A detailed map of the primary sensory cortex of humans was developed by Penfield and Boldrey (1937). This map, known as the sensory homunculus, indicated the order and relative extent to which each region of the body was represented in S1. Penfield's studies were performed as he was mapping various cortical areas during surgeries on epileptic patients. He concluded that the majority of the cortical representation of somatic sensation was localized to the postcentral gyrus. He applied near-threshold stimulations to the postcentral gyrus in an orderly fashion and asked patients to report any sensations. The stimulation often resulted in sensations of numbness or tingling in localized regions. Penfield was able to create the homunculus based on his patient's responses and found that the sequence was nearly identical each time.

Penfield's findings complemented similar studies that were being done at that time in primates. Marshall, Woolsey and Bard found that evoked potentials could be observed in S1 following cutaneous stimulation in monkeys. Using the potentials as a guide, they were able to create a detailed map of the primate's body surface in S1. This somatotopic organization of the primary somatosensory cortex has been documented for many other mammals including mice, rats, rabbits and cats. In each case, the map forms a distorted representation of the body surface of the animal based on the relative importance of each region. For instance in the human, the hand and the tongue occupy the largest portion of the map whereas in the rodent, the whiskers are the largest representation (Woolsey and Van der Loos 1970).

Barrels

The region of the primary somatosensory cortex that corresponds to the whisker representation in rodents is referred to as the barrel cortex. This term was coined by Woolsey and Van der Loos (1970) when after tangentially slicing Nissl-stained mouse cortex they observed the presence of cylindrical units in layer IV. The pattern of these units or barrels was observed to be similar to the pattern of the whiskers on the mystacial pad. It was later discovered that there was a one-to-one, non-overlapping correlation between each barrel and a corresponding whisker on the contralateral whisker pad (Welker 1971). The whiskers (and corresponding barrels) are organized into rows and arcs. On the mystacial pad, the whisker rows are labeled A-E and run along the anterior-posterior axis. The arcs (labeled 1, 2, 3…) run orthogonal to the whisker rows (Woolsey and Van der Loos 1970).

Early research in barrel development found that barrels become visible in mice in the trilaminar cortical plate between the third and fourth postnatal day (Rice and Van der Loos 1977). Septa (the area surrounding the barrel) are visible at postnatal day 6. Rice and Van der Loos (1977) found that when they compared the growth of the barrel arcs to the barrel rows the development of the barrels arcs was disproportionately greater. A revised timetable was created by Schlaggar and O' Leary (1994) who investigated the role of afferents from the ventroposterior nucleus (VP) of the thalamus in the developing barrels. Using acetylcholinesterase (AchE) histochemistry to mark the VP thalamocortical afferents (TCA), they found that these afferents form a barrel related pattern that can be seen in layers 5/6 of rats on

postnatal day (P) 0. They found while the VP afferents innervated layer VI as early as embryonic day (E) 20, the cortical barrel clustering was not apparent until 24-48 hours later.

M1 Map

In humans, the primary motor cortex corresponds to the precentral gyrus of the cortex and is responsible for the executions of motor movements. John Hughlings Jackson was the first to present evidence for the existence of a human motor cortex in the late 1800's. In studying epileptic patients during the late 1800's, Jackson found that the patient's convulsions were often limited to one side of the body and when "organic disease" was found to be present in the brain it was located contralaterally to the side that experience the convulsions. The first experimental studies to demonstrate that this region existed were performed by Eduard Hitzig in 1870. Hitzig and his colleague Gustav Fritsch found that electrical stimulation of discrete areas of the dog's frontal cortex resulted in correlated movements of the face or limbs on the opposite side of the body. A few years later David Ferrier (1876) created the first true map of the motor cortex based on stimulation studies in primates.

The motor map of the primary motor cortex becomes defined after birth and the rate of its development is highly variable between species. At the time of birth, brainstem motor systems are well developed but the corticospinal spinal system is not (Martin et al. 1980). In cats, the motor map is not developed until two months after birth (Bruce and Tatton 1980). Stimulation of the motor cortex will not evoke a motor response before this time period. Chakrabarty and Martin (2000) evaluated the

representation patterns in the primary motor cortex of the cat using intracortical microstimulation and found that four major changes occur between two and three months of age: an increase in sites that produce a motor effect in response to microstimulation, a decrease in current threshold, a proximal- to- distal elaboration of the motor map and an increase in overlap (present after post-natal day 71). Similarly, electrical stimulation of M1 in mice does not result in evoked whisker movement until the third post-natal week (Danny Tam, unpublished observations).

Whisker representation in M1

In the rodent, the area of the cortex that is responsible for initiating voluntary whisker movement is the whisker representation of the primary motor cortex (wM1). M1 contains a topographic map similar to that of S1, but there appears to be a greater degree of overlap in M1. Li and Waters (1991) used intracortical microstimulation techniques (ICMS) to map the primary motor area of the mouse. Within the map of M1 they found three maps of the whisker representation, only two of which were contiguous. A large degree of overlap was found between the whisker regions and surrounding areas including the forelimb, neck and trunk representation.

Cortical Circuitry

Cortical connections are not random; in fact they follow a highly organized pattern of connectivity. Hubel and Wiesel (1962, 1968) proposed a hierarchal model of cortical function based on their studies of the visual system. This model states that there are two basic pathways by which information can travel within the brain:

feedforward (FF) or feedback (FB). In a feedforward pathway information is traveling through a series of neurons having progressively more complex receptive fields. Thalamocortical pathways are an example of feedforward or "bottom up" pathways. In the case of the barrel cortex, simple cells in layer 4 receive information directly from the thalamus and then there is a convergence of information as the simple cells synapse onto complex cells to incorporate information from surrounding whiskers. Feedback pathways process information in the opposite manner such as corticothalamic connections (Jones 1995). More recent evidence indicates that feedback and feedforward mechanisms are not the only mechanisms of cortical processing. Lateral processing has been added to describe processing that occurs within the same hierarchal level (Felleman and Van Essen1991). The response of a cell to a stimulus is often modulated by cells in surrounding areas and different patterns of connectivity can account for variability in how information is received and processed (Hubel and Wiesel 1962; Levitt and Lund 1997; Angelucci et al. 2002).

Currently, much of what we know about the characteristics of feedforward and feedback pathways has been derived from studies of the visual system. In this system it has been found that these pathways can be differentiated based on several factors, one of which is laminar distribution (Rockland and Pandya 1979). In the visual system of primates, forward pathways generally originate in superficial layers and terminate mainly in Layer IV, while feedback pathways originate in both superficial and deep layers and generally terminate outside of Layer IV (Rockland and Virga 1989, 1990; Maunsell and Van Essen 1983; Fig 1). The specific laminar pattern of feedforward and feedback connections does differ somewhat between primates and

rodents but the basic principles remain constant (i.e., forward pathways project primarily to layer 4 and feedback connections generally avoid layer 4) (Coogan and Burkalter 1993). Another morphological characteristic that differentiates these pathways, at least in the visual system, is arbor size. It has been observed that in general, feedback connections in the visual system are more divergent and less specific feedforward axonal arbors (Rockland 2002). Studies in the visual system of primates and monkeys indicate that feedback connections serve to network cells that respond to widely separated regions of visual space (Angelucci et al. 2002, Canton et al. 2005). Conduction velocities between feedforward and feedback connection of V1 and V2 in primates are rapid but comparable, both averaging approximately 3.5 meters per second (Girard et al. 2000).

Intracellular recordings in layer 2/3 of rat visual cortex indicate that these pathways also have different physiological response properties. Stimulation of feedback inputs resulted in depolarizing monosynaptic responses in the primate visual cortex. Conversely, stimulation of feedforward pathways in rodents evoked monosynaptic excitatory postsynaptic potentials followed by disynaptic, hyperpolarizing inhibitory postsynaptic potentials (Shao and Burkhalter 1996). One factor that may contribute to these varied physiological responses in the rodent is these pathway's synaptic inputs to GABAergic neurons. The feedforward and feedback pathways of the rat visual cortex target the same proportion of GABAergic (10%) and non-GABAergic (90%) cells (Gonchar and Burkhalter 1999). Though the inputs are the same in terms of proportion, differences have been observed in the types of synapses that occur in each pathway in rodents. Feedforward inputs prefer to

synapse onto thick parvalbumin (PV)-expressing GABAergic dendrites neurons while feedback pathways favor thin dendrites (Yamashita et al. 2003). This preference may explain why there is greater inhibition in the feedforward pathway. These distinct circuits, however, are only observable after P15 once the eyes have opened, suggesting that the strength of inhibition in of the FF and FB pathways is not stabilized until after the eyes are open.

Feedforward and feedback connections are thought to have very different roles in information processing. In the case of the visual system, feedforward connections are thought to be responsible for the representation of retinal images while feedback connections are thought to be involved in the selection and interpretation of information (Dong 2004, Shao and Burkhalter 1996). It was discovered that feedback connections impact visual processing through alterations in receptive field properties (Hupe et al. 1998). Areas V1, V2 and V3 all receive feedback connections from the medial temporal area (MT). Hupe and others found that inactivation of MT led to a weakening of center response and center-surround interactions especially for low salience stimuli. These results suggest that feedback connections act to boost the gain of center response mechanisms and, in combination with horizontal connections, create center-surround interactions.

Input/Output of S1 Whisker

In the rodent, the primary whisker-barrel pathway begins in the principle trigeminal nucleus where information regarding whisker movement is relayed to a cluster of cells termed "barrelettes" (Gibson and Welker 1983; Jacquin et al. 1993; Deschenes 1998). Trigeminal sensory neurons surround the whisker follicles and send information about whisker movement to the principle trigeminal nucleus. This information is then sent to the ventral posterior medial (VPm) nucleus of the thalamus where there exists another organized cluster of cells known as the "barreloids" (Van der Loos 1976). The information from the barreloids is then sent in a somatoptic fashion to the layer IV barrels. This pathway is referred to as the lemniscal pathway and is the primary signaling pathway from the whiskers to the cortex. An additional pathway known as the paralemniscal pathway also transmits information from the whiskers to the cortex. This pathway integrates information across multiple whiskers and is therefore less specific in that it does not preserve the discrete topographical map of the whisker pad (Diamond et al. 1992).

As with most of the sensory cortical areas, the primary source of input to the barrel cortex is the thalamus. The VPm sends input primarily to the layer IV barrels, while the posterior medial nucleus (POm) sends information to layer IV septa and layers II/III and V/VI (Woolsey and Van der Loos 1970; Koralek et al. 1988; Fig. 2). Neurons with receptive fields dominated by a single whisker send input via the VPm to the layer IV barrels, which activates layer II/III neurons within the barrel column. Once in layer II/III this activation is spread beyond the individual column through horizontal connections (Petersen and Sakmann 2000). Broader-tuned input (cells with multiwhisker receptive fields) is thought to be processed primarily in the nongranular

layers via inputs from the POm and integration of individual whisker (barrel) sensory information.

Input/Output of M1 Whisker

Porter and White (1983) used anterograde (tritated amino acids) and retrograde (horseradish peroxidase (HRP)) tracing techniques to define the afferent and efferent pathways of the primary motor cortex in the mouse. They found that within the cortex, wM1 was reciprocally connected to the ipsilateral barrel field in S1, the face area of the second somatosensory cortex (SII), and the homotypic region of contralateral wM1. In both SI and SII labeled cells were primarily located in layers 2/3 and layer 5. In the homotypic region of contralateral wM1 cell bodies were found mostly in layers 3 and 5. They also found that wM1 had many subcortical connections including thalamic nuclei (ventralis lateralis and centralis lateralis) and the zona incerta.

More recent studies have elaborated on the input-output organization of wM1 revealing that connections also exist with the superior colliculus (Miyashita et al. 1994). The laminar distributions of afferents and efferents were similar to what was found previously, but with some new findings (Fig. 3). Reciprocal connections were found between wM1 and the primary and secondary somatosensory cortex, lateral and ventrolateral orbital cortex, retrosplenial cortex and perirhinal cortex. These corticortical afferent connections originated in layers 2/3, and 5 and sometimes layer 6 (SI only). Efferent connections from wM1 to these areas terminated mainly in layer 2/3. It was also discovered that wM1 projects primarily ipsilaterally to the superior

colliculus. The findings of these studies indicate that wM1 has significant interconnections with thalamic nuclei and other cortical areas, especially S1. These connections allow for integration of sensorimotor information and modulation of behavior.

Sensorimotor Integration

For most species, many functions necessary for survival rely on intercortical connectivity. One such function is the process of sensorimotor integration. Sensorimotor integration is the process by which information is transformed between sensory and motor areas in order to properly update motor plans in response to the sensory environment.

Rodent Sensorimotor Integration

Rodent whisking behavior provides a useful model for the study of sensorimotor integration. Rodents use their whiskers to navigate in the environment through a behavior known as whisking (Bermejo and Zeigler 2000). When whisking, an animal rhythmically moves its whiskers back and forth at a rate of approximately 10 Hz and the protraction of the whiskers is usually synchronous and of equal amplitude across both sides of the face (Welker 1964; Carvell and Simons 1990). Whisking allows the animal to gather information about the location (Bermejo and Zeigler 2000), size (Krupa et al. 2001) and texture (Carvell and Simons 1990) of the object in the environment. Movements of the whiskers have been shown to correlate with changes in the somatosensory cortex. Whole-cell membrane potential recordings in the barrel

cortex of awake mice at rest reveal slow, large amplitude membrane potential changes. When the animal begins to whisk, these potential changes become small, fast fluctuations that correlate with whisker position. Passive whisker stimulation and active whisker contact with an object result in robust subthreshold responses (Crochet and Peterson 2006).

Rodents can be reliably trained to use their whiskers to discriminate between rough and smooth surface textures (Carvell and Simons 1990). This and other tactile learning tasks rely on sensorimotor integration. Disruptions in active touch have been observed in whisker-trimmed animals. Animals (P70) that have had their whiskers trimmed from birth to P45 were able to discriminate between rough and smooth textures as well as non-trimmed animals; however, they were impaired in their ability to discriminate between two different rough textures (Carvell and Simons 1996). These results indicate that a disruption in sensory input early in life can lead to disruptions in sensorimotor integration, particularly the ability to make fine discriminations. Bilateral ablation of the cortical barrel field in rats results in significant differences in the mean amplitude of whisker protractions between the right and left side of the face (Harvey et al. 2001). These results offer insight into behavioral studies of whisking that have shown impaired abilities of rats on tactile discrimination tasks following bilateral ablation of the barrel field (Guic-Robles E et al. 1992). Unilateral ablation of the whisker motor cortex results in a disruption of the spatial and temporal organization of whisking movements, but does not abolish whisker movement on either side of the face (Gao et al. 2003). In this study, the

effects were most evident on the whisker pad contralateral to the lesion, but neither side exhibited a normal whisking pattern.

Human Sensorimotor Integration

When grasping an object, humans and primates use sensory feedback about the weight and surface texture of the object to determine how to grasp it properly. An example would be grasping an egg with enough force to lift it without cracking the shell. Grip force increases as friction decreases in order to prevent slipping (Johansson and Westling 1984). This ability requires that afferent sensory information regarding the properties of the object be sent to the primary motor area to allow for the proper grip force.

Studies of humans with peripheral sensory neuropathy provide insight into the function of afferent sensory information in motor functions. Patients who suffer from severe peripheral neuropathy show normal motor strength as well as normal preprogrammed finger movements and the ability to match forces. However these individuals cannot accurately judge weights of objects without visual feedback and they lack the ability to perform coordinated finger movements (e.g., grasping a pen) (Rothwell et al. 1982). Experimental studies in monkeys have shown similar results. Inactivation of the finger area of S1 by injections of muscimol (GABA agonist) leads to a loss of finger coordination (Hikosaka et al. 1985). In both cases the inactivation of S1 did not alter the finger strength or reaching abilities.

The ability of the deafferented patient to discriminate object weights in the presence of visual feedback indicates that he is utilizing an alternate strategy. Fleury

and others (1995) also found that deafferented subjects could discriminate weight of objects as well as controls when visual feedback was present. In the deafferented subject a significant correlation was found between weight and peak velocity, which was not found in any of the control subjects. The deafferented subjects appear to use the visual cue of peak velocity as an alternate way of determining object weight. This ability is dependent, in part, on vestibular processing. Deafferented subjects under head- fixed conditions could not discriminate small (light) differences in object weight, but large differences could still be discriminated in the absence of visual feedback. In these subjects vestibular feedback appears to play a role in weight discrimination especially when determining subtle changes.

Primate studies have shown that a lack of afferent input to the S1 hand representation leads to an increase in grip force (Brochier et al. 1999). Primates and humans vary their grip force depending on the weight and texture of the object that they are grasping. Inactivation of the S1 hand representation in monkeys leads to an initial increase in grip force, which was followed by a loss of coordination. These results indicate that feedback from S1 is also necessary for fine control of grip forces. Damage to the motor cortical hand area in monkeys leads to significant dexterity impairments, specifically in individuated finger movements which results in slower and less efficient execution of fine motor tasks (Roullier EM et al. 1998; Schieber and Poliakov 1998).

Cellular Components of Sensorimotor Integration

Neurons in the primary somatosensory cortex respond preferentially respond to various aspects of grasping movements. The majority of the receptive fields of the neurons located within the area 3b hand representation of the monkey are cutaneous and represent less than one digit (Salimi et al. 1999a). Two major categories of cells were identified based on their firing patterns. Dynamic cells respond primarily to the grip onset while static cells show increased activity during stationary holding phases. Peak discharges were analyzed in single cell recordings in the thumb and index finger region of the monkey during a grip task. Eighty-seven percent of the cells recorded from showed significant changes in peak firing rate in response to changes in texture, while only 58% showed similar responses to changes in weight (Salimi et al. 1999b). Cells also exhibited preferential responses to certain textures; some showed increased activity in response to smooth textures while others responded to rough textures. These individuated responses support the idea that processing and transformation of efferent signals occurs in S1, which may form the representation of object surfaces that are then relayed to M1.

The receptive field properties of neurons in the hand area of the monkey motor cortex are very similar to what is seen in S1 (Picard and Smith 1992a). Just as in S1, more cells respond to texture as compared to weight and there was a differential response to smooth versus rough surfaces. During dynamic phase of the task, monkeys increased grip force in multiple steps indicating that they relied on sensory feedback. It can be concluded that somatosensory feedback contributes to the

regulation of grip force by modifying motor cortex activity in response to texture input.

Cortico-cortical connections made by pyramidal neurons are principally excitatory, and they influence other cells through the release of the excitatory neurotransmitter, glutamate. Glutamate receptors fall into two major categories: NMDA and non-NMDA. Shima and Tanji (1998) reported that there is a greater contribution of non-NMDA receptors in M1 in response to S1 stimulation in adult monkeys. Recordings in M1 were made while stimulation was applied in S1 during trained motor task. Application of non-NMDA antagonist (CNQX) suppressed the output of the majority of movement related neurons in M1. Thus the input from S1 to M1, which is essential in making somatosensory adjustments to motor movements, is predominately mediated by non-NMDA receptors.

Long distance cortical connections are usually made by axons of pyramidal cells (White, 1989). Many studies across various species have found that the cortical connections responsible for sensorimotor integration are localized to layers 2, 3 and 5 in both M1 and S1 (Prud'homme et al. 1994; Farkas et al. 1999; Alloway et al. 2004). In the rodent, the primary projection to the primary motor cortex from the barrel cortex is located above and below the septal regions of the barrel cortex and it is organized into multiple vertically oriented columns (Alloway et. al. 2004). The septal region is thought to contain cells that have primarily multiwhisker receptive fields (Simons 1989). This pattern suggests that information being sent to wM1 has been processed to incorporate the movement of the object across the row of whiskers. This

organization of M1 projecting neurons may represent a circuit specific to sensorimotor integration.

Pathway of sensorimotor integration

One question that is debated in the literature is at what level in the pathway does sensorimotor integration occur? There are many pathways and proposed parallel cortical loops responsible for the integration of sensory input with motor control (Ahissar and Kleinfeld 2003; Farkas et al. 1999). Within each of these loops both fast and slow signals exist (Kleinfeld et al. 1999). Fast signals travel quickly (approximately 2.0-2.5 ms in the rodent) and are purely cortico-cortical as their response times are too quick to involve any subcortical relays, while slow signals presumably involve various subcortical structures, though variability in conduction speed and synaptic input may also alter signal speed as well (Herman et al. 1985 ; Farkas et al. 1999; Gasparini 2006)

Integration of sensory and motor information is likely to occur in areas where these pathways converge. It has been shown that S1 projects to various motor areas including M1, the neostriatum and the basal pons (Alloway et al. 1999 ;Hoffer et al. 2003). Of the motor projecting S1 neurons, labeled projections to the neostriatum show the largest number of variscosities and occupy the greatest area (Hoffer et al. 2005). Additionally, projections from corresponding whisker representations in M1 and S1 show significant overlap in the neostriatum (Hoffer and Alloway 2001) and that these corticostriatal projections converge on target neurons (Ramanathan et al. 2002). Projections from adjacent regions of S1 show the largest degree of overlap in

the basal pons suggesting that the integrating information from different regions of S1 is likely performed in this region (Hoffer et al. 2005).

Some degree of sensorimotor processing appears to be taking place at the level of the cortex. Firing frequencies in S1 cortex of monkey reflect an interaction of both the texture and the weight of the object, which may represent a coding of the object surface (Salimi et al. 1999c). However, how this "coded" somatosensory information is used by the motor cortex is unclear. The dynamics of this intracortical sensorimotor system is unclear, largely due methodological constraints involved in studying long-range connections.

The rodent whisker sensorimotor pathway provides a useful model in which to study sensorimotor interactions. Though the rodent pathway is likely to be less complex than the pathway that exists in humans, the fundamental circuitry is likely comparable. This is evidenced by the rodent's ability to utilize its whiskers for discrimination. Similar to the way in which humans can discriminate objects with only tactile information from the hand, rodents too can differentiate between textures though the use of their whiskers as seen above. Additionally, the highly structured organization of the barrel cortex in the rodent can provide insight into how these transformations are made within a well defined circuit. This study will introduce a novel preparation in which intracortical feedforward and feedback pathways of the rodent sensorimotor pathway can be investigated through the creation of an *in vitro* sensorimotor slice. Using this preparation, we have explored the anatomical connections between the wS1 and wM1 and the dynamics of the connectivity between these two areas.

Specific Aims

It is clear from studies of humans and primates that primary motor (M1) and primary somatosensory (S1) cortices communicate directly through feedforward and feedback mechanisms and that their communication is necessary for proper motor control and functioning. This connection allows the motor cortex to rapidly update its motor plans in response to sensory stimuli. The present study was designed to evaluate the anatomical and physiological properties of the S1-M1 pathway using the mouse neocortex as a model. Our aim was to create an *in vitro* sensorimotor slice preparation that contains both whisker S1 (wS1) and M1 (wM1) and maintains their reciprocal connectivity. The creation of this novel slice preparation will enable future studies of functional connectivity between these two areas.

Specific Aim 1: To create a novel slice preparation containing both primary motor (M1) and primary somatosensory (S1) areas while maintaining connectivity between the two areas.

A. *In vivo* experiments were performed to determine the optimal stereological coordinates used to target whisker representation in M1 and S1. S1 was identified through insertion of a recording electrode into the designated area, followed by contralateral whisker deflection. The location of wM1 was confirmed by insertion of a bipolar stimulating electrode. Contralateral whisker movement corresponding to the stimulus pulse served as confirmation.

B. In order to ensure that the slice contained the least number of transected axons in the pathway for both directions, we optimized the angle of sectioning and the section thickness. M1 and S1 whisker representations were labeled *in vivo* through pressure injection of food coloring. Only sections containing markers for both areas were used and fiduciary marks were made to ensure visibility.

C. To confirm that the pathway was captured in our *in vitro* sensorimotor slice, biocytin was injected into M1 and S1. Injections were made by applying biocytin directly to the tip of a needle, which was then inserted into the slice at the confirmed location. The slice was kept in the chamber for at least two hours to allow for complete transport of biocytin.

Specific Aim 2: Morphologically define the axonal pathway between wM1 and wS1.

A. *In vivo* biotinylated dextran amine (BDA) injections were made into physiologically identified wS1 and wM1 to determine the projection pathway in both directions. To insure proper transport of BDA, two to three days separated the date of injection from the date of sectioning. Tissue was sectioned and stained to determine location of BDA transport.

B. Using the sensorimotor slice and the BDA-labeled axons we quantified the axonal pathway. For both directions, measurements were taken to

determine the location of the pathway in the cortical plate and the tortuosity of the axons.

C. Large volume biotinylated dextran amine (BDA) injections were made *in vivo* into physiologically identified wM1 to investigate synaptic specificity in wS1. Tissue was counterstained with cytochrome oxidase (CO) and cut tangentially in order to visualize whisker barrels. Infragranular bouton populations were compared between the area below the barrels (target) and the area between the injection site and the target.

Specific Aim 3: Characterize the dynamics of the S1-M1 pathway *in vitro*.

A. To determine that functional connectivity has been maintained after sectioning the sensorimotor slice, extracellular field potentials were recorded in wS1 and wM1 in response to stimulation in the corresponding region.

B. Using current clamp techniques, whole cell recordings were performed on wM1 and wS1 cells within the sensorimotor slice. Intrinsic cell properties were identified by quantifying responses to depolarizing step currents. Synaptic properties were determined by analyzing individual cell responses to stimulation applied in the reciprocal location.

C. Electrodes used to record from individual cells were filled with biocytin so that morphological data could be collected.

General Methods

Experimental procedures: All experiments were performed on white laboratory adult Swiss mice (CD-1, postnatal day 15–60) of either sex (Charles River Laboratories, Wilmington, MA). All procedures were in accordance with the Institutional Animal Care and Use Committee guidelines of Queens College, CUNY (protocol #100). For all surgical procedures, mice were anesthetized through i.p. injection of ketamine/xylazine (153 mg/kg/2.23 mg/kg) until they were unresponsive to a noxious stimulus (toe pinch). All *in vivo* recordings were performed while animals were fixed in place using a small animal stereotaxic apparatus (Kopf Instruments) and given supplemental doses of anesthesia as needed.

In vivo microstimulation and mapping: An approximately 1 mm × 1 mm window was made in the skull to expose the cortex above the whisker representations of S1 (wS1) and M1 (wM1) using published stereotaxic coordinates (Franklin and Paxinos, 1997). To confirm the location of M1, a bipolar stimulating electrode (500 μm intertip distance, Frederick Haer Co., Brunswick, ME) was inserted perpendicular to the pial surface to a depth of approximately 300 μm into the cortex of the right hemisphere. Stimulating pulses were applied via a stimulus isolation unit (World Precision Instruments), controlled by a Master-8 (AMPI) beginning at low intensity (0.1 mA) and gradually increasing until isolated contralateral (left) whisker movement was observed. The location of whisker S1 (barrel cortex) was confirmed by inserting a tungsten microelectrode (3–4 MΩ, Frederick Haer Co.) perpendicular to the pial surface and manually driven to a depth of approximately 300 μm. Activity was

amplified, digitized and recorded (A-M systems amplifier, Digidata analog-to-digital system (Axon Instruments), Axoscope version 8.0 (Axon Instruments) while whiskers were being manually deflected contralateral to the recording location. Robust unambiguous responses to contralateral whisker deflection were used as confirmation of barrel cortex. For early sensorimotor slice experiments, both regions were marked with cresyl violet injections (2.5 g/1.5 ml, dissolved in acetate buffer) *in vivo* (wM1 and wS1) to ensure that the section contained both physiologically confirmed areas. Once the slice was developed, the section was identified by number and confirmed by the presence and location of previously identified subcortical structures.

Tissue processing: Sensorimotor (SM) sections containing identified wM1 and wS1 were cut parasagitally at a 45° angle relative to midline (Ted Pella Vibratome (vt 1000s, Leica; Fig. 4) at 350 μm. As shown in Figure 4, brains were hemisected and the medial edge was glued to an angled agar block (45-45-90 triangle). Using this method, one sensorimotor slice is created per hemisphere, which can be identified by the location of the subcortical structures seen in Fig 4. With the rostral end of the brain facing upward, the tissue was sliced at 350 μm. For some anatomical studies tangential sections (90 μm) were made through Layer IV of the barrel cortex to view synaptic densities relative to the layer IV barrel field following large BDA injections.

For all morphology experiments, the following staining protocol was utilized (Alloway et al., 2004; Brumberg et al., 2003; Pucak et al., 1996). Free floating 350 μm sections were rinsed (3 × 10 min) in 0.05 M cold PBS. Sections were then incubated twice (30 min each) in a blocking solution of 0.05 M PBS, 0.4% Triton-X

(Sigma) and 0.5 mg/ml Bovine Serum Albumin (Fisher Scientific). Biotinylated dextran amine (BDA) and biocytin-filled cells were revealed using the avidin–biotin-peroxidase complex method (ABC, Vector Laboratories) with 3,3′-diaminobenzidine (DAB; 5 mg/ml in 0.1 M PB Fluka; 0.5% H_2O_2) and nickel ammonium sulfate (NAS, 1.10 g/10 ml H_2O) as the chromagen for the peroxidase reaction. Sections were incubated in the avidin–biotin solution overnight at 4°C. Sections were then rinsed at room temperature in 0.1 MPB (4 × 10 min). Slices were incubated in DAB/NAS solutions (0.4 ml NAS/20 ml DAB) for 12 min exactly. Hydrogen peroxide was added drop wise until a black precipitate formed. Sections were immediately rinsed in 0.1M PB (3 × 10 min), dehydrated, mounted and coverslipped using mounting media (Shurmount, Triangle Biomedical Sciences). Mounted sections were viewed with an Olympus BX51 microscope using 4× (0.1 numerical aperture (NA)), 10× (0.4 NA) and 60× (1.4 NA, oil immersion) objectives. Digital images were taken using an Optronics Microfire camera attached to a dedicated PC via firewire connection.

Experiment 1: Methods

Retrograde tracer injections: Following localization of the target region (i.e. wM1 or wS1), tracer injections were made via glass micropipettes. All injections were made in the right hemisphere. Glass micropipettes (O.D. /I.D. in mm; 1.0/0.58) were fashioned on a Sutter micro-pipette puller (P-87, Sutter Instruments), and were filled with BDA (BDA; 2.5 g/ml in 0.01 M Phosphate Buffered Saline (PBS), Molecular Probes). Approximately 0.5µl of the BDA solution was pressure injected (Toohey Company) into the region of interest using several pulses of pressurized N_2 of duration of less than 1 ms. Large volume (up to 1 µl) BDA injections were made using a Hamilton Syringe (Hamilton Company). Animals were recovered and survived for at least two days to allow for adequate transport. Mice were anesthetized through an i.p. injection of Nembutal (0.1 mg/100 g) and perfused with 0.9% saline followed by 4% paraformaldehyde in 0.1 M phosphate buffer (PB). Tissue was post fixed overnight at 4^{o}C. Tissue was sectioned in the sensorimotor plane or tangentially as previously described.

To confirm the presence of unsevered axons connecting wS1 and wM1 within the sensorimotor slice, crystals of biocytin were placed in live 350 µm sensorimotor sections. Crystals were placed into either wM1 or wS1 via a 27-gauge needle that was pushed into the slice. Fiduciary marks were made in the gray matter lateral to the identified areas for later identification. Slices were held in an interface chamber perfused with artificial cerebral spinal fluid (ACSF, see below for contents) at 33^{o}C for approximately 6–8 h to ensure transport of the biocytin between locations. Slices

were carefully removed and post fixed overnight in a 4% paraformaldehyde solution. Slices were then processed, mounted and coverslipped as described above.

Axon tracing and stereology: Axons were reconstructed using the Neurolucida program (MicroBrightField, Williston, VT) under 60× magnification and analyzed using NeuroExplorer (MicroBrightField). Contours of each section were also constructed at 4× and included the pial surface, white matter border and tracer injection site. Axonal trajectories were computed by measuring their tortuosity which compares the actual path length of an axon in three-dimensions to its shortest possible path length; a value of 1.0 indicates a perfectly straight line.

StereoInvestigator software (MicroBrightField, Williston, VT) was used to perform bouton quantification using the optical fractionator method. The barrel region was outlined in Layer IV under low (4×) magnification. The corresponding region in Layer V of the same animal was also outlined using the same procedures and aligned using the local vasculature. Within the same Layer V section, the area between the injection site and the area below the barrels was also outlined. Approximately 15 random sampling sites were used for analysis for each area (area below barrels and the area in between the injection site and target) throughout the depth of the tissue. Each bouton observed within the sampling sites were marked which was used to estimate the total number of boutons per location.

Data Analysis: T- tests were used to compare axon tortuosity and thickness of M1 projecting cells to S1 projecting cells (alpha level $p < 0.05$). Bouton estimates were normalized for area and directly compared.

Experiment 2: Methods

Preparation of tissue for in vitro recording studies: Adult mice of either sex were anesthetized as previously described. The brain was quickly removed and sectioned in the sensorimotor plane in chilled, oxygenated artificial cerebral spinal fluid (ACSF) solution (in mM: 124 NaCl, 2.5 KCl, 2 $MgSO_4$, 1.25 NaH_2PO_4, 1.2 $CaCl_2$, 26 $NaHCO_3$, 10 dextrose). Sections were kept in oxygenated ACSF and kept at 34 °C for at least 1 h before the start of the experiment.

Extracellular recordings: Bipolar stimulating electrodes similar to those used *in vivo* were placed in either S1 or M1 and a recording electrode was placed opposite to the location of the stimulating electrode (3–4 MΩ, Frederick Haer Co., Brunswick, ME). Recorded data were amplified 1000 fold and filtered at 100 Hz–5 kHz (A-M Systems Model 1700) and digitized using the Digidata system (Axon Instruments) and recorded with Axoscope 8.0 (Axon Instruments). Analysis was done using PClamp software (version 8.0, Axon Instruments).

For some experiments, 5 µl of an excitatory synaptic blocking solution of CNQX (40µm)/APV(50µm) (Sigma–Aldrich), dissolved in ACSF, was added directly to the slice after recording baseline field potentials. To inactivate S1 or M1 selectively we applied 1 mM Muscimol (Sigma–Aldrich) at the stimulation site which hyperpolarizes the somata without affecting fibers of passage (see Hirsch, 1995). Stimulation was immediately applied following the application of the pharmacological agents and responses were recorded as stated above.

Whole cell recordings: Cells were visualized with infra red – differential interference contrast optics (Olympus BX51WI). Intracellular recording electrodes were pulled from fire-polished thick-wall glass (1.5mm O.D., 0.8 I.D.) on a microelectrode puller (see above) resulting in a final resistance of approximately 3MΩ. Electrodes were filled with (in mM) 120 KGlu, 10 NaCl, 20 KCl, 10 HEPES, 2 Mg-ATP, 0.3 Na-GTP, 0.5 EGTA, and 0.3-1% biocytin (wt/vol) for subsequent visualization of the neurons. Cells were recorded using current clamp methods from infragranular layers. Once a stable recording was obtained (resting V_m of <-55 mV, ability to generate action potentials in response to a depolarizing current pulse) intrinsic properties were assessed. Resting membrane potential was determined by measuring the membrane voltage in the absence of current input. Intrinsic properties were determined by quantifying responses to a series of 1 s steps (ranging from -300 to 300 pA) applied from rest. To calculate action potential characteristics, we analyzed responses of cells to threshold currents for generating action potentials. The input resistance for peak (R_{in} Peak) was calculated using Ohm's Law based on the maximum voltage deflection in response to a hyperpolarizing current step of -30 pA . The input resistance ratio (R_{in}) was calculated based on responses to a 1s step current of -30 pA. The value is equal to the resistance at the maximum hyperpolarized value divided by the resistance at 100 ms prior to the stimulus offset. The slope of the firing current (FI) relationship was determined by analyzed responses of cells to threshold currents for activating action potentials to responses to two times the threshold value. Once intrinsic properties were assessed, synaptic response data was collected by placing a stimulating electrode (see above) in the infragranular layers of the whisker

representation (e.g. M1) while recording in the target area (e.g. S1). A response threshold was determined by stimulating with a series of 100μs current pulses (ranging from (1μA to 10mA) until a reliable response was observed. If a response was not observed to a single stimulus pulse, a train of 3 pulses was then applied at various frequencies (10 Hz to 100 Hz).

Neuronal reconstruction: Biocytin-filled cells from whole cell recordings were reconstructed for morphological analysis using the Neurolucida software program (MicroBrightField, Williston, VT). Contours of each section were drawn at 4× and cells were marked. Tracing of soma and dendrites was done at 60×, and axons were tracing using a 100× lens. The following soma characteristics were analyzed with the same program: Feret Maximum (longest diameter of the soma), Feret Minimum (longest diameter perpendicular to the feret maximum), Aspect Ratio ((Feret Max)/ (Feret Min); as the aspect ratio approaches one, it is indicative that the soma is closer to a symmetrical shape (e.g. circle or square)) and Roundness ((4x Area)/ (π x Feret Max^2)).

Data Analysis: Off-line analyses were performed using Clampfit 9.2 (Molecular Devices). Extracelluar paired-pulse responses were analyzed with an ANOVA. Pairwise comparisons were made post-hoc using Fisher's LSD. Cells categorized based on their response to the stimulus. T-tests were used to perform between intrinsic membrane and firing properties. Mann-Whitney test was used to compare synaptic response results due to unequal variance. Chi-Square test was used to

compare population distributions. Statistical analyses were done with Statistica (StatSoft).

Experiment I: The sensorimotor slice.

Introduction

Despite the role that intercortical connections have in cognitive computations, research has traditionally focused on the response properties (*in vivo* studies) or the physiological properties (*in vitro* studies) of neurons found in specific cortical areas. Furthermore, little research has focused on interactions between cortical areas, particularly those serving different functions (e.g. sensory and motor). The lack of a model preparation that contains interconnected cortical areas has been a hindrance to this line of research and the development of such a preparation is an important step towards understanding intercortical connectivity.

At present it is unknown what pathways the axons that connect S1 and M1 traverse, or what the synaptic targets of these pathways are. Despite the fact that motor cortex and somatosensory cortex are adjacent to each other, little work has been done to develop a slice which contains these two areas and their reciprocal connections. In the case of the rodent somatosensory, visual and auditory systems it is possible to cut a slice that contains both the thalamus and cortex with some degree of connectivity maintained (Agmon and Connors 1991; Cruikshank et al. 2002, MacLean et al. 2006).

The advantage of a slice that contains S1 and M1 would be the ability to study the relationship between cortical feedforward and feedback networks in the same slice. A similar approach has been utilized to effectively study the interactions and the spread of epileptic activity between the hippocampus and adjacent cortical areas such as the

entorhinal cortex (Breustedt et al. 2002) and the parahippocampal cortex (Bear and Lothman 1993). Additionally, feedforward and feedback connections between V1 and V2 of the rodent visual system have been investigated using a visual cortex slice containing these areas and their reciprocal connections (Domenici et al. 1995). In order to study the interconnectivity between whisker M1 and whisker S1 we have developed an *in vitro* preparation that contains these areas and maintains their synaptic interconnectivity. In this study we utilize neuroanatomical tract tracing techniques to morphologically define the axonal pathway between S1 and M1.

Results

In this study we created an *in vitro* preparation that contains the whisker representations of both primary motor and primary cortical sensory areas while also maintaining their synaptic interconnectivity. The precise locations of wM1 and wS1 were identified *in vivo* prior to slice preparation. In our anatomical studies, both areas of interest were marked and the brain was subsequently hemisected and sectioned at a 45 degree angle relative to the midline. We found this to be the optimal angle of sectioning in which to capture the whisker representations of M1 and S1 within the same cortical slice (see Figure 4).

Connectivity in the sensorimotor slice

The first step in creating the sensorimotor slice was to determine the relative location of the axonal pathway between wS1 to wM1 in order to maximize our ability to maintain these pathways and their synaptic targets within one cortical section. *In vivo* injections of rhodamine conjugated BDA were used to visualize the axonal pathway and synaptic targets of these two regions. In separate experiments, injections of a fluorescent tracer were made in wS1 and wM1. The results of these experiments revealed an axonal pathway (in both directions) that projects mainly via the infragranular layers connecting these two areas (Figure 5A). The labeled pathway extends the entire distance (≈ 3 mm) between S1 and M1 (Figure 5B). Some sparse axonal labeling was observed in the supragranular layers, however these axons are not included in the analyses because the few that are observed all are transected and do not extend greater than a few hundred microns from the injection site. The results

of these fluorescent tracer studies enabled us to determine the optimum angle at which to section the tissue in order to maintain the infragranular axonal pathway between wS1 and wM1.

In order to better quantify the connections between whisker M1 and S1, BDA was injected into either area and allowed to transport (Figure 6). The projection site (e.g. M1 if BDA was injected into S1) was marked with an injection of cresyl violet just prior to perfusing the animal for future localization. Transport across the entire length of the pathway was observed in all animals (n = 20 of 20) regardless of injection location. Similar patterns of labeled axons were observed in the S1 injected (Figure 6, A-C) and M1 injected (Figure 6, D-E) animals. Labeled cells (Figure 6A) were observed at the injection sites and at various locations throughout the pathway. Injections of large volumes of BDA into whisker S1 reveal the outlines of the layer IV barrels (see the unstained areas highlighted by asterisks in Figure 6C) providing additional confirmation of the correct placement of our BDA injections. The lack of staining of the barrels confirms that neurons involved in the pathway from S1 to M1 do not originate from the barrel. Control experiments were done to determine the specificity of the connections observed in the sensorimotor slice. *In vivo* BDA injections were made into the forepaw representation of S1 (n=3) and M1 (n=3) and sectioned in the identical sensorimotor plane (see methods). While there was some axonal labeling observed in these forepaw-area-injected sections, these projections were sparse and nonspecific and very different from those observed following injections into the whisker representations of M1 or S1 (not shown). These results indicate that the whisker S1-M1 pathway is topographically specified.

It is possible that axons connecting S1 and M1 may be transected during slice preparation and that the observed pathway may be an incomplete representation since the injections were made *in vivo* prior to slice preparation. To address this issue, injections of biocytin were made during separate *in vitro* experiments in either S1 or M1 in slices maintained in an interface style chamber. After six to eight hours the slices were fixed and reacted for biocytin. Results of these *in vitro* labeling experiments (Figure 7) revealed analogous patterns of connectivity as the *in vivo* BDA injection experiments. These results indicate that a significant number of axons are preserved in our plane of section (n=6).

Quantitative characterization of sensorimotor axons

There are several factors that can affect the transfer of information between cortical areas. One factor that is particularly important is the speed of axonal conduction which can be mediated by several factors including axonal diameter and tortuosity. In order to determine if the axonal properties differed between M1 projecting and S1 projecting cells, we quantified their axonal diameters and the directness of their pathway from origin (e.g. M1) to target (e.g. S1) through the utilization of a computer -assisted morphometric analysis system (Neurolucida). A reconstruction of a sensorimotor section can be seen in Figure 5B. Both the BDA injection site (S1) and the marker injection site (M1) are delineated. The distance between the anterior border of S1 and the posterior border of M1 is approximately 3 mm. The reconstruction data show that while many of the axons that connect the two areas are preserved in this plane, a portion of the axons are transected during

sectioning. Due to the number of axons labeled and the difficulty in reconstructing them over several millimeters, we are not able to calculate what percentage of the connection is maintained.

We quantified two aspects of the axons that may influence their physiological functioning, their diameter and the directness of the path that they took from their origin to their target (e.g., S1 to M1). Using a 60 x (1.4 NA) objective, the diameters of 52 S1 projecting axons and 38 M1 projecting axons were measured. Axons originating from M1 had an average diameter of 0.61 μm ± 0.23 standard deviation (S.D.) whereas those originating in S1 were significantly smaller in diameter ($t = 3.06$, $p < .01$) with an average of 0.48 μm ± 0.12 S.D. (Figure 8A). Thus the feedforward (FF) S1 to M1 pathway had smaller diameter axons then the feedback (FB) pathway from M1 to S1.

To assess the trajectory of the path that the two axonal populations took we computed their tortusoity (see methods). Tortuosity is a measure of "straightness" where a value of 1.0 indicates the shortest possible path between the origin and target of the axon. The average tortuosity (Figure 8B) value for M1 originating axons was 1.03 ± 0.02 S.D. (range 1.00-1.14, $n = 52$). The tortuosity values for S1 originating axons did not differ significantly from M1 injected animals with an average value of 1.02 ± 0.01 S.D. (range 1.00-1.07, $n = 38$). These results suggest that axons in the reciprocal sensorimotor pathway take the most direct route between their origin and target. Further analysis revealed that the axons labeled in the *in vivo* and *in vitro* experiments were found in the same depths of the cortical plate and when their axon

morphologies (diameter and tortuosity) were compared there were no significant differences.

In order to better visualize the synaptic targets of the S1 projecting cells, large volume BDA injections were made in M1 and tissue was tangentially sectioned and counterstained with cytochrome oxidase (CO) so that barrels could be identified (Figure 9). Infragranular sections display dense staining of the axonal pathway and indicate that M1 projecting cells avoid the barrels (Figure 9A). Stereological estimates were performed to compare the relative population of boutons in the axonal pathway between wS1 and wM1 to those observed in barrel region (Figure 9D). It was estimated that there are approximately two times more M1 cell boutons in S1 ($0.07/\mu m^2$) (the target location) than there are within cortical area between the two locations ($0.03/\mu m^2$). One possibility was that the axons that connect S1 and M1 have putative synapses (boutons) along their entire extent, which appears not to be the case since a greater number of boutons was observed in S1 when compared to the region between M1 and S1 (see Figure 9C). These results suggest that that the cells in M1 may directly and preferentially target cells in S1.

Summary of Experiment I

Many studies have utilized *in vivo* techniques to learn more about sensorimotor processing (Smith 1983; Wannier 1991). Though these studies have contributed greatly to our knowledge of this pathway, they do not allow for the direct investigation of how sensorimotor information is processed. Through the creation of

our novel slice preparation these connections can now be studied for the first time *in vitro*, which will allow for more detailed investigations of this pathway.

Our results indicate that the axonal pathway between whisker S1 and whisker M1 is maintained in the sensorimotor slice as confirmed by our *in vitro* tracing experiments. We have found that this reciprocal pathway is topographically specific and is primarily restricted to the infragranular layers in both directions (FF and FB). The axons comprising this pathway extend the entire distance between the two regions (approximately 3 mm) and vary in their morphological structure depending on their target location. We have found that axons of the FB pathway (M1 to S1) have significantly larger diameters those axons of the FF pathway (S1 to M1). The axons of both pathways follow a relatively straight path. There appears to be specificity in the synaptic targets of these cells as there is a greater estimated bouton density at the target location (S1) compared to within the pathway itself. In sum these novel results reveal that sensorimotor interactions between S1 and M1 can be studied *in vitro.* This preparation allows for detailed analyses of the neurons of these pathways and their synaptic connectivity which will provide a better understanding how the brain adapts its motor plan to changes in the sensory environment.

Experiment II: *In vitro* characterization of the dynamics of the sensorimotor pathway.

Introduction

Sensory input provides information about our environment. Often, this information is translated into a motor response which either allows us to gain more information about the sensory stimuli or navigate away from it. While we are aware that the sensory and motor cortices communicate, the neural mechanisms underlying this communication remain largely unknown.

The functional dynamics of feedforward and feedback connections have been widely studied within the visual system. These studies have shown that feedforward and feedback connections often vary in their laminar distribution and in their synaptic targets (Lund et al. 1976; Weller and Kaas 1978; Johnson and Burkhalter 1996). They have also shown that these pathways vary in their responsiveness to stimuli (Shao and Burkhalter 1996). Presently it is unknown if these findings apply to all intracortical feedforward and feedback connections. Is this pattern specific to connections of the same modality or does it apply to extrinsic connections as well? Does the same pattern of connectivity exist in the sensorimotor system? Gaining knowledge of the components of these pathways and how they function is an important step towards understanding how the brain translates sensory input into a motor response and the role of feedback in the sensorimotor circuit. This will provide insight into the processes underlying sensorimotor integration and cortical connectivity in general.

With the development of the sensorimotor slice (experiment 1) we can now directly investigate the feedforward and feedback connections within the rodent sensorimotor pathway. In the present study we have used *in vitro* extracellular and whole cell recording techniques to characterize the synaptic properties of the sensorimotor system. Morphological data and intrinsic cell membrane and firing properties are utilized to identify the components of each circuit.

Results

The results of Experiment 1 indicate that the targeted axonal pathway between wS1 and wM1 is preserved within the sensorimotor slice, and that this pathway is largely restricted to the infragranular layers. To determine if functional connectivity is maintained after sectioning, we recorded from one target area (e.g. S1) while stimulating in the reciprocal location (e.g. M1) using both extracellular and whole cell recording techniques. For whole cell recordings, electrodes used to record from individual cells were filled with biocytin so that morphological data could also be collected.

Functional connectivity is maintained in the sensorimotor slice

The presence of an anatomical connection between whisker M1 and S1 does not prove that the observed pathway is functional. Electrophysiological analyses were performed to determine if functional connections were also maintained in the sensorimotor slice. Initially, wS1 and wM1 were identified *in vivo* (see *in vivo microstimulation and mapping* in the methods section) and non-toxic food coloring was injected into each location. Once slices were placed in the interface chamber, fiduciary marks were made slightly anterior to the M1 injection site and slightly posterior to the S1 injection site to allow for recognition of the two locations since the food coloring washed out in the interface chamber after several minutes. Additionally, subcortical markers such as the relative position of the hippocampus

and striatum provide further identifiers of the target locations within the sensorimotor slice (see Figure 4C).

To test for a functional connection, a bipolar stimulating electrode was placed in either identified wS1 or wM1 while a recording electrode was placed in the reciprocal area. We stimulated slices with a negative current pulse of 200 μs duration and 200-500 μA of current and resulting field potentials were recorded in the reciprocal location. In normal ACSF, robust responses were seen in the reciprocal area following stimulation (e.g. M1 after S1 stimulation, Figure 10A black line).

We next sought to determine if this connection was glutamatergic, using locally application of glutamatergic antagonists CNQX (40 μM) and APV (50 μM). CNQX/APV application led to a 70% decrease in the evoked field potential in S1 (n=3) and a 77% decrease of the field potential in M1 (n=3) following stimulation in the reciprocal area (Figure 10 A, B grey lines). The diminution of the response following application of glutamatergic antagonists strongly suggests that some degree of synaptic connectivity is maintained in the sensorimotor slice and that the reciprocal connection is mediated by glutamate. In several cases the original amplitude of the field potential could be recovered following washout. These results coupled with the anatomical findings demonstrate that synaptic connections are maintained between whisker S1 and whisker M1 in the sensorimotor slice.

The short term dynamics of the connection between the two areas were assessed in response to paired-pulse stimulation between S1 and M1 (see Figure 11) using extracellular recording techniques. Following stimulation in M1 a facillitory response in S1 was observed across most interstimulus intervals assessed (n=16),

whereas facilitation was rarely observed following stimulation in S1 and recording in M1 (n=16). This differential responding is most evident at interstimulus intervals below 20 ms ($F= 3.26$, $p <.001$). These results suggest that that facilitation is more likely to occur in the feedback pathway (M1 to S1).

To determine the influence of antidromic activation within this preparation, we inhibited the stimulation site by hyperpolarizing the neurons in that location with local application of 1mM muscimol ($GABA_A$ agonist). We then repeated the stimulation protocol described above. Muscimol application at the stimulation site significantly reduced the evoked field in the reciprocal area (see Figure 12). Since muscimol should have no effect on axons (they lack $GABA_A$ receptors) and the resultant antidromic activity, the reduction of the evoked field potential suggests that antidromic activation is being minimized in our preparation.

Direct connections are observed between S1 and M1

To investigate individual cell responses whole cell current clamp recordings were made in S1 and M1 within the sensorimotor slice. The large distance between the recording and stimulating locations (≈ 3 mm) posed a number of challenges. One such challenge was in placement of the harp used to stabilize the slice. The slice had to be positioned such that it was secured beneath the harp, but at the same time the wS1 and wM1 areas had to be accessible to the stimulating and recording electrodes. Once the harp was in place, the regions within wS1 and wM1 that were suitable for recording were limited. The only areas where we could target cells were those exposed regions where the cortex between the target locations was not transected by

the strings of the harp. For this reason, we were not able to systematically sample cells from various locations within each location as we were limited to whatever suitable area was remaining. Laminar distributions of cells are estimated post-hoc following tissue processing to reveal biocytin-filled cells (see Figure 19). Physiological data was collected and included intrinsic membrane and firing properties as well as synaptic response properties for each cell when possible. To evaluate intrinsic firing properties, responses to depolarizing and hyperpolarizing step currents (-100 pA to +300 pA by 10 pA steps) were used. Synaptic properties were assessed by evaluating post-synaptic responses to bipolar stimulation in the reciprocal area.

There were 33 cells recorded from in S1 across 6 different mice, and 20 cells recorded from in M1 across 5 different mice (n= 53; Table 1). A majority of the cells that were recorded from in S1 (21 of 33) and M1 (14 of 20) were able to be visualized following biocytin processing. For each of these recovered cells, laminar locations of cell bodies were determined in S1 (21 of 33) and M1 (14 of 20). A large portion of the recovered cells were able to be reconstructed in S1 (16 of 21) and M1 (11 of 14). This allowed us to gather additional morphological data including the shape and area of the cell body, as well as dendritic arborization patterns. Due to the large number of cells recorded from in each section and the close proximity of the cells to one another, it was not always possible to pair the physiological and morphological data across every measure. For those cells that did not fill completely, we were able to match only the laminar distribution with the physiological data (S1 = 14 of 33; M1 = 14 of 20). For cells that were able to be reconstructed, we were able to determine the shape

of the cell body (pyramidal or nonpyramidal) which we could then correlate with physiological response properties (S1 = 9 of 33; M1 = 11 of 20). We were able to completely match 9 cells in S1 and 5 cells in M1 on all physiological (intrinsic and synaptic), and morphological (layer and soma properties) features (n=14 of 53).

Table 1. Summary of sample totals and analyses by location.

	S1 Total	*M1 Total*
Animals	6	5
Individual Cells recordings	33	20
Complete Intrinsic data	31	20
Cells Recovered (layer)	21	14
Reconstructed Cells (shape)	16	11
Intrinsic * Response	31	20
Layer * Response	14	14
Shape * Response	9	11
Shape* Layer* Response* Intrinsic	9	5

The following synaptic response categories were identified based on individual cell responses to stimulation in the reciprocal area: direct (presumed mono-synaptic connections), indirect (presumed poly-synaptic connections), both (direct and indirect) and no response. Direct responses were those that occurred immediately (< 150 ms) following the stimulus and that were reliably present across multiple trials (Figure 13B). Indirect responses were responses that occurred after the presentation of the stimulus, but with latency > 150 ms (Figure 13A). Two additional categories

were also created to capture more general response properties: direct and both (includes cells with any direct responses) and any response (includes direct, indirect and both categories). Cells were characterized based on their responses to approximately 10 trials of stimulation at approximately 110% of the minimal intensity necessary to evoke a post-synaptic response. Cells considered to be responsive to the stimulus were those within the 'any response' category and unresponsive cells were those in the 'no response' category. Despite the vast distance (>3mm) between the two regions, direct responses were observed in both regions following stimulation in the reciprocal area. These results provide evidence that direct (mono-synaptic) connections exist in both the feedforward and feedback pathway and these connections are maintained within the sensorimotor slice.

Intrinsic properties of responsive and non responsive cells

Intrinsic membrane and firing properties of both M1 and S1 neurons were assessed identically by quantifying responses to a series of depolarizing and hyperpolarizing step currents of 200 ms duration. Complete data was obtained from the majority of cells recorded from in S1 (31 of 33) and all cells recorded from in M1 (20 of 20). All cells were categorized by their spike pattern according to previously published results (McCormick et al 1985; Agmon and Connors 1989; Kawaguchi 1993, 1995). The majority of cells recorded from in S1 were found to be regular spiking (28 of 31) based on their intrinsic firing properties. A few fast spiking cells were observed (2 of 31) and one cell in this area was intrinsically bursting. A large portion of the cells recorded from in M1 were also found to be regular spiking (RS,

12 of 20). Additionally, low threshold spiking (LTS, 6 of 20) and fast spiking (FS, 2 of 20) cells were also observed in M1. While we are not able to systematically sample from different populations of cells, our sample does contain a variety of cell types that would be expected to be encountered in these two areas based on the published literature (White 1978; Peters and Jones 1984; McCormick et al. 1985; Agmon and Connors 1989; Kawaguchi 1993).

Cells were characterized as being responsive or non-responsive based on their synaptic responses to stimulation in the reciprocal area. Responsive cells are those that had any response to stimulation (direct, indirect or both) and non-responsive cells are those that did not show any response. A large proportion of the cells in S1 (18 of 33) were responsive to stimuli in the reciprocal area as were the majority of cells in M1 (18 of 20).

The majority of regular spiking cells recorded from in S1 (17 of 28) were found to be responsive to stimuli in the reciprocal area (Table 2). Approximately half of these responsive RS cells (9 of 17) showed a direct response. Of the three non regular spiking S1 cells, only one was responsive to M1 stimulation; this cell showed a direct response. Nearly all of the regular spiking cells found in M1 responded to stimuli in S1 (11 of 12), almost all of which were direct responses (10 of 11). The response probabilities of the low threshold cells (5 of 6) and the fast spiking cells (2 of 2) in M1 were also very high. All of the fast spiking cells (2 of 2) and all but one of the low threshold cells (4 of 5) showed a direct response. These results indicate that in both S1 and M1, multiple cell types are responsive to stimuli in the reciprocal area. In the case of M1, regular spiking and non-regular spiking cells had approximately equal

proportions of responsive cells. All cell types in M1 exhibited primarily direct responses. In S1, the majority of cells sampled were regular spiking. A portion of the regular spiking responsive cells in S1 also exhibit direct responses, however the likelihood of encountering a direct RS cell in was higher in M1 compared to S1.

Table 2. Intrinsic firing properties and synaptic responses.

	S1		**M1**	
	Responsive	*Non Responsive*	*Responsive*	*Non Responsive*
RS	17	11	11	1
nRS	1	2	7	1

	S1		**M1**	
	Responsive	*Non Responsive*	*Responsive*	*Non Responsive*
RS	17 *(9)*	11	11 *(10)*	1
IB	0	1	0	0
FS	1 *(1)*	1	2 *(2)*	0
LTS	0	0	5 *(4)*	1

Numbers represent total number of cells within a given category. RS=regular spiking, nRS= non regular spiking, LTS= low-threshold spiking, FS=fast-spiking, IB=intrinsically bursting. Number of direct responses is shown in parentheses.

Intrinsic properties of responsive cells in S1 (n=18) and M1 (n=18) were compared. These comparisons are between all cells in both regions that fell into the any response category, regardless of their morphology (Figure 14). The results are summarized below in Table 3. Responsive cells in S1 had a significantly greater spike amplitude ($t=5.54$, $p<0.01$), input resistance ratio ($U=53$, $p < .01$), and duration of

spike afterhyperpolarization when compared to responsive M1 cells (t= 2.09, p <.05). M1 responsive cells had a significantly greater magnitude of afterhyperpolarization than S1 responsive cells (t=-4.37, p< .01). S1 and M1 responsive cells did not differ significantly on measures of resting membrane potential, spike threshold, spike rise time or slope of the FI curve (Figure 15). These results suggest that within our sample, responsive cells in S1 and M1 are comparable on most intrinsic membrane measures, but differ physiologically in some aspects of their firing properties such as action potential amplitude and AHP dynamics.

Table 3. Intrinsic membrane properties of responsive S1 and M1 cells.

	S1	*M1*
N	18	18
Vm (mV)	-66.42 ± 1.90	-70.70 ± 1.49
AP threshold (mV)	-43.93 ± 1.79	-37.28 ± 4.54
AP amplitude (mV)	87.30 ± 2.89 **	62.50 ± 3.41
AP rise (ms)	4.40 ± 2.45	2.23 ± 0.56
R_{in} Peak (MOhm)	306 ± 24	406 ± 43 †
R_{in} Ratio	1.27 ± 0.04 **	1.21 ± 0.03
FI slope	0.06 ± 0.01	0.07 ± 0.02
AHP magnitude (mV)	9.69 ± 1.35	17.33 ± 1.08 **
AHP duration (ms)	241.19 ± 31.48 *	143.99 ± 34.15

Values reported as means ± SE for cells in S1 and M1 that were responsive to stimuli in the reciprocal area. Statistics were calculated from t-tests. † Indicates a p value of 0.055. Significant group differences are indicated as * where $p < 0.05$ and ** where $p < 0.01$. FI slope= slope of the frequency versus injected current curve; R_{in} ratio = ratio of input resistance measures; AP= action potential; AHP= afterhyperpolarization.

Synaptic properties of the S1-M1 pathway

Once intrinsic properties were assessed for a given cell, electrical stimulation was applied to the reciprocal area via a bipolar electrode (see methods) and any resulting post-synaptic response was recorded. Initial attempts were made using a single pulse of stimulation of moderate stimulus intensity (+5.0 mA). Stimulus parameters were adjusted to achieve a reliable response. If no response was observed following a single pulse, a train of three pulses was then applied, and stimulus frequency was varied (10-100 Hz), to maximize responding. Final parameters were noted and all responses used for analyses are averaged over a minimum of 10 traces to ensure reliability. Direct comparisons between cells are only done for those with identical stimulus parameters.

Overall, M1 cells (18 of 20) were more responsive than S1 cells (18 of 33) to stimulation in the reciprocal area. In addition, cells in M1 (16 of 20) were more likely to have a direct response to stimulation in the reciprocal area than S1 cells (10 of 33).

Cells in S1 had a higher proportion (8 of 33) of purely indirectly responding cells than those in M1 (2 of 20). S1 cells also showed the greatest proportion of non responsive cells (15 of 33) when compared to M1 (2 of 20). The distribution of cells in the any response and no response categories is significantly different between S1 and M1 cells. (χ^2= 7.19, $p<0.01$, Figure 16). These results indicate that cells receiving feedforward input (M1 cells) have a higher synaptic response probability. These cells are also more likely to be directly connected to cells in the reciprocal area.

The differential responsiveness of S1 cells and M1 cells is also evidenced by directly comparing the both the *number* of cells in each area that directly responded to low intensity stimulation (single pulse < +5.0 mA), and the average *magnitude* of the direct responses of these cells (Figures 17-18). Of the 33 sampled S1 cells, only 4 cells showed a reliable direct response to low intensity stimulation in M1 with an average magnitude of 2.62 ± 0.85 mV. Conversely, of 20 M1 cells sampled, 9 cells directly responded to low intensity stimuli with a significantly higher average response of 33.29 ± 8.64 mV ($U = 34$, $p < .05$; Figure 18C)

Significant differences were also observed in the average latency of direct synaptic responses of S1 and M1 cells (Figure 18B). When M1 was stimulated with a single pulse of less the +5.0 mA of current, cells in S1 had an average response latency (time to peak) of 19 ± 0.50 ms. This was significantly faster than the response latency observed in M1 cells when similar stimulation is applied to S1 (106 ± 31 ms; $U = 36$, $p < .01$). Assuming a 3 mm separation between the stimulation site and the recording site (see below) the axons projecting from S1 to M1 (FF) have an average conduction rate (including the synaptic delay) of ~0.03 m/s compared to a speed of ~0.16m/s in the reverse direction (FB). These findings indicate that the feedforward input to M1 from S1 results in a large response which likely results from primarily direct connections. The feedback input to S1 from M1 results in a comparatively smaller response, but occurs with a shorter latency. These results are in agreement with our previous anatomical studies which found significantly smaller axon diameters in the feedforward pathway which may provide one explanation as to why this pathway appears to have longer response latency.

Laminar location of recovered cells

Given the limited area of potential recording sites within each section and the physical limitations of the recording setup (see *direct connections* section above) we were unable to systematically target cells by their laminar location in our experiments. However, the laminar position of these cells was of interest to us, as previous studies have shown variability in the laminar distribution of feedforward vs. feedback cells (Rockland and Pandya 1979; Rockland and Virga 1989, 1990). To obtain this information, we measured the relative location of recovered cells in S1 and M1, and when possible, used this information to examine the relationship between synaptic connectivity and position within the cortical plate.

Morphological data (including laminar location) were collected for each of the recovered cells. Laminar locations of cell bodies were determined in S1 (21 of 33) and M1 (14 of 20). For all recovered cells, measurements were made to determine the cells' relative location within the cortical plate. It was determined post-hoc that the average distance between the stimulating electrode and the cell recorded from was 2.97 ± 0.17 mm across all experiments (n=35). This is consistent with our previous measurements collected during anatomical experiments where M1 and S1 were physiologically confirmed. Since there is currently no good indication of the laminar distribution in this plane of section, we measured the location of the barrels within the cortical plate and used this measure as a reference point in determining the relative cell depths. Cell locations are reported as the relative location of the soma where the

white matter border is 0 and the pial surface is 1. The distributions of cells within the cortical plate for S1 and M1 can be seen in Figure 19.

On average, the barrel region within the S1 portion of the sensorimotor slice occupied from 0.40 to 0.60. Based on this approximation, the cells whose somas lie within this region in S1 will be considered to be within layer 4. Cells whose somas are below 0.40 will be considered infragranular and those above 0.60 will be considered supragranular. The majority of cells recovered within S1 (15 of 21) were in the infragranular layers, followed by cells in layer 4 (5 of 21) and only one of the recovered cells in S1 was located in the supragranular region. The majority of these cells (14 of 21) could be accurately paired with their synaptic response type.

For measurements in M1, we divided the cortex into three equal parts, lower third (0-0.32), middle third (0.33-0.66) and upper third (0.67-1.00). The lower third will be considered the infragranular layers and the upper third will be referred to as the supragranular layers. The majority of recovered M1 cells (11 of 14) were in the infragranular layers (lower third). The remaining M1 cells (3 of 14) were in the middle third. All 14 of the recovered cells in M1 could be matched with their synaptic response type. For both S1 and M1 the probability of finding a post-synaptic response following stimulation in the reciprocal area was higher in the infragranular layers, which was consistent with the termination patterns of the axonal projections.

Morphological categorization of recovered cells

The majority of cells recorded from in M1 (14 of 20) were recovered, most of which (11 of 14) were able to be reconstructed. A large proportion of the S1 cells recorded from were also recovered (21 of 33), most of which (16 of 21) were also able to be reconstructed. Of the 16 fully reconstructed cells in S1, 15 had pyramidal cell bodies. Of the 11 cells recovered from M1, 4 were pyramidal in shape and 7 were nonpyramidal (Table 4).

Table 4. Quantitative cell body measurements for S1 and M1 cells.

	S1 Pyramidal	*M1 Non-Pyramidal*
n	15	7
Perimeter(μm)	50.93 ± 10.84	45.58 ± 6.84
Area(μm²)	164.91 ± 68.79	128.10 ± 31.90
Feret Max (μm)	16.88 ± 3.44	16.13 ± 3.18
Feret Min (μm)	12.87 ± 2.77	10.92 ± 1.68
Aspect Ratio	1.32 ± 0.13	1.50 ± 0.37
Roundness	0.72 ± 0.08	0.65 ± 0.16

Values reported are the means ± SD for recovered cells.

Of the 16 reconstructed cells in S1, 9 could be matched with their synaptic response types. All 11 of the reconstructed M1 cells could be paired with their synaptic response types (Table 5).

Table 5. Soma morphologies of identified responsive and non responsive cells.

	S1		**M1**	
	Responsive	*Non Responsive*	*Responsive*	*Non Responsive*
Pyramidal	6	2	4	0
Non Pyramidal	1	0	5	2

Responsive cells did not appear to be restricted to a particular morphological cell type. Unfortunately, due to our small sample of recovered cells, we are unable to determine any patterns of responsiveness based on soma characteristics.

Nearly half of the recovered cells in S1 (9 of 21) and more than a third of the cells recovered in M1 (5 of 14) could be paired with their intracellular recordings. For these cells (n = 14) the intrinsic, synaptic and morphological properties are known (Table 6a, b; Figure 20).

Table 6a. Morphological and physiological properties of identified S1 cells.

Experiment	*Location*	*Shape*	*Firing*	*Synaptic*
070502A	Infragranular	Pyramidal	RS	Indirect
070502C	Granular	Pyramidal	RS	Indirect
070503A	Infragranular	Non-Pyr	FS	Direct
070503B	Infragranular	Pyramidal	RS	Indirect
070503C	Infragranular	Pyramidal	RS	Direct
070503D	Infragranular	Pyramidal	RS	Indirect
070503E	Infragranular	Pyramidal	RS	Both
070502B	Granular	Pyramidal	RS	None
070502D	Infragranular	Pyramidal	RS	None

RS= regular spiking; FS= fast spiking.

Table 6b. Morphological and physiological properties of identified M1 cells.

Experiment	*Location*	*Shape*	*Firing*	*Synaptic*
080128A	Middle Third	Non-Pyr	RSNP	None
070128B	Lower Third	Non-Pyr	LTS	None
070128C	Middle Third	Pyramidal	RS	Indirect
070128D	Lower Third	Non-Pyr	RS	Both
070128E	Lower Third	Non-Pyr	LTS	Indirect

RSNP= regular spiking, nonpyramidal; LTS= low-threshold spiking; RS= regular spiking.

Due to the fact that our sample of recovered cells is small and we did not use any unbiased techniques in selecting them, we are unable to make many inferences about these populations as a whole. We have, however, clearly determined that direct responses occur in both the feedforward and feedback pathway. It is also evident based on our results that these direct responses do not appear to be restricted to a particular cell class or morphological subtype, which may be different from the pattern observed in the visual system (Shao and Burkhalter 1996).

Summary of Experiment II

Many studies have used *in vitro* preparations to investigate cortical connectivity (Agmon and Connors 1991; Shao and Burkhalter 1996). This is the first *in vitro* study using whole cell recording techniques to quantify connections between S1 and M1. Despite the large distance separating the whisker representations in S1 and M1, we can conclude that direct connections exist in both the feedforward and feedback pathway within the sensorimotor pathway in the rodent. The results of this

study indicate that the sensorimotor slice is a viable method for studying the functional connections between whisker representations in S1 and M1 in the mouse.

In our initial extracellular studies of the sensorimotor pathway, we determined that the synaptic connections observed between S1 and M1 are predominately glutamatergic and that antidromic activity is not responsible for the resulting field potentials. More detailed whole cell recordings revealed that multiple cell types in S1 and M1 are responsive to stimuli in the reciprocal area. The majority of the cells sampled from in both areas were regular spiking. Overall, the M1 cells sampled were more diverse than those found in S1 in terms of their cell morphology and intrinsic firing properties. In comparing intrinsic firing and membrane properties of responsive S1 cells to responsive M1 cells, some significant differences were observed, however, these differences do not sufficiently explain the differential synaptic responses observed in the FF and FB pathway.

For both pathways the probability of finding a post-synaptic response following stimulation in the reciprocal area was higher in the infragranular layers which is consistent with the observed termination patterns of the axonal projections. In our sample of cells receiving feedforward input (M1 cells) there was a higher likelihood of a synaptic response as well as a greater probability of observing a direct connection. Comparisons of synaptic responses of responsive S1 and M1 also revealed significant differences in the latency and magnitude of the postsynaptic EPSP. In comparing synaptic responses under identical stimulation conditions, feedforward input from S1 to M1 resulted in significantly larger responses, but with significantly longer latencies than feedback responses. These results are in agreement

with our previous anatomical studies which found significantly smaller axon diameters in the feedforward pathway which may provide one explanation as to why this pathway appears to have longer response latencies. Paired-pulse experiments suggested that facilitation is more likely to occur in the feedback direction (M1 to S1).

General Discussion

These data provide the first *in vitro* evidence indicating that a direct reciprocal axonal pathway exists between whisker sensory and motor cortices. With the use of the sensorimotor slice, we have shown that direct single cell responses can be recorded in both S1 and M1 in response to stimulation in the reciprocal area. The results of this study indicate that sensorimotor feedforward (FF) feedback (FB) circuits vary in their response to pathway stimulation. This novel preparation provides a useful tool for future studies of sensorimotor integration and cortical connections in general.

We have characterized the reciprocal axonal pathway that transverses the infragranular layers between S1 and M1. These axons differ morphologically in that the FB axons (M1 to S1) are significantly larger than the axons comprising the FF pathway. The projections of the FB pathway appear to preferentially target S1 as there is a greater bouton density there than within the pathway itself. Whole-cell recordings in both areas reveal that direct projections exist in both directions (FF and FB). Synaptic responses to stimuli in the reciprocal area vary by location. Stimulation of the FB pathway resulted in a smaller response than stimulation of the FF pathway; however, the FB response occurred at a shorter latency.

The rodent whisker model

Rodents use their whiskers to gain information about their environment through a process known as whisking (Welker 1971). Through this process these

animals can capture details about a surface or object similar to how we use our hands for tactile discrimination (Guic-Robles et al. 1989; Carvell and Simons 1990). Tasks such a tactile discrimination are reliant on sensorimotor integration. While this process seems to be essential to the survival of many species, the details of how it occurs is still largely unknown. The rodent whisker barrel system provides an ideal model in which to study this process.

The barrel cortex of the rodent has been extensively studied and well-defined. The topographic arrangement of the mystacial whisker pad within layer IV of the primary somatosensory cortex (S1) reveals a one-to-one correspondence between each barrel and its corresponding (principal) whisker (Woolsey and Van der Loos, 1970; Welker 1971; Simons 1978). Within the barrels there are structured circuits that define how individual cells within this region will respond to stimuli. The barrel cortex exhibits a columnar organizational pattern whereby cells in the extragranular layer surrounding a barrel will be preferentially activated by that same barrels principal whisker (Simons 1978, 1985; Brumberg et al. 1996). Between each barrel lies an area known as the septal region. This area is not as widely studied as the barrels themselves, but it is thought that this region comprises a separate circuit within the same cortical area (Alloway et al. 2004, 2008). In support of this hypothesis, anatomical studies have shown that separate afferent pathways convey sensory information to these two regions (Woolsey and Van der Loos 1970; Koralek et al. 1988; Lu and Lin 1993 Figure 2). While the barrels receive most of their thalamic afferents from the ventral posterior medial (VPM) nucleus, the septal regions receive dense inputs from the medial part of the posterior (POm) nucleus.

Additionally, there are distinct projections originating from neurons aligned with the layer IV septa (i.e., septal columns) that terminate in brain regions associated with the motor system; however there are no distinct projection systems that originate from the barrel columns (Welker et al. 1988; Alloway et al. 1999)

There are functional differences that differentiate the barrel and the septal circuits as well. It is thought that barrel columns are important for encoding spatial (Harvey et al. 2001; Krupa et al. 2001; Arabzadeh et al. 2005) and temporal (Ahissar 1998, 2000) stimulus properties, while septal circuits process information about the rate of whisker movements (Melzer, Champney et al. 2006; Melzer, Sachdev et al. 2006). While these circuits are distinct they must communicate in order for sensorimotor integration to occur. The precise neuronal mechanism underlying this communication remains unclear.

The functional organization of the rodent motor cortex has also been widely investigated. While a topographic map exists in the motor cortex of the rodent as well, it does not appear to be as well-defined as what is observed in the somatosensory cortex (Donoghue and Wise 1982; Li and Waters 1991). One distinct feature of motor cortical neurons is their long, horizontal branches. An *in vitro* study using sagittal and coronal sections of the motor cortex of rats found that axon collaterals in layer III project horizontally within that layer for distances greater than 1.5mm. Cells in layer V were also found to have long, horizontal and oblique axon collaterals, but these cells have a more extensive terminal field, extending to layers II-V (Aroniadou and Keller 1993).

Anatomical studies have shown that direct, reciprocal connections exist between the primary motor and primary sensory cortical areas in the rodent (White and DeAmicis 1977; Porter and White 1983; Miyashita et al. 1994; Israeli and Porter 1995; Hoffer et al. 2003; Alloway 2008). The cell bodies of corticocortical efferents from S1 to M1 are located primarily in layer V and also in upper layer VI (Israeli and Porter 1995). These cells terminate throughout the cortical plate in M1 (Hoffer et al. 2003). A similar study found that most of the cells in M1 projecting to S1 are in layers II/III and V (Porter and White 1983). These cells terminate in every layer but layer IV in S1 (Miyashita et al. 1994).

These connections between S1 and M1 are somatotopically organized. Retrograde labeling experiments targeting individual whisker regions in M1 have shown that the S1 representation of a whisker is morphologically connected to the same whisker representation in M1, though some degree of overlap between surrounding whiskers is present (Porter and White 1983; Miyashita et al. 1994). The overlapping projections from S1 to M1 facilitate integration of information of barrels that are within the same row (Hoffer et al. 2003). Cells projecting to M1 from S1 are vertically aligned with septa above and below layer IV (Alloway et al. 2004). Cells projecting from M1 to S1 follow a columnar arrangement as well, but the highest density of cells appears to be within layer V within the rodent (White and DeAmicis 1977; Veinante and Deschenes 2003).

The neocortical loop between S1 and M1 provides a good model in which to study feedforward and feedback circuitry. The rodent sensorimotor system is a particularly advantageous model system as the behavior (whisking) is largely a one-

dimensional movement that can be easily and accurately quantified. However, many of the past and present studies investigating these types of interactions are based on studies of the visual system. While these types of interactions are known to occur within the sensorimotor system as well, the study of these interactions has been limited by physical distance between these two areas and the lack of an existing preparation in which to study their intracortical pathway.

In vitro preparation

In general, *in vitro* models provide a useful method in which to study the details of cortical circuitry. This method enables the study of individual cell responses and allows for detailed characterization of these neurons. Several methods have been utilized to define the connections between the sensory and motor cortices in rodents. Anterograde and retrograde tracers have been used to identify the projections and targets of these cells. The laminar location of these projections can be determined through traditional coronal sectioning. In the case of the somatosensory cortex, the location of these cells in relationship to the barrels and septa can be quantified by making tangential sections of the flattened cortex to reveal the barrel field. To some extent, the processes of these cells can also captured and analyzed, but usually this is limited to a small distance because most of the axons in this pathway are transected using traditional slicing methods. The sensorimotor slice is the only current preparation that allows for quantifiable visualization of the axonal pathway between S1 and M1.

In terms of defining connectivity an advantage of *in vitro* methods over *in vivo* is that they allow for the investigation of activity in the infragranular layers. Methods such as calcium dye imaging are only capturing activity that is occurring within the supragranular layers. While this information is useful, it does not take into account the connections that are occurring at the infragranular level, which have shown to play a large role in intracortical connections in the rodent (Porter and White 1983; Israeli and Porter 1995). Finally, while sensorimotor integration occurs at multiple levels of the neuroaxis (brainstem, thalamus, and cortex), the fast response that is observed is likely due to the direct connections observed between the sensory and motor cortical areas (Kleinfeld et al. 1999). These responses most likely play the largest role in guiding fine dexterous movements (Guic-Robles et al. 1992). An *in vitro* neocortical sensorimotor slice allows for the direct investigation of this circuit.

A reciprocal infragranular pathway

Previous studies have shown that a reciprocal axonal pathway exists between the whisker areas of S1 and M1 (Porter and White 1983; Israeli and Porter 1995). These studies have reported on the laminar location of the cells projecting between these regions, but little attention has focused on the actual axonal pathway due to the aforementioned methodological constraints. Our novel slice preparation allows for the first time these axons to be visualized throughout the entire length of the pathway. A recent *in vivo* study utilized fluorescently labeled lentivirus to visualize the projections of the barrel cortex (Ferezou et al. 2007). Through this method the axonal connections can be visualized throughout the pathway and their results are in

agreement with our findings that axons from S1 extend the entire 3 mm distance to M1 resulting in a direct connection between these two areas.

Due to the fact that FF and FB connections carry out different functions within central nervous system, it is of interest to determine if they also vary morphologically. Quantification of FF and FB axons has been performed in the visual system of primates and rodents. One caveat is that intracortical connections in the primate are primarily achieved through layers II/III, while in the rodent they appear to primarily utilize layer V (Jones et al. 1975). Another relevant point is that most quantification of FF and FB pathways has been achieved by studying connections within the visual system (primary visual cortex, secondary visual cortex and middle temporal cortex). The factors governing these intrinsic connections may vary somewhat from those of extrinsic connections (e.g. sensory to motor).

Most studies report that FF projections originate in the suprgranular layers and terminate in layer IV while FB projections originate in the infragranular and supragranular layers and terminate outside of layer IV. It does not appear that the FF and FB pathways within the sensorimotor system follow the prototypical patterns of these pathways (based on studies of the visual system; Figure 1). This may in part be due to the fact that they are extrinsic connections and laminar distribution of cells is not identical under these conditions. Even within the visual system, variability has been observed in the laminar distribution of feedforward and feedback connections. Reciprocal connections between the primary visual cortex (V1) and the secondary visual cortex (V2) of primates follows the pattern shown in Figure 1, while reciprocal connection between V1 and the middle temporal cortex (MT) primarily utilize layers

IVb and VI (Lund et al. 1976; Weller and Kaas 1983). This suggests that the pattern of FF and FB projections may be area specific to some extent. In general, there is some debate over the laminar distribution of FF and FB pathways and the consensus is that it appears to be less orderly in rodents than in primates (Nowak et al. 1997, Coogan and Burkhalter 1993).

While previous studies have not traced the entire axonal pathway between S1 and M1, they have noted the location of the axons as they enter and exit the target areas. These studies report observing a horizontal axon pathway extending through the deep infragranular layers (White and DeAmicis 1977; Israeli and Porter 1995). Our finding of an infragranular, reciprocal axonal pathway between S1 and M1 is in agreement these studies and with others indicating that cells responsible for long-range connections between the primary motor and sensory areas reside in these layers within the rodent cortex.

Our results indicate that the axonal diameters of the FB pathway (M1 to S1) are larger than those of the FF pathway (S1 to M1). Axonal diameters of FF and FB pathways have also been measured within the primate visual system. In primates the axons comprising the FF and FB connections between V1 and V2 do not differ significantly in their axonal diameters (Rockland and Virga 1989, 1990). Several factors may account for this discrepancy. The relative distance between V1 and V2 is much smaller than that of S1 to M1. It may be the case that long range connections have different properties than those extending a shorter distance. As stated above, extrinsic FF and FB connections may have different properties than connection that are intrinsic. Finally, it may be related to the cell types that comprise these

connections. Given the extent of layer V in the motor cortex, it is probable that axons contributing to the FB pathway are extending from the large pyramidal cells are typically observed in this layer. These axons are likely to be larger than those of the typical pyramidal cells found in the somatosensory cortex which may account for their larger axonal diameter (Rockland 1995).

In addition to the existence of an infragranular axonal pathway, we have also found that infragranular cells in S1 and M1 receive direct input from one another. These results do not imply that direct connections between these areas do not exist in other layers however, as we primarily targeted cells in the infragranular region. Within our sample, we did find a greater likelihood of a direct connection within the infragranular layers. These results should be interpreted with caution as we did not systematically target specific layers within each area, but it is likely that layer V cells in both areas play a large role in the direct sensorimotor pathway in the rodent given the results of previous anatomical studies (White and DeAmicis 1977; Israeli and Porter 1995).

Sensorimotor feedforward and feedback responses differ in timing and magnitude

In both feedforward and feedback directions, direct, presumably monosynaptic responses were observed. These results are in agreement with what is known in the rodent visual system (Shao and Burkhalter 1996) and in the sensorimotor system (Keneko 1994; Porter 1996). Our results differ from previous studies of the dynamics of FF and FB connections in several ways. The latency of our responses is longer than what would be expected based on reported *in vivo* conduction velocity studies (Kelly et al. 2001). *In vivo* studies suggest that M1

responses to S1 stimuli occur on average within 8 ms based on subthreshold voltage changes in the supragranular layers (Ferezou et al. 2007). Our latency is approximately 10 fold higher, which is likely due to the fact that we are using an *in vitro* preparation which is not maintained at 37^{o}C as the *in vivo* condition.

We have also observed relative differences in conduction rates for FF and FB connections, which has been previously been found in the rodent visual system, but not in primates (Girard et al. 2000). Our findings are in agreement with the previous results showing longer conduction times for the FF pathway. Our observed differences in conduction time were correlated with differences in the axonal diameters as well. The conduction speed is consistent with our axonal diameter results in that the larger diameter axons (M1 to S1) relayed information faster.

Our results agree with previous findings indicating differences in magnitude in FF and FB connections. FF connections appear to be stronger than FB. In an *in vitro* preparation of rodent cortex containing V1 and V2, FF connections to V2 result in significantly larger amplitude EPSP's than those resulting from FB connections (Shao and Burkhalter 1996). One explanation for these results may be the density of the projections between the two areas. Feedback inputs to area 17 in V1 of the rodent are about 50% less numerous than forward inputs to LM (the rat homology of V2, Shao and Burkhalter 1996). Similarly, significantly smaller projections were observed in the FB from M1 to V1 when compared to the FF direction (Maunsell and Van Essen 1983). Anecdotally, we have observed this as well, and this may account for the difference in magnitude (Figure 6).

Some differences in intrinsic properties were observed when comparing S1 responsive cells to M1 responsive cells. These differences in firing properties are reflective of the fact that the population of cells sampled from was not homogeneous. The sample of S1 cells was primarily pyramidal while the M1 cells were a mixture of pyramidal and nonpyramidal. The differences in input resistance ratios are likely due to the greater presence of an inward rectifying (I_h) current in the S1 cells due to the fact that these cells are mostly layer V pyramidal cells. When we quantified the 'sag' of these neurons the S1 neurons had greater 'sag' then the M1 neurons (Spain, Schwindt and Crill 1987). In general the observed differences in firing properties between these groups did not correlate with the differences observed in synaptic properties.

Previous studies have shown that FF and FB connections are made predominately by pyramidal cells that use glutamate (Johnson and Burkhalter 1996). However, differences have been observed in the proportion of pyramidal vs. nonpyramidal cells between these two pathways. In the rodent visual system, FF and FB pathways make monosynaptic connections to pyramidal and GABAergic interneurons. In the FF pathway 10% of synapses are made onto GABAergic cells, while in the FB only 2% of the cells synapse on GABAergic targets (Johnson and Burkhalter 1996). Similarly, we found a greater proportion of nonpyramidal cells in M1 (FF) compared to S1 (FB). While we can not confirm that these are in fact GABAergic interneurons, their shape and intrinsic properties imply that there is a greater probability that they are not excitatory neurons. In contrast to the Burkhalter studies (Shao and Burkhalter 1996) which showed an EPSP typically followed by an

IPSP, we did not see any IPSPs.). The results of our paired-pulse experiments indicate that FF and FB information is not processed in the same way within the sensorimotor system. The facilitory response of the FB pathway may be in part reflective of differences in the cortical circuitry of these regions.

Functional relevance: Whisking dynamics

Rodents generally exhibit two types of whisking: exploratory and discriminative (Welker 1964; Gao et al. 2003). Exploratory is rhythmic whisking that occurs in the absence of stimulation. However, whisking patterns change (bilateral synchrony, amplitude, etc.) when in contact with surfaces (Welker 1964, Carvell and Simons 1990). These adaptive changes are what allow rodents to discriminate between objects in their environment and provide a basic example of sensorimotor processing.

Many studies have attempted to determine the role of sensory and motor processing in whisking dynamics. Exploratory whisking appears to reflect the output of a central pattern generator as it persists even in decerebrated rats (Lovick 1972; Cramer et al. 2007). This idea is supported by results indicating that bilateral deafferentation of whiskers does not affect the generation, patterning or bilateral coordination of exploratory whisking (Gao 2001). Large-amplitude, exploratory whisking is also undisturbed by ablation of the motor cortex (Welker 1964). More detailed studies of unilateral ablation have shown discrete deficits in whisking behavior. Unilateral ablation of the cortical barrel field resulted in amplitude differences between the right and left side of the face (Harvey et al. 2001), while

unilateral ablation of motor cortex produced a bilateral shift in whisking frequency and an increase in both the amplitude and velocity of whisker protractions contralateral to the lesion (Gao et al. 2003). These types of changes which disrupt the balance of whisking dynamics have been shown to cause impairments on tasks of discrimination that involve sensorimotor integration (Guic-Robels et al. 1992).

It appears that M1 responses to whisker stimuli are dependant on S1 processing. Significant reductions have been observed in M1 stimulus-evoked responses following inactivation or ablation of S1 (Asanuma et al. 1980; Farkas et al. 1999). *In vivo* calcium imaging has shown that a single, brief whisker defection results initially in a strong depolarization in S1 followed by motor cortex depolarization. While S1 is not necessary to produce whisking, the FF projections that are sent to M1 are important in regulating whisking dynamics. The role of FB projections are generally not well understood. In the whisker pathway, they may serve to synchronize firing of cells that respond to similar stimuli as seen in the visual system (Sillito et al. 1994). In general this process would serve to focus the activation such that only a specific subset of cells would be excited. This distinct activation could then cause an alteration of whisker movements that would allow for better discrimination. These results highlight the fact that while S1 and M1 likely play distinct roles in sensorimotor processing, both cortical regions are necessary in order to make fine-tuned discriminations.

Recent studies have shown that responses to whisker stimulation appear to be context-dependant and may vary based on the behavioral state of the animal. *In vivo* barrel cortex responses to a passive whisker defection were more robust when the

animal was in a quite wakeful state (non-whisking) than when the animal was already actively whisking. Active whisker contact of real objects during exploratory whisking also produced robust responses (Crochet and Peterson 2006; Ferezou et al. 2007). The way that stimuli are transformed under these different conditions is likely the result of subcortical processing within the sensorimotor loop. It has recent been suggested that the zona incerta (ZI), through its connections to the posterior nucleus of the thalamus (Po), may play a role in gating this state-dependant activity (Urbain and Deschenes 2007).

A proposed circuit

The neocortical circuit connecting S1 and M1 represents one part of a much larger loop that is responsible for sensorimotor integration in the whisker pathway. While the details of the entire pathway is still unknown, recently physiological and anatomical data have shed light on what areas are likely involved. As seen in Figure 21, there are presumably many targets involved in this pathway throughout the neuroaxis. These stages of processing are likely occurring on various timescales as not all information is processed at the same speed within the nervous system (Swadlow and Weyand 1981). The cortical component of this pathway is presumed to be the fastest and is most likely responsible for the rapid updating of motor output in response to sensory stimuli.

Our findings indicate the FF and FB pathways of the sensorimotor system have different neuronal targets. While we did not reliably observed any IPSP's in either location, there were a greater number of cells in M1 that were likely to be

inhibitory based on their physiological and morphological characteristics. It appears that FB connections (M1 to S1) target almost exclusively excitatory pyramidal cells, while FF connections likely target excitatory and inhibitory cells (Figure 22). This finding is in agreement with observations in the rodent visual system (Johnson and Burkhalter 1996). The absence of IPSPs in our experiments could be due to multiple factors. The most likely contributing factor is likely the degree of synaptic connectivity maintained within the sensorimotor slice. While we are aware that the infragranular pathway is maintained within this plane of section, we do not know how cutting at this angle affects local cortical connections. Additionally, the overall proportion of GABAergic cells targeted by the FF connections is likely to be small; in the visual system it is estimated to be only 10% (Johnson and Burkhalter 1996). This further limits the likelihood of our recordings targeting a cell that is connected to one of these cells given our limited viable sampling areas.

Final remarks

Sensorimotor connections are crucial to an animal's ability to consistently update its motor plan in response to changes in sensory input. While this fundamental pathway is known to exist, the details of its location and structure have yet to be quantitatively defined. A hindrance to the study of this pathway has been the relative location of its endpoints and the lack of an existing preparation that allows for quantitative investigation of its connectivity.

Our results indicate that there are morphological and physiological differences observed in the FF and FB pathway of the sensorimotor system. These differences are

likely reflective of the different functions that are carried out by these two stages of processing. These data show that the direct, monosynaptic connections and the axonal pathway between S1 and M1 are preserved within the sensorimotor slice. This preparation provides a useful tool to study sensorimotor integration and cortical connections in general.

Figures

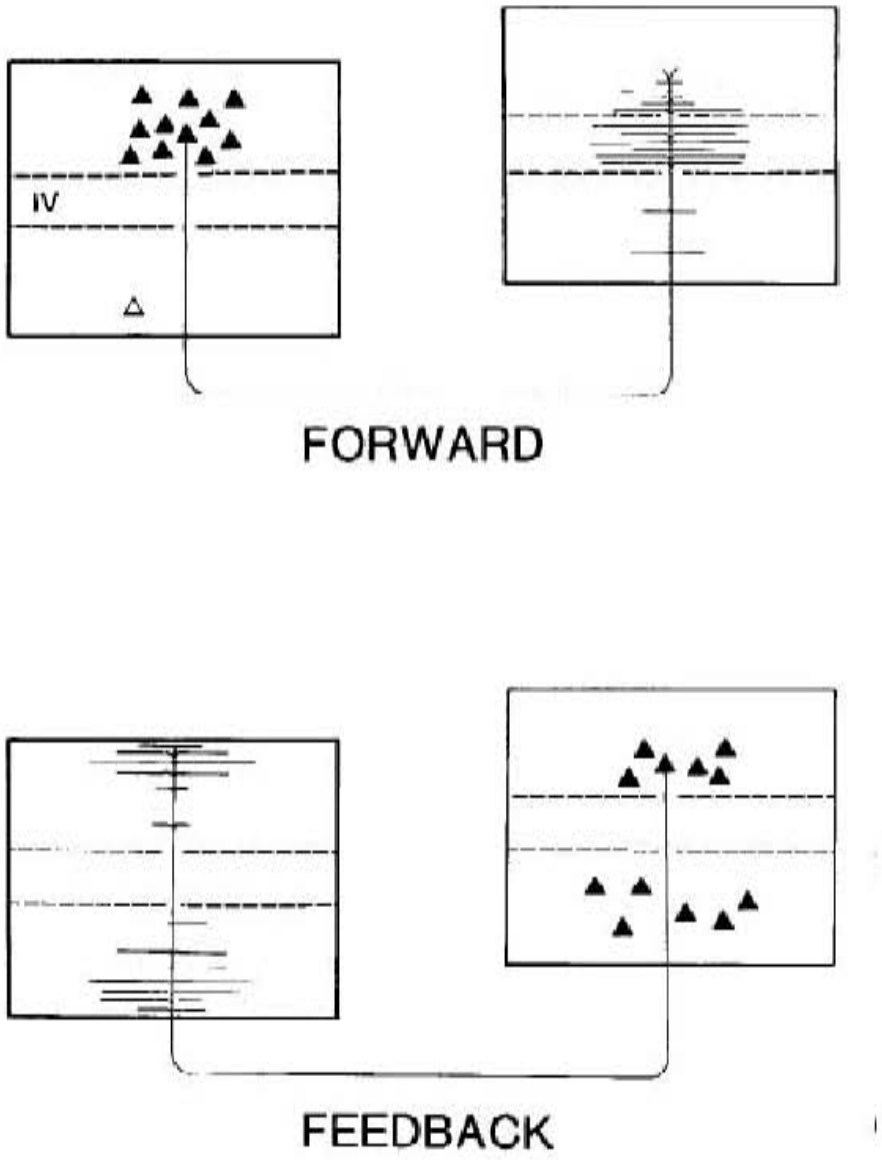

Figure 1. Laminar distributions of cell bodies and terminals in feedforward and feedback pathways as depicted by Maunsell and Van Essen 1983. Feedforward pathways originate mainly in superficial layers and terminate in layer 4. Feedback pathways originate in superficial and deep layers and usually terminate outside of layer 4.

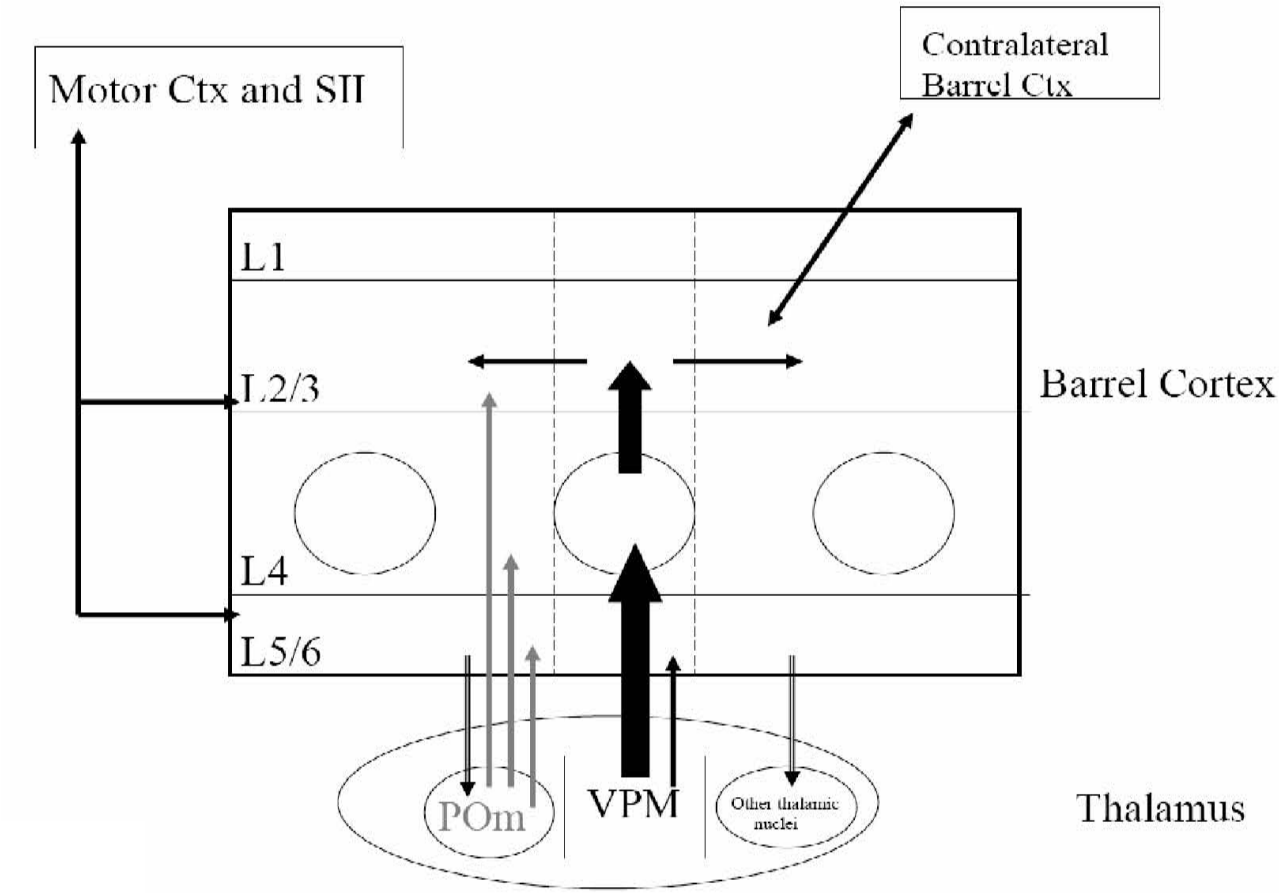

Figure 2. Input-output organization of the rodent barrel cortex. Neurons within the ventral posterior medial (VPM) nucleus of the thalamus project to layer 4, the primary somatosensory cortex, where they terminate in somatotopically organized clusters known as barrels. These cells also terminate in a less-dense manner in layers 5/6. The posterior medial nucleus (POm) of the thalamus also projects to the primary somatosensory cortex. These cells terminate mainly in the area between the barrels within layer 4 (known as the septa), as well as layers 2/3 and 5/6. The majority of intracortical processing occurs within layers 2/3 and 5, with dense reciprocal connections between the contralateral barrel cortex, the primary motor cortex and the secondary somatosensory cortex (SII).

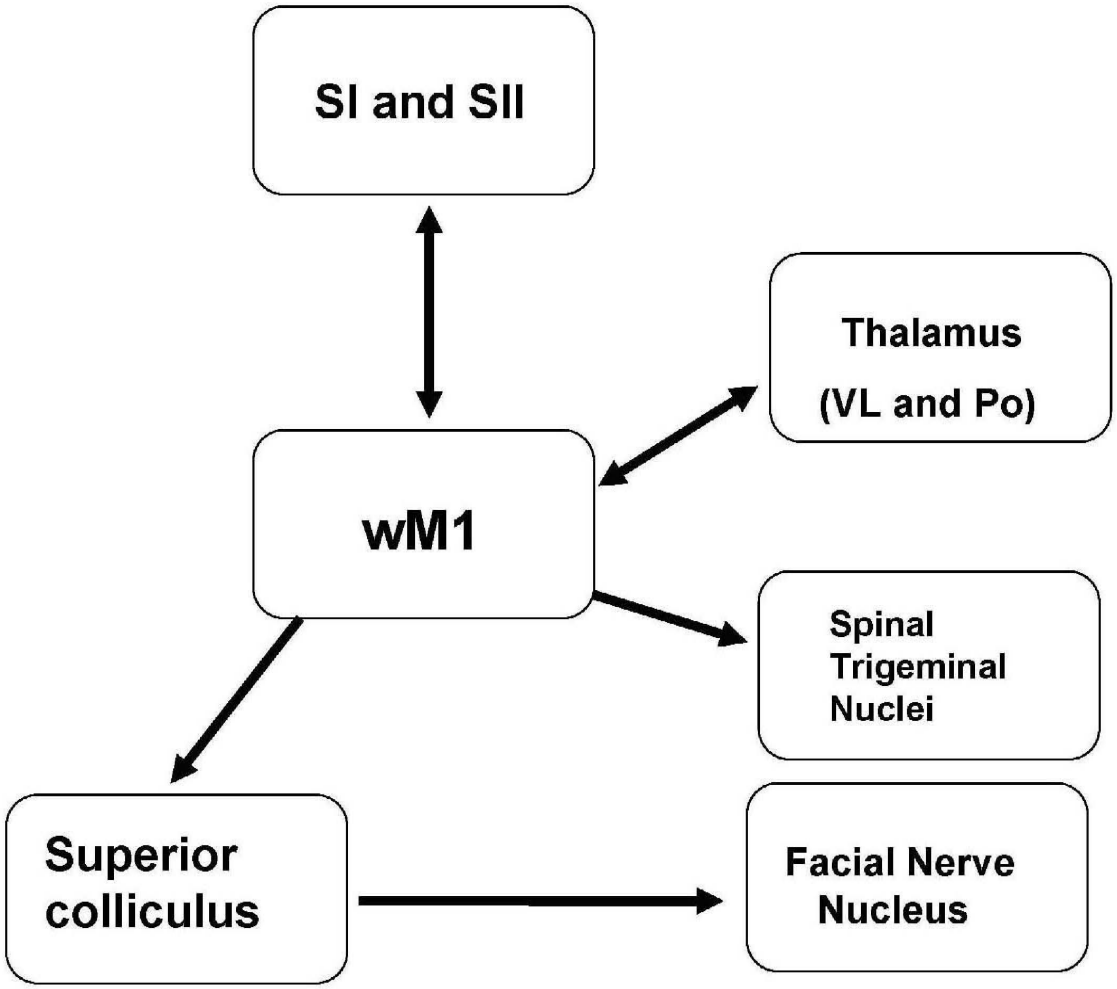

Figure 3. Input-output organization of the vibrissa area of the motor cortex. The vibrissa region of the motor cortex is reciprocally connected to the primary and secondary somatosensory cortices as well as the ventrolateral (VL) and posterior (Po) nuclei of the thalamus. This area also sends projections to the superior colliculus and the spinal trigeminal nuclei. Figure adapted from Miyashita et al. 1994.

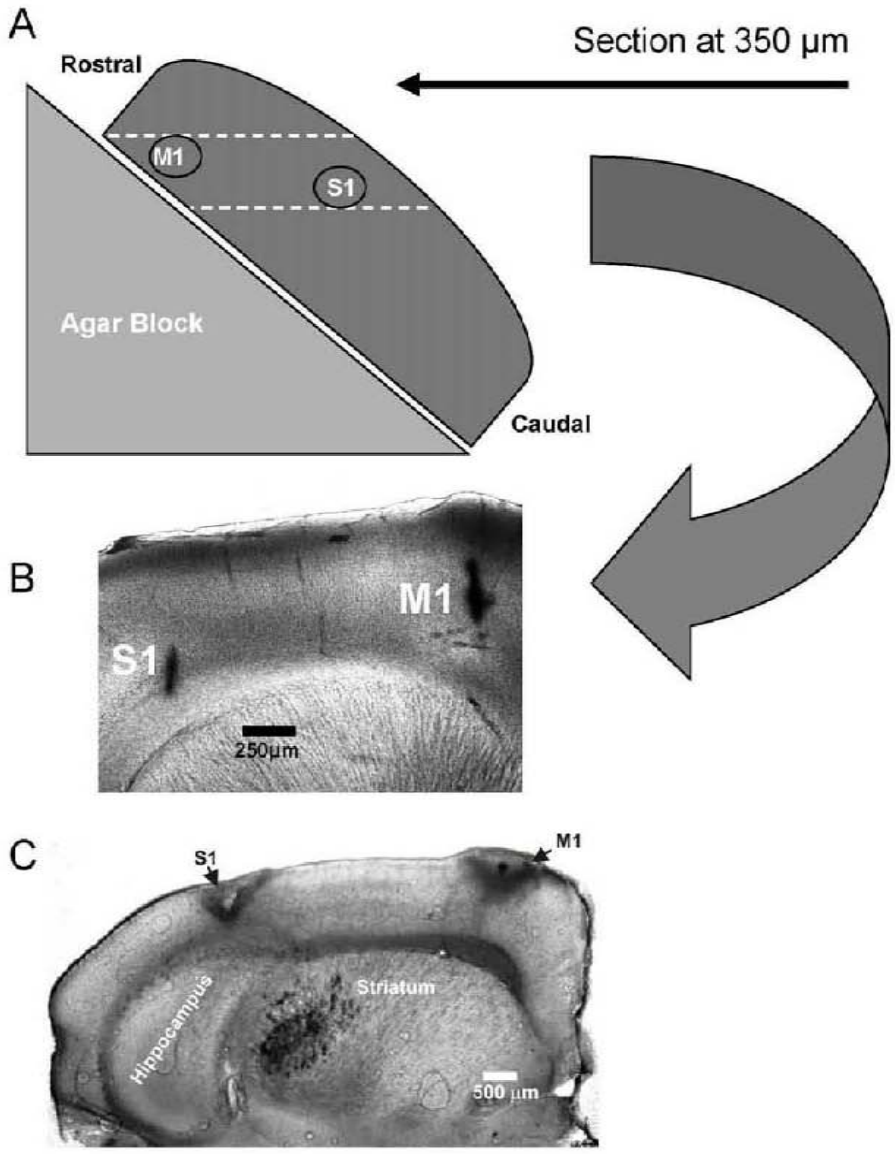

Figure 4. The sensorimotor slice. (A) The position of the injected hemisphere in the vibratome when creating the slice. 350 µm sections are cut at a 45° degree angle relative to the midline. (B) An example of the sensorimotor slice where cresyl violet was injected in vivo into whisker M1 and whisker S1; note that both injection sites are recovered in the same plane of section. (C) A low magnification image of the sensorimotor slice with prominent subcortical areas labeled.

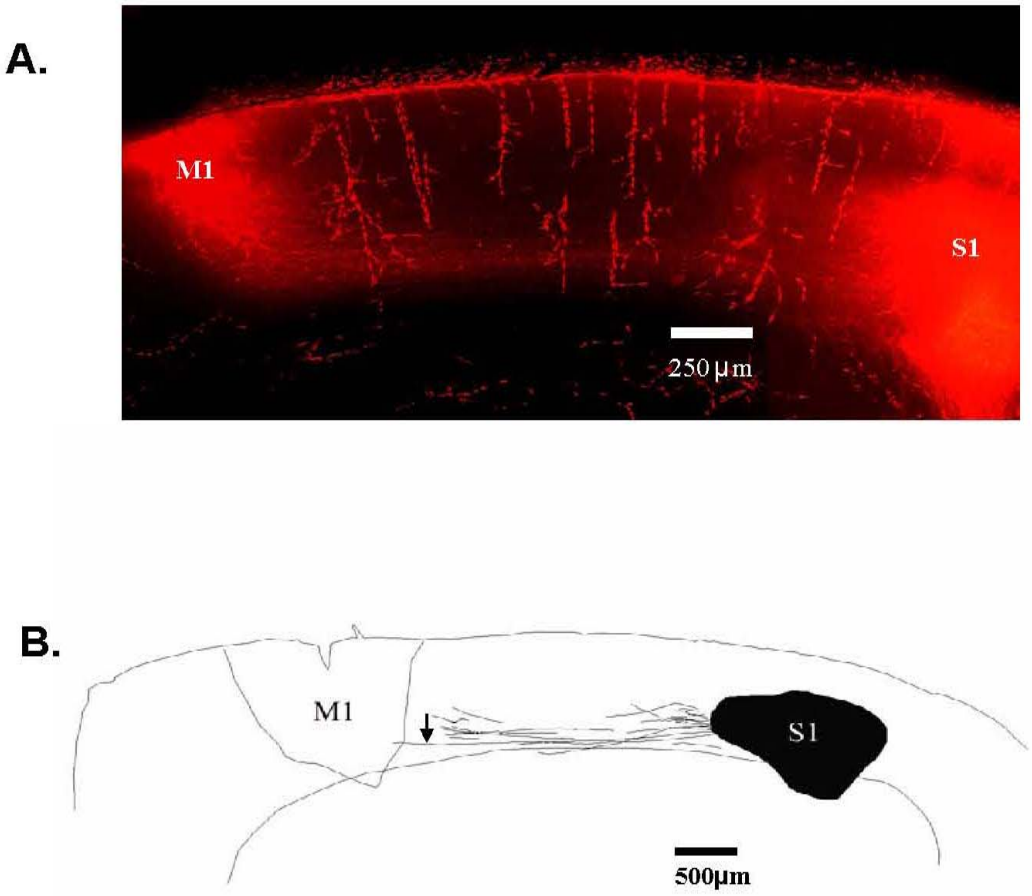

Figure 5. Visualization of the sensorimotor pathway. (A) Anterograde axon labeling observed two days after an injection of flouro-ruby conjugated biotinylated dextran amine in whisker S1. (B) A Neurolucida reconstruction of the sensorimotor slice illustrating the S1 to M1 axon pathway in a BDA injected animal. Whisker S1 and M1 were injected *in vivo* within the same animal. An injection of BDA was made in whisker S1 and cresyl violet was injected into whisker M1 to serve as a marker. Both injection sites are traces as well as the pial surface and white matter border. Horizontal lines represent all visible anterogradely labeled axons that were traced within this section. Note that axons can be traced from the injection site (S1) to the projection site (M1) (arrow).

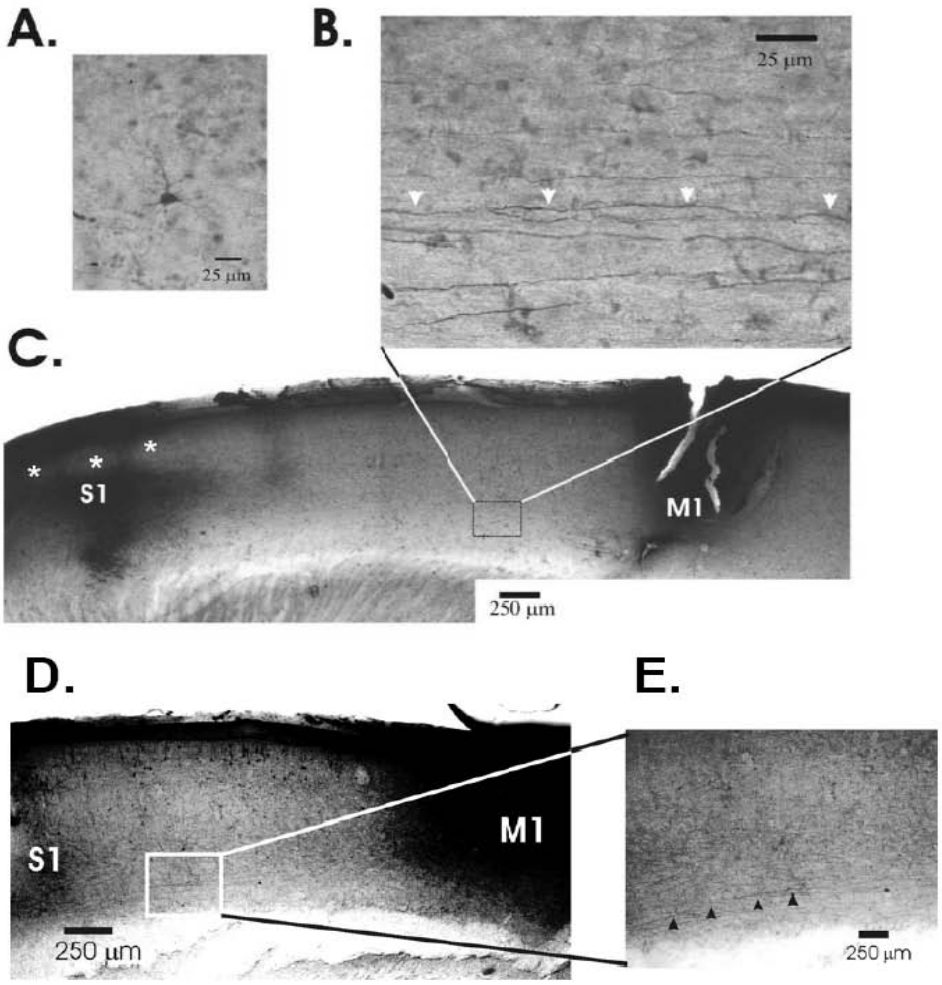

Figure 6. Axonal labeling in the sensorimotor slice. Anterograde axon labeling observed two days after an injection of biotinylated dextran amine in whisker S1 (A-C) and whisker M1 (D-E). (A) Labeled neurons can be seen surrounding the injection site (S1). (C, D) In both S1 and M1 injected animals, BDA labeled axons can be seen throughout the entire distance between these two areas. Asterisk denotes barrel center which is largely devoid of barrel staining. (B, E) Axons originating in S1 and M1 follows a similar course, traveling primarily through the deeper cortical layers (see arrows).

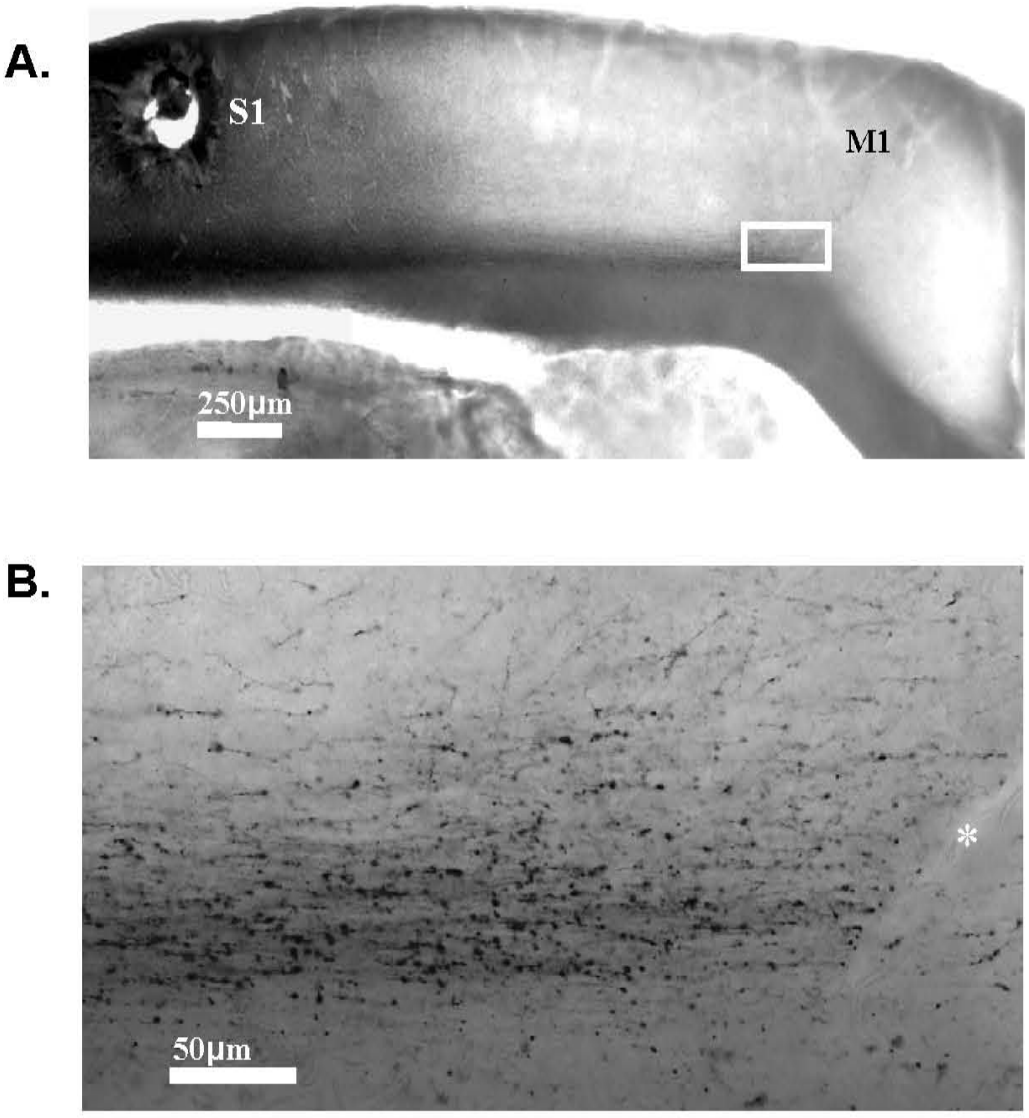

Figure 7. Axonal connections are maintained following the preparation of the sensorimotor slice. (A) A live sensorimotor slice is prepared and placed in an interface chamber. Biocytin crystals are inserted into S1 (hole) and allowed six hours to transport. (B) Inset seen in panel A. Labeled axons travel the entire distance from S1 to M1 in the prepared slice. The asterisk marks the location of the stimulated electrode tract used to mark the location of whisker M1 prior to slice preparation.

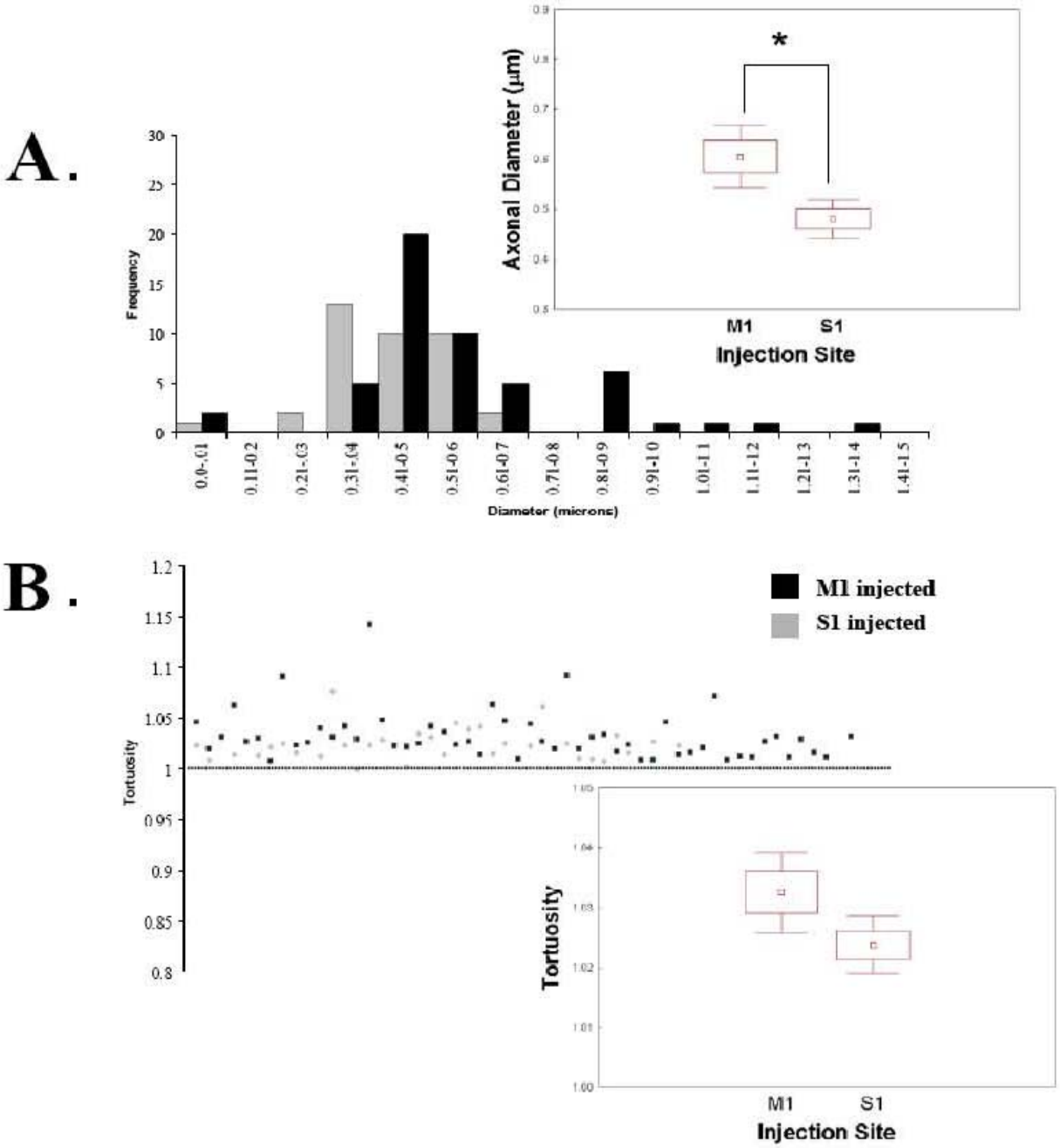

Figure 8. Characterization of sensorimotor axons. (A) Cells projecting to S1 (M1 injection, n=52) had a significantly larger diameter than those projecting to M1 (S1 injected, n=38) (t= 3.06, p< .01). (B) Individual tortuosity measurements of S1 and M1 projecting axons indicate that axons traveling in both directions travel in relatively straight paths.

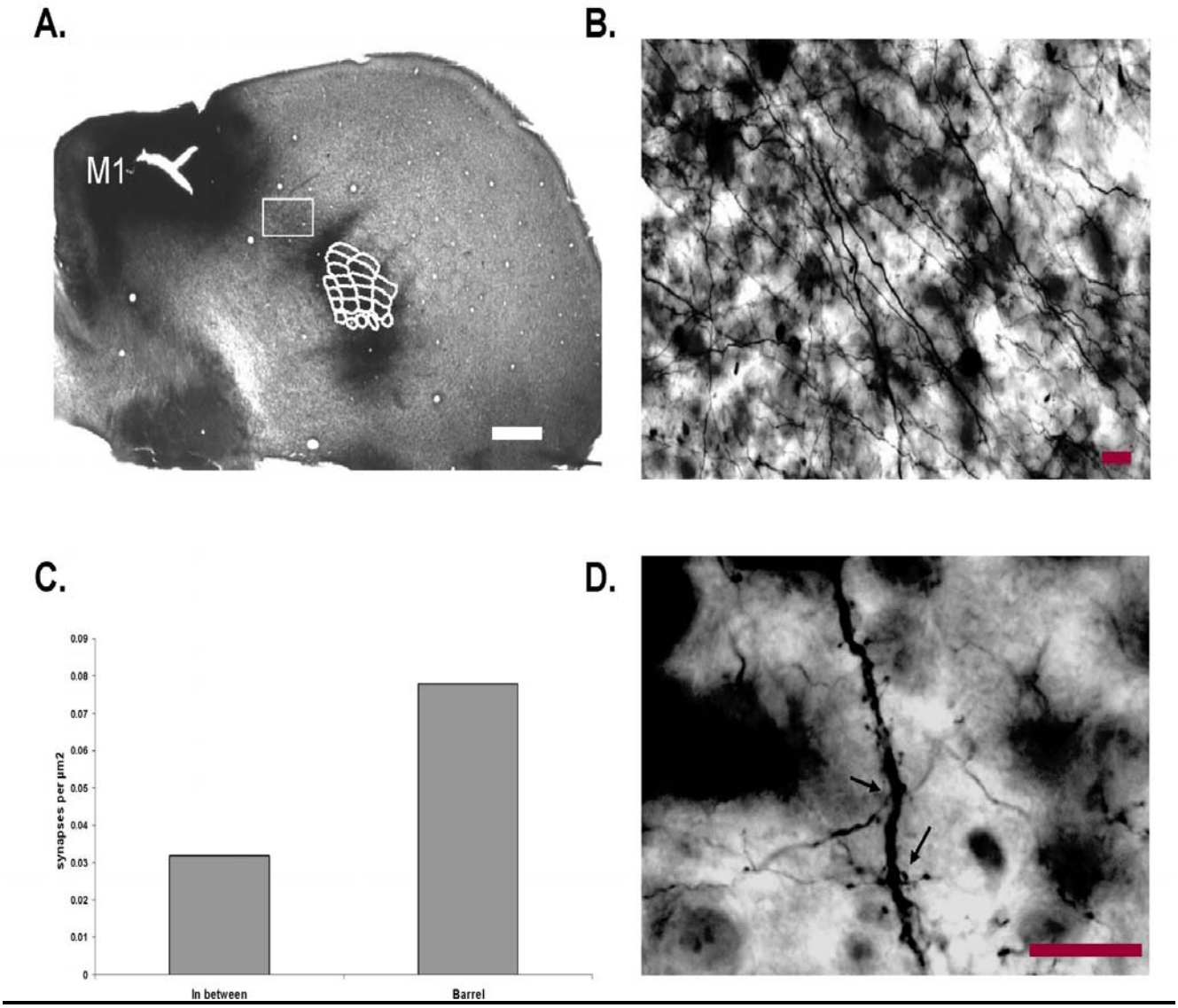

Figure 9. A tangential view of the sensorimotor pathway. A large volume injection of BDA in whisker M1 results in dense staining of the axonal pathway between the areas and the projection site (whisker S1). (A) A tangential section of the infragranular cortex two days after BDA injection. The barrels have been reconstructed from an adjacent section to highlight their location. (B) The inset shown in panel A, this is a magnified view of axons traveling from M1 to S1, note axons of different diameters. (C) Stereological estimates of synapse populations were made for the stained area between M1 and S1 and the projection site (S1). Higher densities of pre-synaptic boutons were observed in the projection site (S1) when compared to the area between M1 and S1. (D) Axo-dendritic synapses observed in S1. Scale bar in panel A represents 250µm, all others are 25µm.

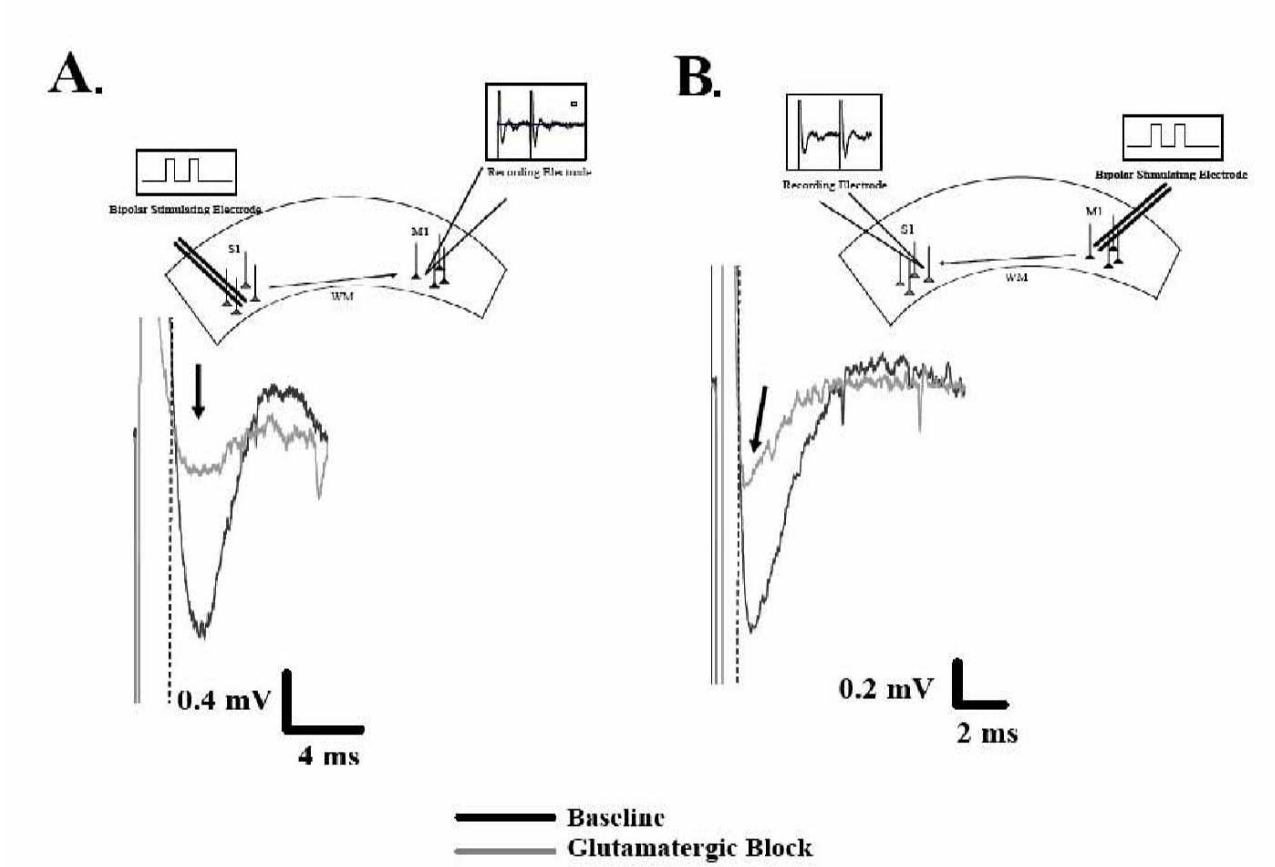

Figure 10. Functional connectivity is maintained in the sensorimotor slice. Slices were stimulated with a negative current pulse of 0.5 mA in either S1 or M1 and field potentials were recorded in the reciprocal area. (A, B) Field potentials were observed in both M1 and S1 following stimulation, both of which were reduced by the application of glutametergic agonists (CNQX (40 μM) + APV (50μM)).

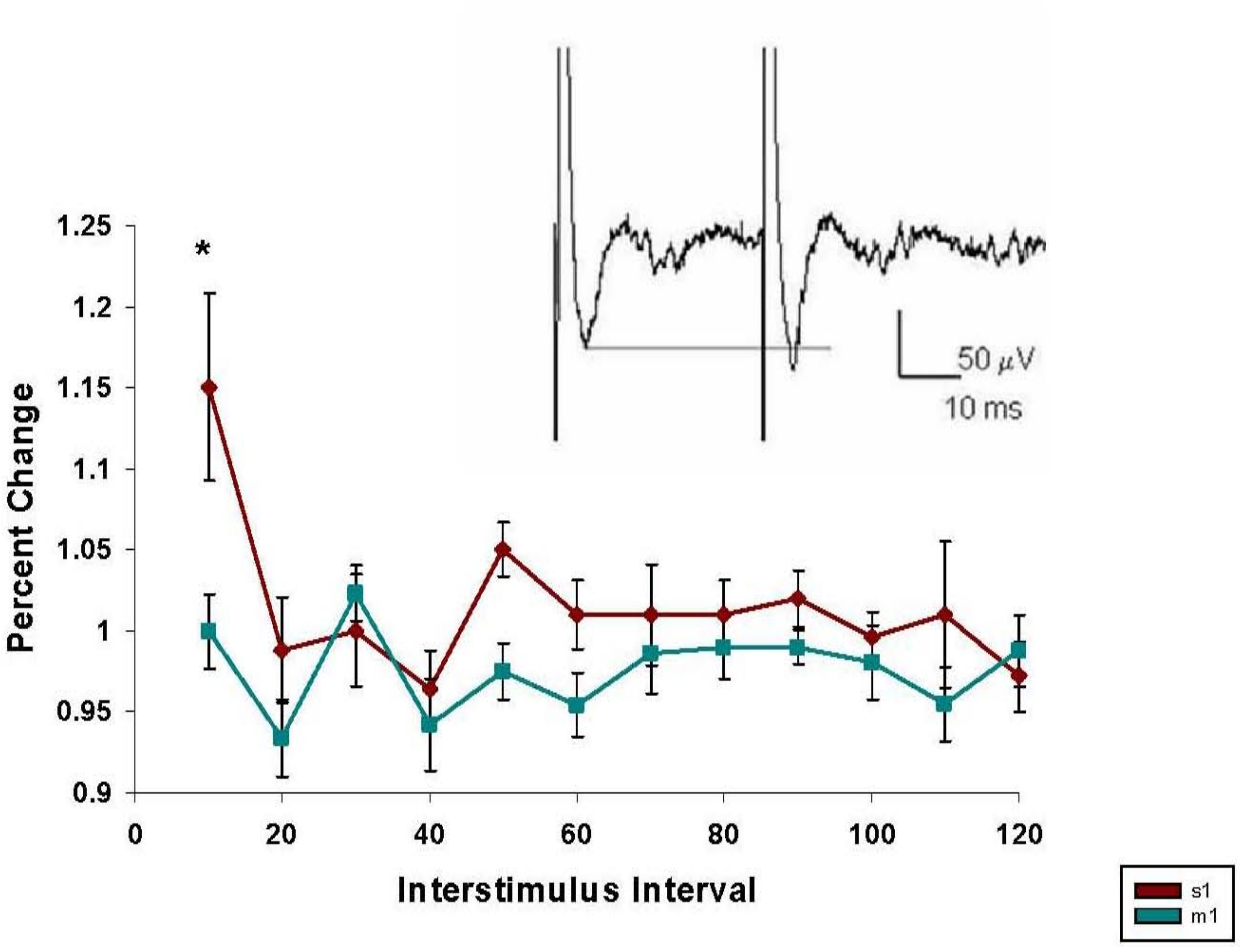

Figure 11. Extracellular responses to 0.3 mA paired-pulse stimuli in M1 (n=16) and S1 (n=16). A stimulating electrode was place in either S1 or M1 within the sensorimotor slice and resulting potentials were recorded. The percent change between the first and second response is shown across various interstimulus intervals for both M1 and S1. Cells in S1 show a greater facilitatory response overall when compared to M1 cells. This difference is most apparent an interstimulus interval of 10 ms ($F= 3.26$, $p< .01$). Inset shows example an extracellular response in S1 following paired-pulse stimulation in M1.

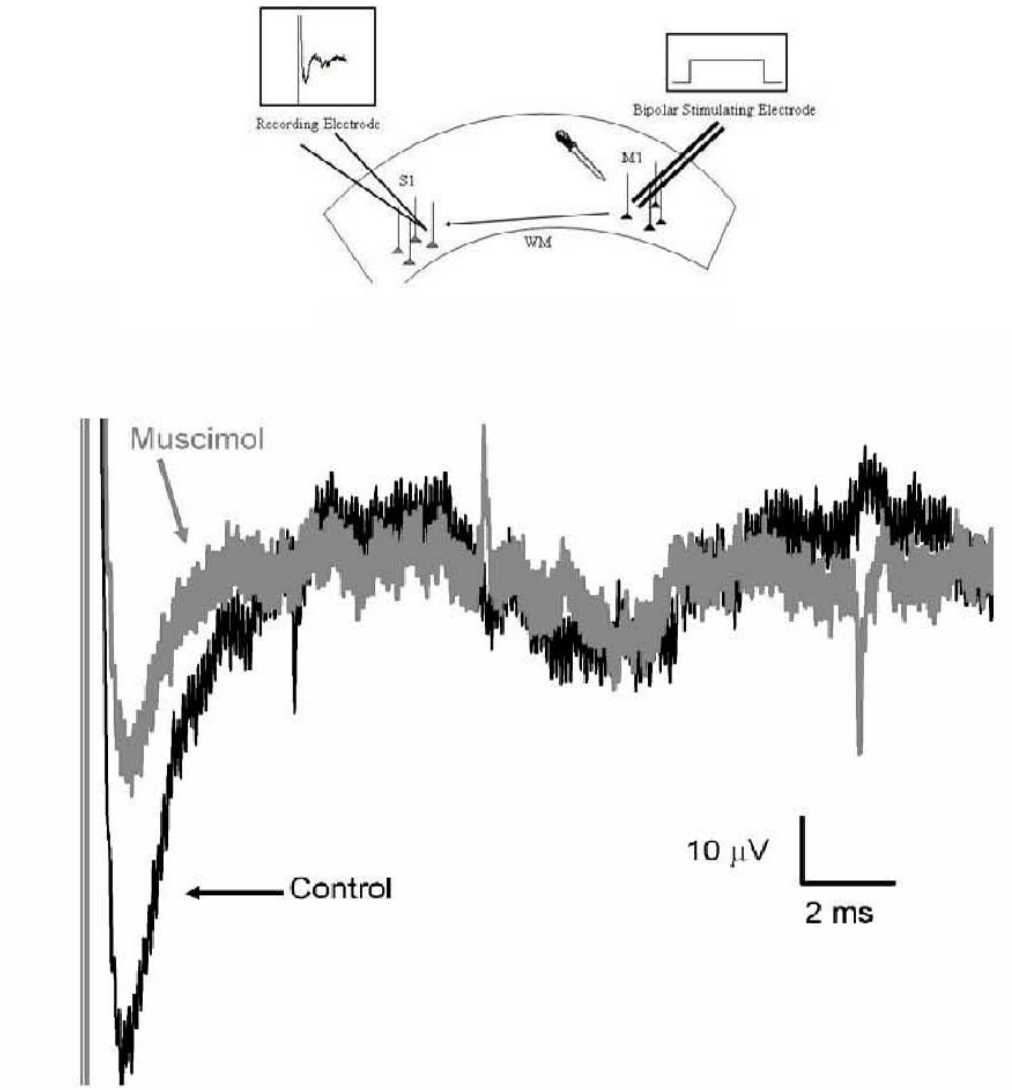

Figure 12. Minimal contribution of antidromic activity. Muscimol (1 mM) applied at the stimulation site (M1) resulted in a significantly reduced evoked response in S1 suggesting few neurons were antidromically activated.

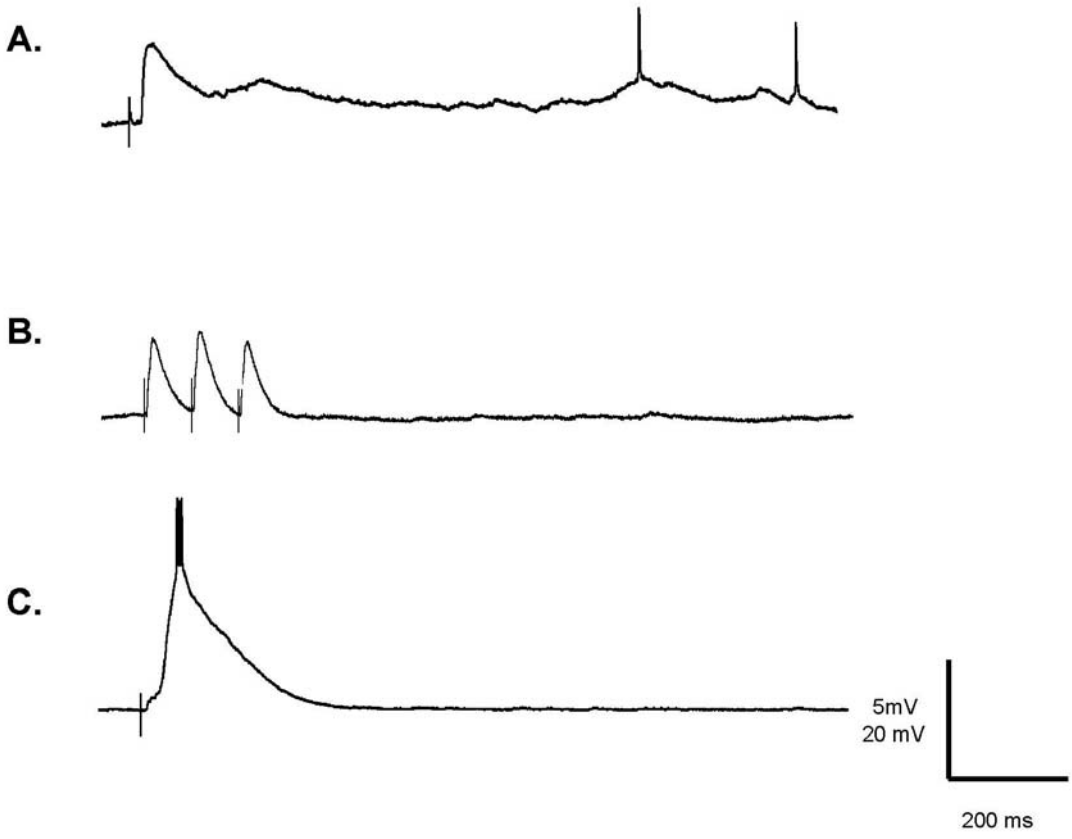

Figure 13. Synaptic response types observed in S1 and M1. Average traces (10-20 sweeps) recorded from cells in M1 and S1 following stimulation in the reciprocal area. (A) A cell in S1 has a direct and an indirect response to stimulation of 8 mA in M1, this cell would be categorized as both. (B) An S1 cell responds directly to each pulse of a 3 mA, 10 Hz train of stimuli in M1. (C) A large direct response is observed in an M1 cell following a single pulse of 5mA stimulation in S1. For traces A and B, the scale bars represent 5 mV and 200 ms; for trace C it is 20 mV and 200 ms.

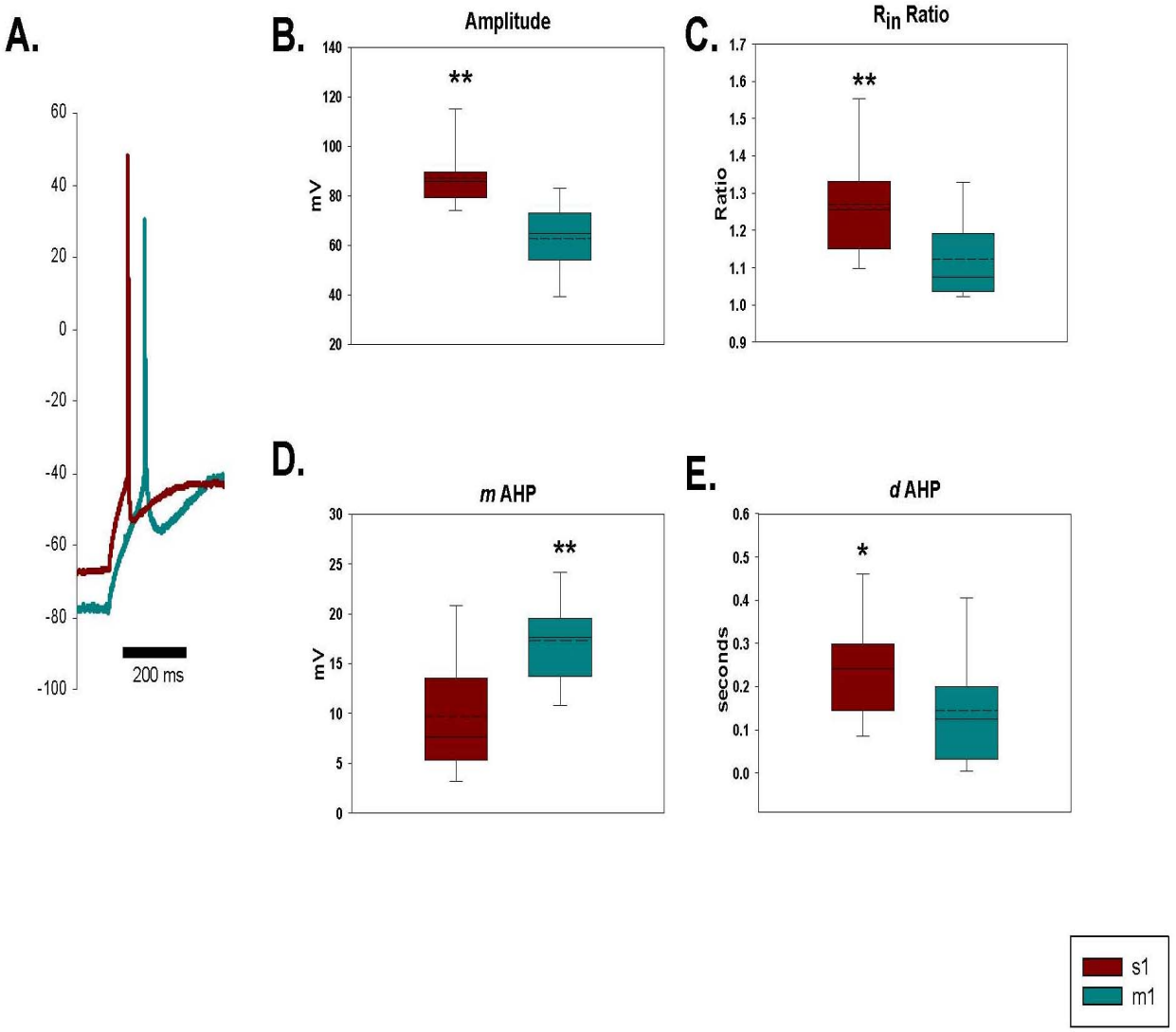

Figure 14. (A) Action potentials in an M1 and S1 cell resulting from injection of a 1s current pulse of 60 pA. (B) The spike amplitude of responding cells was significantly greater in S1 cells compared to M1 cells ($t = 5.54$, $p < .01$). (C) The input resistance ratio (R_{in}) was significantly greater in S1 cells compared to M1 cells ($U = 53$, $p < .01$). (D) The magnitude of the spike afterhyperpolarization (mAHP) was significantly greater in M1 cells when compared to S1 cells ($t = -4.37$, $p < .01$). (E) The duration of the afterhyperpolariztion (dAHP) was significantly greater in S1 cells when compared to M1 cells ($t = 2.09$, $p < .05$).

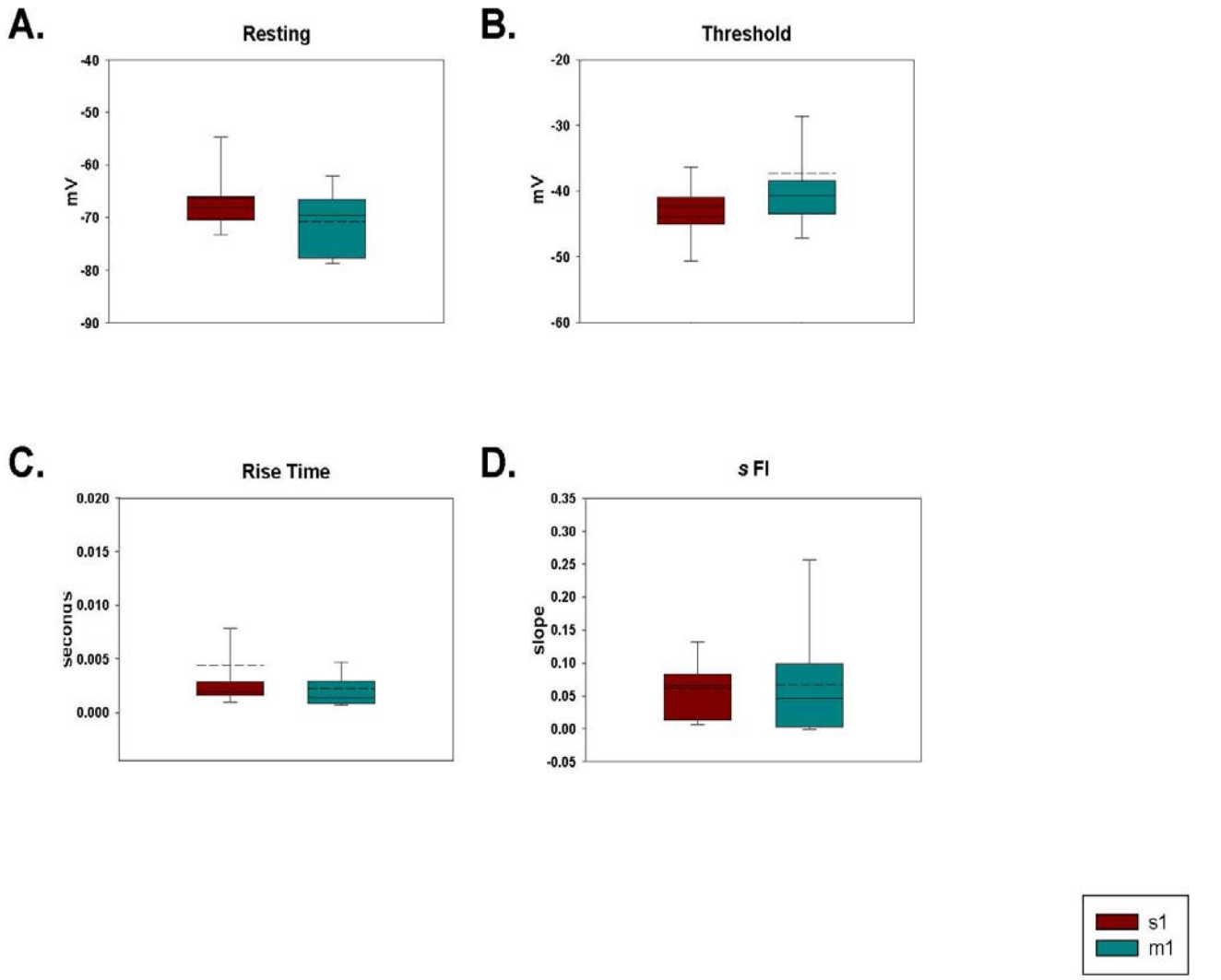

Figure 15. Intrinsic response properties of S1 (n=18) and M1 (n=18) cells that respond to stimuli in the reciprocal area (cells in the any response category). Responsive cells in S1 and M1 did not differ significantly in their resting membrane potential (A), spike threshold (B), spike rise time (C), or slope of their FI curve (sFI).

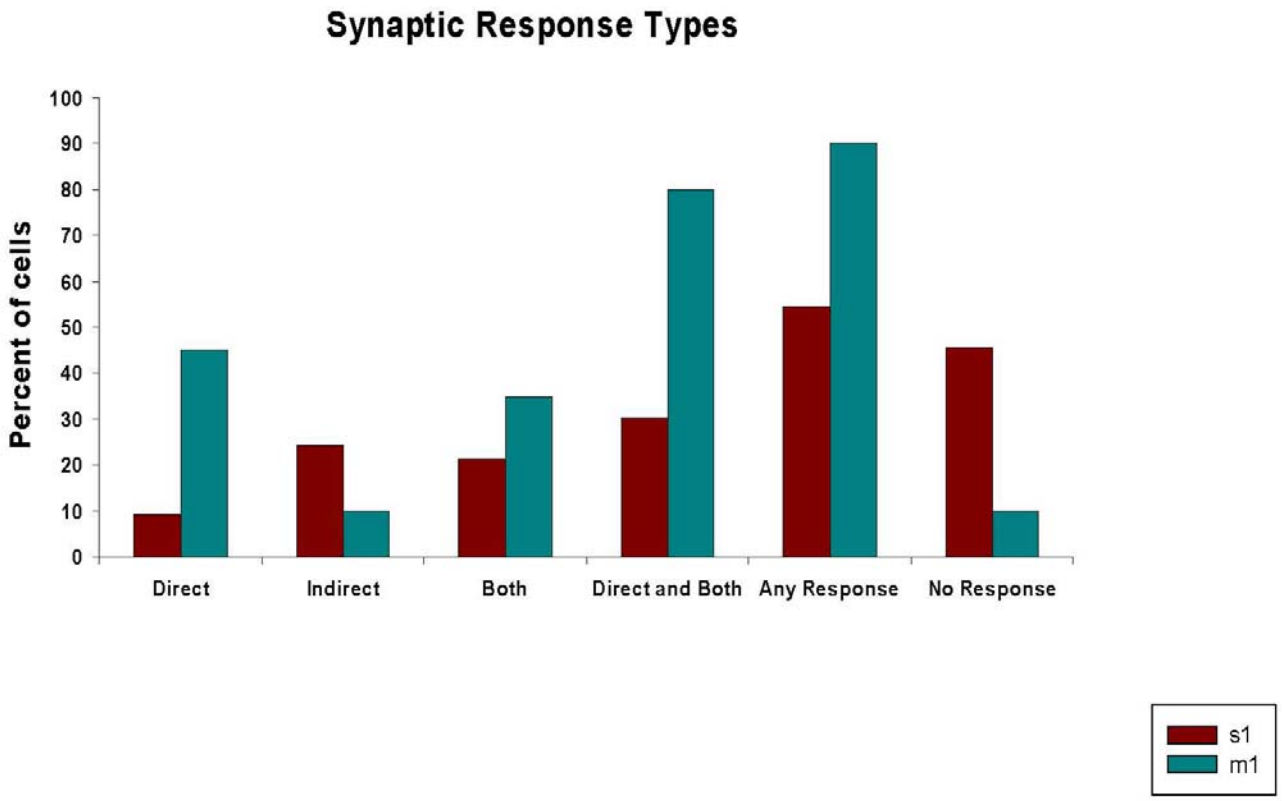

Figure 16. Synaptic responses observed in S1 (red) and M1 (green) cells following stimulation in the reciprocal area. Whole cell recordings of cell activity in both locations resulted in one of four synaptic responses: direct, indirect, both direct and indirect or no response. The any category includes cells from the direct, indirect and both categories. M1 had a higher proportion of responsive cells overall as well as a larger proportion of cells that exhibited a direct response S1 stimulation. A greater proportion of cells that responded indirectly to stimulation were found in S1 when stimulating in M1. The distribution of responsive (any response) and non-responsive (no response) cells was significantly different between S1 and M1 (χ^2=7.19, p<.01).

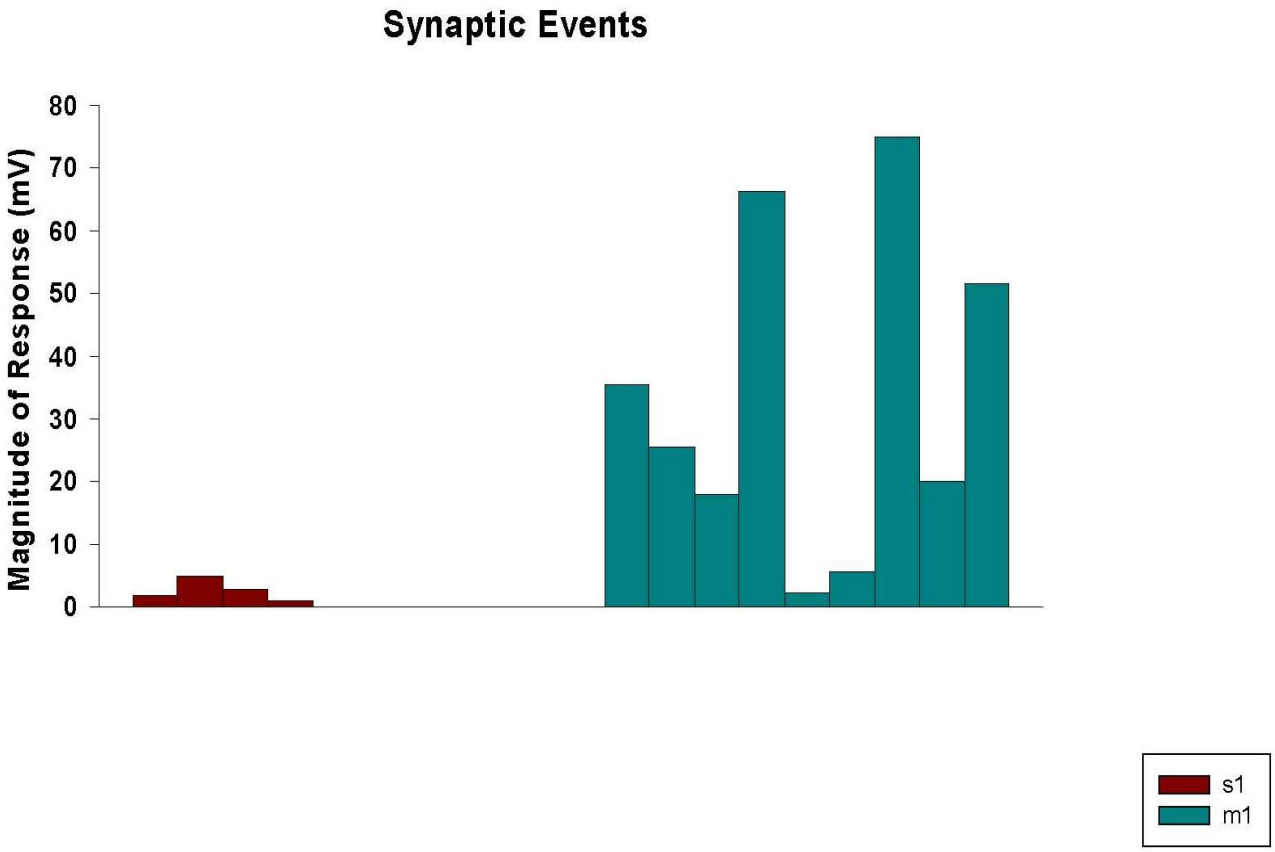

Figure 17. Response magnitude of M1 and S1 cells following stimulation in the reciprocal area. Individual response magnitudes are shown following a single pulse stimulation of 5 mA or less in the reciprocal area. A greater proportion of M1 cells responded to low levels of stimulation. In comparing the S1 and M1 cells that responded to low stimulation, the M1 cells had a significantly larger magnitude of response.

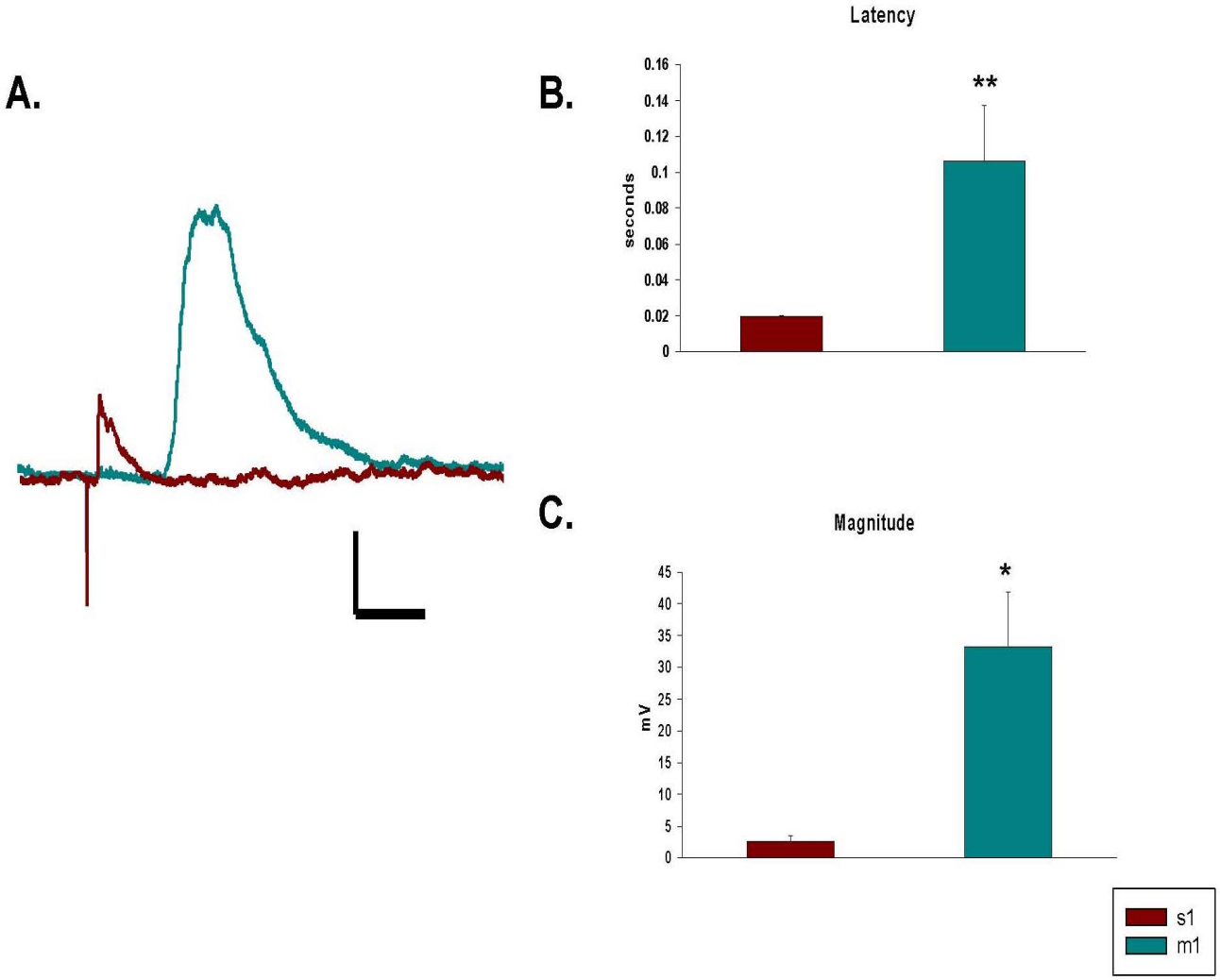

Figure 18. Direct responses observed in S1 and M1 under identical stimulation parameters differed in latency and magnitude. (A) Averaged responses in an S1 and M1 cell following stimulation in the reciprocal area (n=13). The S1 response is following a single pulse of 0.47 mA in M1 and the M1 response is following a single pulse of 8 mA in S1. Note that despite the significantly larger stimulation current used for the S1 recording, the M1 response is still larger. Comparisons of response latency and magnitude were made for cells in both location following single stimulus pulses of less than 5 mA. The range of stimulation currents for S1 cells in this group was 1 to 4 mA, with the average being 2.63mA. The range of injected currents for M1 was 0.3 to 4.7 mA with an average injected current of 1.98 mA. (B) Cells in M1 exhibited a significantly longer response latency than cells in S1 ($U = 36$, $p<.01$). (C) Cells in M1 had a significantly higher response magnitude than cells in S1 when stimulated under the same or weaker stimulus ($U =34$, $p<.05$). Scale bars represent 5 mV and 200 ms.

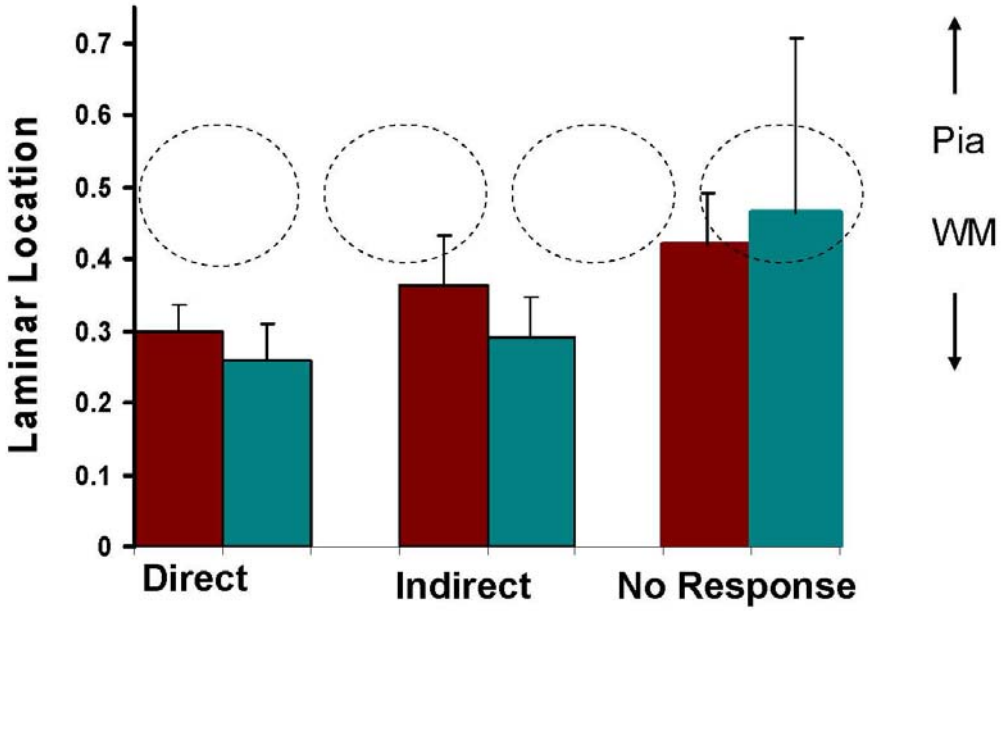

Figure 19. Laminar location of recovered cells by response type. Laminar locations of cell bodies were determined in S1 (n=21) and M1 (n=14). The circles represent the approximate location of Layer 4. For both S1 and M1 the probability of finding a post-synaptic response following stimulation in the reciprocal area was higher in the infragranular layers, which is consistent with the termination patterns of the axonal projections.

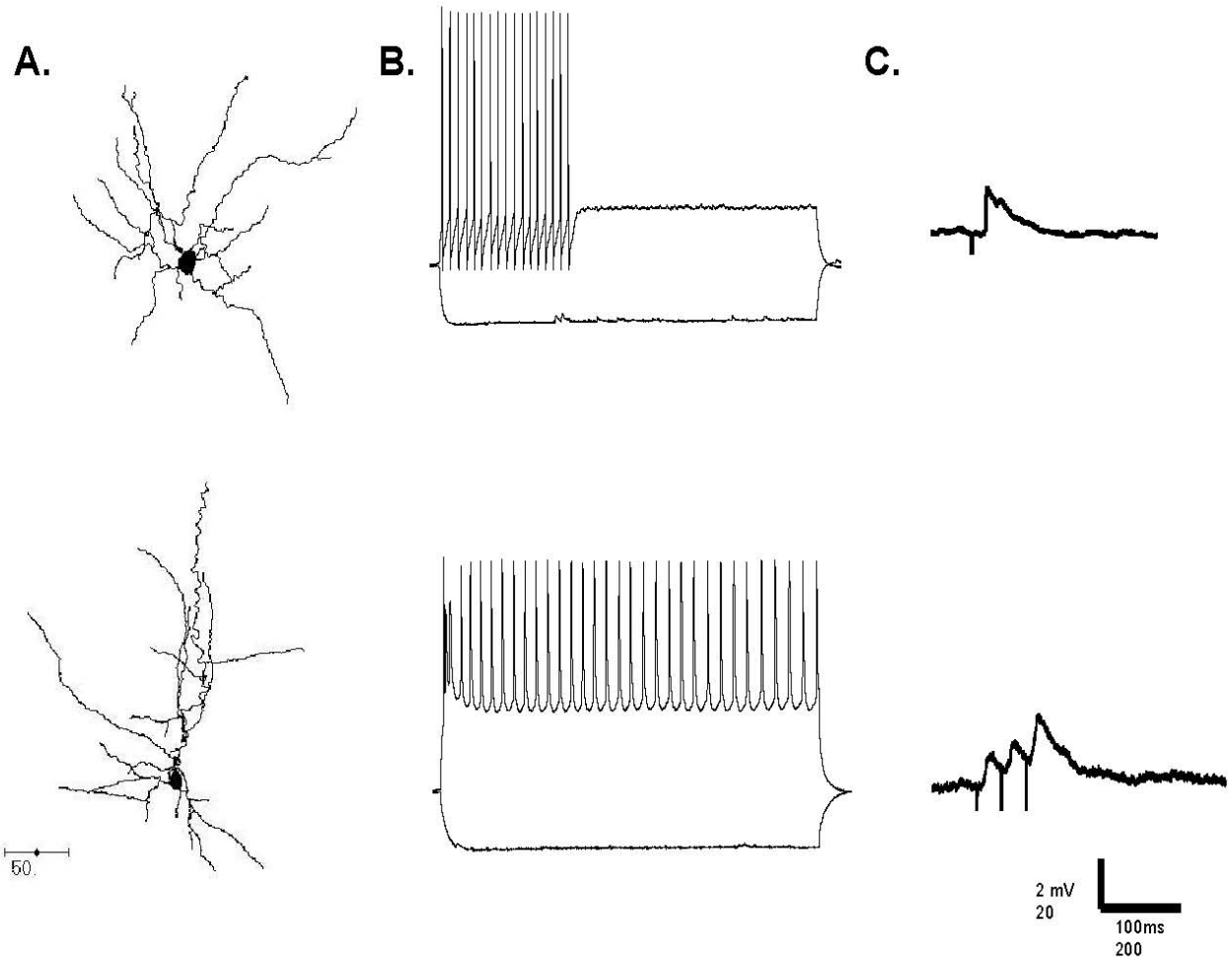

Figure 20. Characterization of recovered S1 cells. Cells were filled with biocytin during recording and recovered cells were reconstructed using Neurolucida. The morphology, intrinsic firing patterns and synaptic responses to two different cells in S1 are shown. (A) A nonpyramidal (top) and pyramidal (bottom) cell recorded from in S1. (B) Individual cell responses of the reconstructed cells following step currents of ±160 pA (top) and ±100 pA (bottom). (C) Each cell's direct response to stimulation in M1. The scale bar represents 20 mV and 200 ms for panel B, and 2mV and 100 ms for panel C.

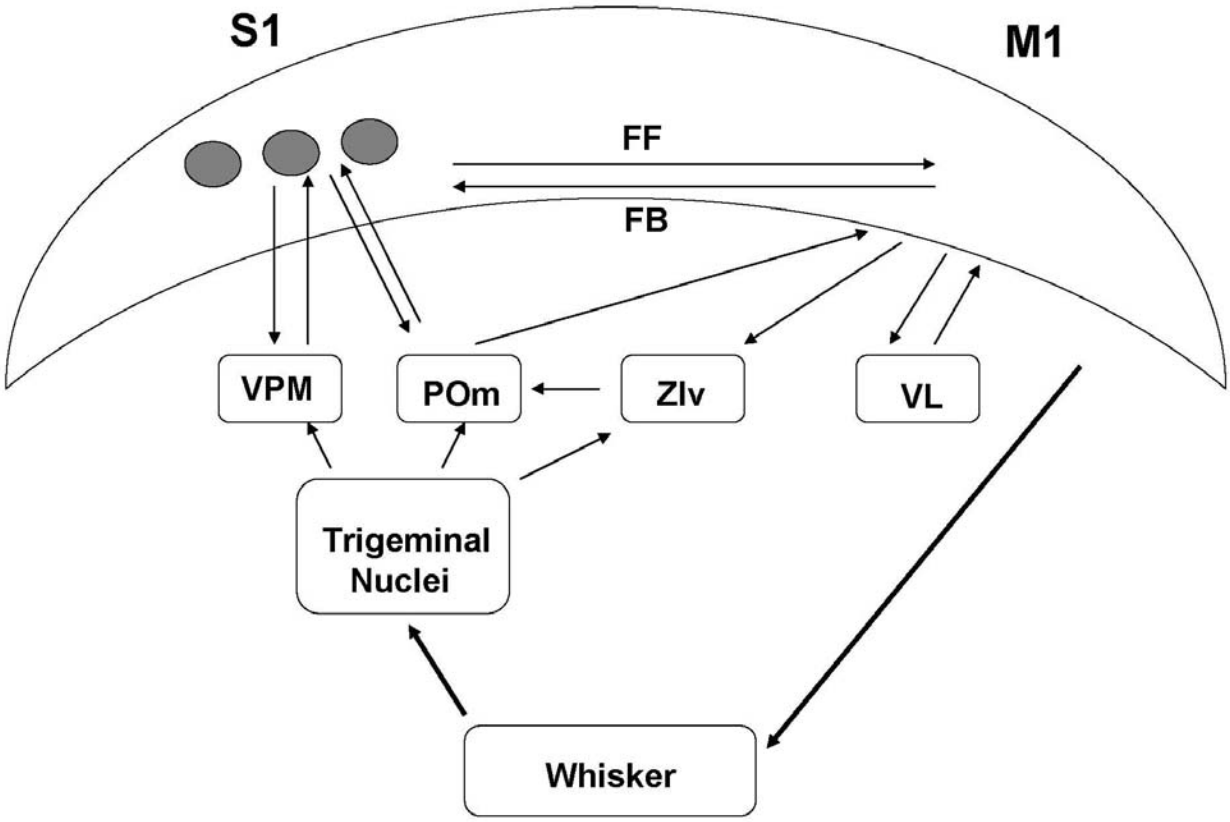

Figure 21. Anatomical connections between the somatosensory and motor cortices. Adapted from Kleinfeld and Waters 2007. Schematic of sensory and motor pathways in the rodent whisker system. VPM= ventral posterior medial thalamus, POm = posterior medial thalamus, VL= ventral lateral thalamus, ZI= zona incerta. The section represents the sensorimotor slice. The arrows within the cortex represent the reciprocal axonal pathway.

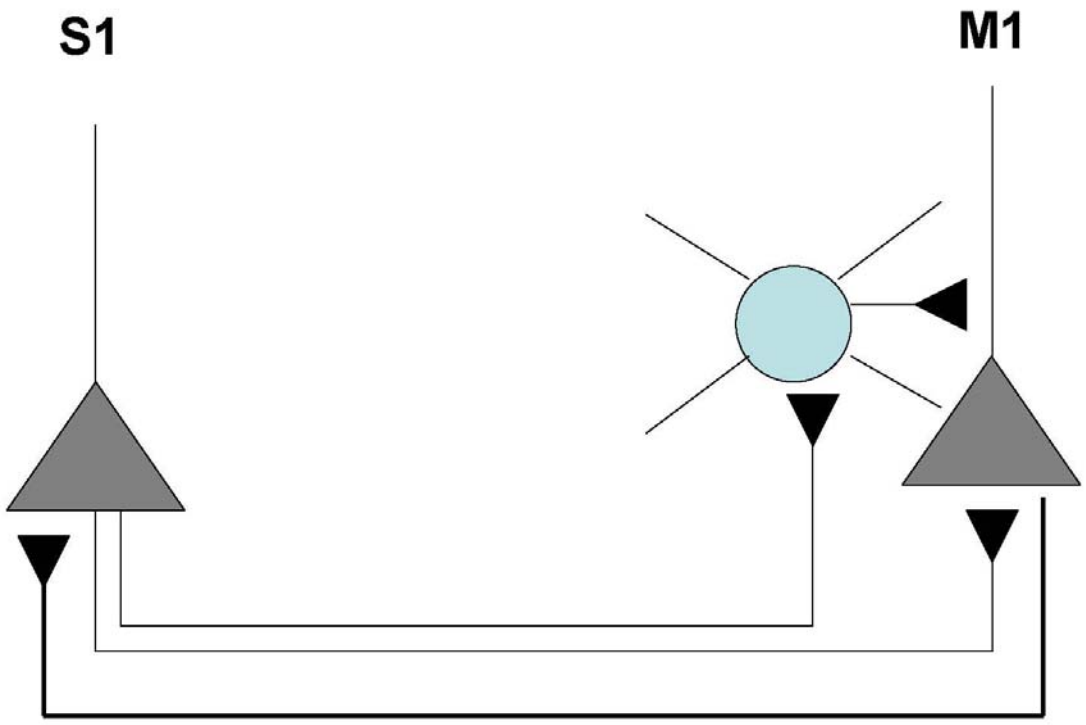

Figure 22. A proposed cortical circuit of sensorimotor processing. The triangular cells represent pyramidal neurons; the circular cell represents a nonpyramidal interneuron. The thicker line in the FB direction represents the larger diameter axons that were observed in this pathway.

References

Abeles M, Goldstein MH Jr.: Functional architecture in cat primary auditory cortex: columnar organization and organization according to depth. J Neurophysiol. 1970 Jan; 33(1):172-87.

Ahissar E. Temporal-code to rate-code conversion by neuronal phase-locked loops Neural Comput. 1998 Apr 1;10(3):597-650.

Ahissar E, Sosnik R, Haidarliu S Transformation from temporal to rate coding in a somatosensory thalamocortical pathway. Nature. 2000 Jul 20;406(6793):302-6.

Ahissar E, Kleinfeld D.:Closed-loop neuronal computations: focus on vibrissa somatosensation in rat. Cereb Cortex. 2003 Jan; 13(1):53-62.

Agmon A, Connors BW. Thalamocortical responses of mouse somatosensory (barrel) cortex in vitro. Neuroscience. 1991;41(2-3):365-79

Alloway KD, Crist J, Mutic JJ, Roy SA: Corticostriatal projections from rat barrel cortex have an anisotropic organization that correlates with vibrissal whisking behavior. J Neurosci. 1999 Dec 15; 19(24):10908-22

Alloway KD, Zhang M, Chakrabarti S.: Septal columns in rodent barrel cortex: functional circuits for modulating whisking behavior.J Comp Neurol. 2004 Dec 13;480(3):299-309.

Alloway KD. Information processing streams in rodent barrel cortex: the differential functions of barrel and septal circuits. Cereb Cortex. 2008 May;18(5):979-89. Epub 2007 Aug 16.

Angelucci A, Levitt JB, Walton EJS, Hupe JM, Bullier J, Lund JS. Circuits for local and global signal integration in primary visual cortex. J Neurosci. 2002 Oct 1; 22(19): 8633-8646.

Arabzadeh E, Zorzin E, Diamond ME. Neuronal encoding of texture in the whisker sensory pathway. PLoS Biol. 2005 Jan;3(1):e17. Epub 2005 Jan 11.

Armstrong-James M, Fox K: Spatiotemporal convergence and divergence in the rat S1 "barrel" cortex. J Comp Neurol. 1987 Sep 8; 263(2):265-81.

Armstrong-James M, Fox K, Das-Gupta A: Flow of excitation within rat barrel cortex on striking a single vibrissa. J Neurophysiol. 1992 Oct;68(4):1345-58.

Aroniadou VA, Keller A. The patterns and synaptic properties of horizontal intracortical connections in the rat motor cortex. J Neurophysiol. 1993 Oct;70(4):1553-69.

Asanuma H, Larsen K, Yumiya H. Peripheral input pathways to the monkey motor cortex. Exp Brain Res. 1980 Feb;38(3):349-55.

Bear J, Lothman EW. An in vitro study of focal epileptogenesis in combined hippocampal-parahippocampal slices. Epilepsy Res. 1993 Mar;14(3):183-93.

Bermejo R, Zeigler HP.: "Real-time" monitoring of vibrissa contacts during rodent whisking. Somatosens Mot Res. 2000; 17(4):373-7.

Brecht M, Sakmann B: Whisker maps of neuronal subclasses of the rat ventral posterior medial thalamus, identified by whole-cell voltage recording and morphological reconstruction. J Physiol. 2002 Jan 15; 538(Pt 2):495-515.

Breustedt J, Gloveli T, Heinemann U. Far field effects of seizure like events induced by application of 4-AP in combined entorhinal cortex hippocampal slices. Brain Res. 2002 Nov 22;956(1):173-7.

Brodmann K: Comparative study of localization in the cerebral cortex (translated title). Barth, Leipzig, Germany.

Brochier T, Boudreau MJ, Pare M, Smith AM: The effects of muscimol inactivation of small regions of motor and somatosensory cortex on independent finger movements and force control in the precision grip. Exp Brain Res. 1999 Sep; 128(1-2):31-40.

Bruce IC, Tatton WG: Synchronous development of motor cortical output to different muscles in the kitten. Exp Brain Res. 1980; 40(3):349-53.

Brumberg JC, Pinto DJ, Simons DJ. Spatial gradients and inhibitory summation in the rat whisker barrel system. J Neurophysiol. 1996 Jul;76(1):130-40.

Brumberg JC, Pinto DJ, Simons DJ: Cortical columnar processing in the rat whisker-to-barrel system. J Neurophysiol. 1999 Oct; 82(4):1808-17.
Cantone G, Xiao J, McFarlane N, Levitt JB: Feedback connections to ferret striate cortex: Direct evidence for visuotopic convergence of feedback inputs. J Comp Neur. 2005; 487: 312-331.

Carvell GE, Simons DJ: Biometric analyses of vibrissal tactile discrimination in the rat.J Neurosci. 1990 Aug; 10(8):2638-48.

Carvell GE, Miller SA, Simons DJ: The relationship of vibrissal motor cortex unit activity to whisking in the awake rat. Somatosens Mot Res. 1996; 13(2):115-27.

Chakrabarty S, Martin JH: Postnatal development of the motor representation in primary motor cortex. J Neurophysiol. 2000 Nov; 84(5):2582-94.

Coogan TA, Burkhalter A: Hierarchical organization of areas in rat visual cortex. J Neurosci. 1993 Sep;13(9):3749-72.

Cramer NP, Li Y, Keller A. The whisking rhythm generator: a novel mammalian network for the generation of movement. J Neurophysiol. 2007 Mar;97(3):2148-58. Epub 2007 Jan 3.

Crochet S, Petersen CC: Correlating whisker behavior with membrane potential in barrel cortex of awake mice.Nat Neurosci. 2006 May;9(5):608-10. Epub 2006 Apr 16.

Cruikshank SJ, Rose HJ, Metherate R. Auditory thalamocortical synaptic transmission in vitro. J Neurophysiol. 2002 Jan;87(1):361-84.

Deschenes M, Veinante P, Zhang ZW: The organization of corticothalamic projections: reciprocity versus parity. Brain Res Brain Res Rev. 1998 Dec;28(3):286-308.

Diamond ME, Armstrong-James M, Budway MJ, Ebner FF: Somatic sensory responses in the rostral sector of the posterior group (POm) and in the ventral posterior medial nucleus (VPM) of the rat thalamus: dependence on the barrel field cortex. J Comp Neurol. 1992 May 1;319(1):66-84.

Domenici L, Harding GW, Burkhalter A. Patterns of synaptic activity in forward and feedback pathways within rat visual cortex. J Neurophysiol. 1995 Dec; 74(6):2649-64

Dong H, Shao Z, Nerbonne JM, Burkhalter A. Differential depression of inhibitory synaptic responses in feedforward and feedback circuits between different areas of mouse visual cortex. J Comp Neurol. 2004 Jul 26;475(3):361-73.

Donoghue JP, Wise SP. The motor cortex of the rat: cytoarchitecture and microstimulation mapping. J Comp Neurol. 1982 Nov 20;212(1):76-88.

Elhanany E and White EL: Intrinsic circuitry: synapses involving the local axon collaterals of corticocortical projection neurons in the mouse primary somatosensory cortex. J Comp Neurol. Jan 1; 291 (1): 43-54.

Farkas T, Kis Z, Toldi J, Wolff JR:Activation of the primary motor cortex by somatosensory stimulation in adult rats is mediated mainly by associational connections from the somatosensory cortex. Neuroscience. 1999 May;90(2):353-61.

Favorov OV, Diamond ME, Whitsel BL: Evidence for a mosaic representation of the body surface in area 3b of the somatic cortex of cat. Proc Natl Acad Sci U S A. 1987 Sep;84(18):6606-10.

Feldman ML, Peters A: The forms of non-pyramidal neurons in the visual cortex of the rat. J Comp Neurol. 1978 Jun 15; 179(4):761-93.

Felleman DJ and Van Essen DC: Distrubuted hierarchial processing in the primate cerebral cortex. Cereb Cortex 1991 Jan-Feb; 1 (1): 1-47.

Ferezou I, Haiss F, Gentet LJ, Aronoff R, Weber B, Petersen CC. Spatiotemporal dynamics of cortical sensorimotor integration in behaving mice. Neuron. 2007 Dec 6;56(5):907-23.

Finger , S: Origins of Neuroscience. New York: Oxford University Press; 1994.

Fleury M, Bard C, Teasdale N, Paillard J, Cole J, Lajoie Y, Lamarre Y: Weight judgment. The discrimination capacity of a deafferented subject.Brain. 1995 Oct; 118 (Pt 5):1149-56.

Gao P, Bermejo R, Zeigler HP. Whisker deafferentation and rodent whisking patterns: behavioral evidence for a central pattern generator. J Neurosci. 2001 Jul 15;21(14):5374-80.

Gao P, Hattox AM, Jones LM, Keller A, Zeigler HP: Whisking motor cortex ablation and whisker movement patterns. Somatos Mot Res. 2003 Sept-Dec; 20 (3-4): 191-198.

Gasparinin S and Magee, JC: State dependant dendritic computation in Hippocampal CA 1 pyramidal neurons. J Neurosci. 2006 Feb 15; 26(7): 2088-2100.

Gibson JM, Welker WI: Quantitative studies of stimulus coding in first-order vibrissa afferents of rats. 1. Receptive field properties and threshold distributions. Somatosens Mot Res. 1983; 1(1):51-67.

Gilbert CD, Wiesel TN: Morphology and intracortical projections of functionally characterised neurones in the cat visual cortex. Nature. 1979 Jul 12; 280(5718):120-5.

Girard P, Hupe JM and Bullier J : Feedfoward and feedback connections between areas V1 and V2 of the monkey have similar rapid conduction velocities. J Neurophysiol. 2001 Mar;85(3):1328-31.

Gonchar Y, Burkhalter A: Differential subcellular localization of forward and feedback interareal inputs to parvalbumin expressing GABAergic neurons in rat visual cortex.J Comp Neurol. 1999 Apr 12; 406(3):346-60.

Guić-Robles E, Valdivieso C, Guajardo G. Rats can learn a roughness discrimination using only their vibrissal system. Behav Brain Res. 1989 Jan 1;31(3):285-9.

Guić-Robles E, Jenkins WM, Bravo, H: Vibrissal roughness discrimination is barrel cortex-dependant. Behav Brain Res 1992; 48 (2): 142-52.

Hartline HK : The receptive fields of optic nerve fibers. Amer. J. Physiol.1940 Oct; 130 (4): 690-699.

Harvey MA, Sachdev RS, Zeigler HP: Cortical barrel field ablation and unconditioned whisker kinematics. Somatosens Mot Res 2001; 18(3): 223-227.

Herman D, Kang R, MacGillis M, Zarzecki P: Responses of cat motor cortex neurons to cortico-cortical and somatosensory inputs. Exp Brain Res. 1985;57(3):598-604.

Hikosaka O, Tanaka M, Sakamoto M, Iwamura Y: Deficits in manipulative behaviors induced by local injections of muscimol in the first somatosensory cortex of the conscious monkey. Brain Res. 1985 Jan 28; 325(1-2):375-80.

Hoffer ZS, Alloway KD: Organization of corticostriatal projections from the vibrissal representations in the primary motor and somatosensory cortical areas of rodents.
J Comp Neurol. 2001 Oct 8; 439(1):87-103.

Hoffer ZS, Hoover JE, Alloway KD: Sensorimotor corticocortical projections from rat barrel cortex have an anisotropic organization that facilitates integration of inputs from whiskers in the same row. J Comp Neurol. 2003 Nov 24; 466(4):525-44.

Hoffer ZS, Arantes HB, Roth RL, Alloway KD:Functional circuits mediating sensorimotor integration: quantitative comparisons of projections from rodent barrel cortex to primary motor cortex, neostriatum, superior colliculus, and the pons.
J Comp Neurol. 2005 Jul 18; 488(1):82-100.

Hubel DH, Wiesel TN: Receptive fields, binocular interaction and functional architecture in the cat's visual cortex. J Physiol. 1962 Jan; 160:106-54. .

Hubel DH, Wiesel TN: Receptive fields and functional architecture of monkey striate cortex.J Physiol. 1968 Mar; 195(1):215-43.

Hubel DH, Wiesel TN: Anatomical demonstration of columns in the monkey striate cortex. Nature. 1969 Feb 22; 221(182):747-50.

Hupe JM, James AC, Payne BR, Lomber SG, Girard P, Bullier J: Cortical feedback improves discrimination between figure and background by V1, V2 and V3 neurons. Nature. 1998 Aug 20; 394(6695):784-7.

Izraeli R, Porter LL. Vibrissal motor cortex in the rat: connections with the barrel field. Exp Brain Res. 1995;104(1):41-54.

Jacquin MF, McCasland JS, Henderson TA, Rhoades RW, Woolsey TA. 2-DG uptake patterns related to single vibrissae during exploratory behaviors in the hamster trigeminal system. J Comp Neurol. 1993 Jun 1; 332(1):38-58.

Johansson RS, Westling G: Roles of glabrous skin receptors and sensorimotor memory in automatic control of precision grip when lifting rougher or more slippery objects. Exp Brain Res. 1984; 56(3):550-64.

Johnson RR, Burkhalter A. Microcircuitry of forward and feedback connections within rat visual cortex. J Comp Neurol. 1996 May 6;368(3):383-98.

Jones EG, Burton H, Porter R. Commissural and cortico-cortical "columns" in the somatic sensory cortex of primates. Science. 1975 Nov 7;190(4214):572-4.

Jones and Diamond: Cerebral Cortex; vol 11. New York: Plenum Press; 1995.

Kandel, Swartz and Jessel: Priniples of Neural Science, Fourth Edition. McGraw-Hill, New York, 2000.

Kaneko T, Caria MA, Asanuma H. Information processing within the motor cortex. I. Responses of morphologically identified motor cortical cells to stimulation of the somatosensory cortex. J Comp Neurol. 1994 Jul 8;345(2):161-71.

Kelly MK, Carvell GE, Hartings JA, Simons DJ. Axonal conduction properties of antidromically identified neurons in rat barrel cortex. Somatosens Mot Res. 2001;18(3):202-10.

Kisvarday ZF, Martin KA, Friedlander MJ, Somogyi P. Evidence for interlaminar inhibitory circuits in the striate cortex of the cat. J Comp Neurol. 1987 Jun 1; 260(1):1-19.

Kleinfeld D, Berg RW, O'Connor SM: Anatomical loops and their electrical dynamics in relation to whisking by rat. Somatosens Mot Res. 1999;16(2):69-88.

Kleinfeld D and Waters J : Wilder Penfield in the age of YouTube: visualizing the sequential activation of sensorimotor areas across the neocortex. Neuron. 2007 Dec 6; 56: 760-762.

Koralek KA, Jensen KF, Killackey HP: Evidence for two complementary patterns of thalamic input to the rat somatosensory cortex. Brain Res. 1988 Nov 1; 463(2):346-51.

Krupa DJ, Matell MS, Brisben AJ, Oliveira LM, Nicolelis MA: Behavioral properties of the trigeminal somatosensory system in rats performing whisker-dependent tactile discriminations. J Neurosci. 2001 Aug 1; 21(15):5752-63.

Levitt JB and Lund JS: Contrast dependence of contextual effects in primate visual cortex. Nature 1997 May 1; 387: 73- 76.

Li CX, Waters RS:Organization of the mouse motor cortex studied by retrograde tracing and intracortical microstimulation (ICMS) mapping. Can J Neurol Sci. 1991 Feb;18(1):28-38.

Lovick TA. The behavioural repertoire of precollicular decerebrate rats. J Physiol. 1972 Oct;226(2):4P-6P.

Lu SM, Lin RC. Thalamic afferents of the rat barrel cortex: a light- and electron-microscopic study using Phaseolus vulgaris leucoagglutinin as an anterograde tracer. Somatosens Mot Res. 1993;10(1):1-16.

Lund JS, Lund RD, Hendrickson AE, Bunt AH, Fuchs AF. The origin of efferent pathways from the primary visual cortex, area 17, of the macaque monkey as shown by retrograde transport of horseradish peroxidase. J Comp Neurol. 1975; 64: 287-303.

MacLean JN, Fenstermaker V, Watson BO, Yuste R. A visual thalamocortical 524 slice. Nat Methods 2006;3:129–34.

Martin GF, Cabana T, Culberson JL, Curry JJ, Tschismadia I: The early development of corticobulbar and corticospinal systems. Studies using the North American opossum. Anat Embryol (Berl). 1980;161(2):197-213.

Maunsell JHR and Van Essen DC : The connections of the middle temporal visual area (MT) and their relationship to a cortical hierarchy in the macaque monkey. J Neurosci. 1983 Dec; 3 (12): 2563-2586.

McDonald CT and Burkhalter A: Organization of long-range inhibitory connections within rat visual cortex. J Neurosci. 1993 Feb; 13 (2): 768-781.

Melzer P, Champney GC, Maguire MJ, Ebner FF. Rate code and temporal code for frequency of whisker stimulation in rat primary and secondary somatic sensory cortex. : Exp Brain Res. 2006 Jul;172(3):370-86. Epub 2006 Feb 3.

Melzer P, Sachdev RN, Jenkinson N, Ebner FF. Stimulus frequency processing in awake rat barrel cortex. J Neurosci. 2006 Nov 22;26(47):12198-205.

Miyashita E, Keller A, Asanuma H: Input-output organization of the rat vibrissal motor cortex. Exp Brain Res. 1994; 99(2):223-32.

Mountcastle VB: Modality and topographic properties of single neurons of cat's somatic sensory cortex. J Neurophysiol. 1957 Jul; 20(4):408-34. .

Nowak LG, James AC, Bullier J. Corticocortical connections between visual areas 17 and 18a of the rat studied in vitro: spatial and temporal organisation of functional synaptic responses. Exp Brain Res. 1997 Nov;117(2):219-41.

Petersen CC, Sakmann B: The excitatory neuronal network of rat layer 4 barrel cortex. J Neurosci. 2000 Oct 15; 20(20):7579-86.

Petersen CC: The barrel cortex--integrating molecular, cellular and systems physiology. Pflugers Arch. 2003 Nov; 447(2):126-34. Epub 2003 Sep 19. .

Picard N, Smith AM: Primary motor cortical responses to perturbations of prehension in the monkey. J Neurophysiol. 1992a Nov; 68(5):1882-94.

Picard N, Smith AM: Primary motor cortical activity related to the weight and texture of grasped objects in the monkey. J Neurophysiol. 1992b Nov; 68(5):1867-81.

Porter LL, White EL: Afferent and efferent pathways of the vibrissal region of primary motor cortex in the mouse. J Comp Neurol. 1983 Mar 1;214(3):279-89.

Porter LL. Somatosensory input onto pyramidal tract neurons in rodent motor cortex. Neuroreport. 1996 Oct 2;7(14):2309-15

Porter LL: Morphological Characterization of a Cortico-cortical relay in the cat sensorimotor cortex. Cereb Cortex. 1997 Mar; 7(2):100-9

Powell TB and Mountcastle VB:The cytoarchitecture of the postcentral gyrus of the monkey Macaca mulatta. Bull Johns Hopkins Hosp. 1959 Sep; 105:108-131.

Price DJ, Lotto RB. Influences of the thalamus on the survival of subplate and cortical plate cells in cultured embryonic mouse brain. J Neurosci. 1996 May 15; 16(10):3247-55.

Prud'homme MJ, Kalaska JF: Proprioceptive activity in primate primary somatosensory cortex during active arm reaching movements. J Neurophysiol. 1994 Nov; 72(5):2280-301.

Ramanathan S, Hanley JJ, Deniau JM, Bolam JP: Synaptic convergence of motor and somatosensory cortical afferents onto GABAergic interneurons in the rat striatum. J Neurosci. 2002 Sep 15; 22(18):8158-69.

Rice FL, Van der Loos H: Development of the barrels and barrel field in the somatosensory cortex of the mouse. J Comp Neurol. 1977 Feb 15; 171(4):545-60.

Rockland KS and Pandya DN : Laminar origins and terminations of cortical connections of the occipital lobe in the rhesus monkey. Brain Research, 1979; 179: 3-20.

Rockland KS, Lund JS, Humphrey AL: Anatomical binding of intrinsic connections in striate cortex of tree shrews (Tupaia glis). J Comp Neurol. 1982 Jul 20; 209(1):41-58.

Rockland KS and Virga A: Terminal arbors of individual "feedback" axons projecting from area V2 to V1 in the macaque monkey: a study using immunohistochemistry of anterogradely transported *phaseolus vulgaris*-leucoagglutinin. J Comp Neurol.1989 258: 54-72.

Rockland KS and Virga A: Organization of individual cortical axons projecting from area V1 (area 17) to V2 (area 18) in the macaque monkey. Vis Neurosci 1990; 4: 11-28.

Rockland KS: Morphology of individual axons projecting from area V2 to MT in the macaque. J Comp Neurol. 1995 Apr 24;355(1):15-26.

Rockland KS: Non-uniformity of extrinsic connections and columnar organization. J Neurocytol. 2002 Mar-Jun;31(3-5):247-53.

Rothwell JC, Traub MM, Day BL, Obeso JA, Thomas PK, Marsden CD: Manual motor performance in a deafferented man. Brain. 1982 Sep;105 (Pt 3):515-42.

Rouiller EM, Yu XH, Moret V, Tempini A, Wisendanger M, Liang F: Dexterity in monkeys following early lesion of the motor cortical hand area: the role of the cortex adjacent to the lesion. Eur J Neurosci. 1998 Feb; 10 (2): 729-40.

Salimi I, Brochier T, Smith AM: Neuronal activity in somatosensory cortex of monkeys using a precision grip. I. Receptive fields and discharge patterns.J Neurophysiol. 1999a Feb;81(2):825-34.

Salimi I, Brochier T, Smith AM: Neuronal activity in somatosensory cortex of monkeys using a precision grip. II. Responses To object texture and weights. J Neurophysiol. 1999b Feb;81(2):835-44.

Salimi I, Brochier T, Smith AM: Neuronal activity in somatosensory cortex of monkeys using a precision grip. III. Responses to altered friction perturbations. J Neurophysiol. 1999c Feb;81(2):845-57.

Schieber MH and Poliakov AV: Partial inactivation of the primary motor cortex hand area: effects on individuated finger movements. J Neurosci. 1998 Nov 1; 18 (21): 9038-9054.

Schlaggar BL, O'Leary DD: Early development of the somatotopic map and barrel patterning in rat somatosensory cortex. J Comp Neurol. 1994 Aug 1;346(1):80-96.

Shao Z, Burkhalter A: Different balance of excitation and inhibition in forward and feedback circuits of rat visual cortex. J Neurosci. 1996 Nov 15;16(22):7353-65.

Shima K, Tanji J: Involvement of NMDA and non-NMDA receptors in the neuronal responses of the primary motor cortex to input from the supplementary motor area and somatosensory cortex: studies of task-performing monkeys. J Physiol. 1998 Aug;48(4):275-90.

Sillito AM, Jones HE, Gerstein GL, West DC. Feature-linked synchronization of thalamic relay cell firing induced by feedback from the visual cortex. Nature. 1994 Jun 9;369(6480):479-82.

Simons DJ.: Response properties of vibrissa units in rat SI somatosensory neocortex. J Neurophysiol. 1978 May;41(3):798-820.

Simons DJ. Temporal and spatial integration in the rat SI vibrissa cortex. J Neurophysiol. 1985 Sep;54(3):615-35.

Simons DJ, Carvell GE: Thalamocortical response transformation in the rat vibrissa/barrel system. J Neurophysiol. 1989 Feb;61(2):311-30.

Simons DJ, Carvell GE, Hershey AE, Bryant DP: Responses of barrel cortex neurons in awake rats and effects of urethane anesthesia. Exp Brain Res. 1992;91(2):259-72.

Spain WJ, Schwindt PC, Crill WE. Anomalous rectification in neurons from cat sensorimotor cortex in vitro. J Neurophysiol. 1987 May;57(5):1555-76.

Streit P, Knecht E, Cuenod M. :Transmitter-specific retrograde labeling in the striato-nigral and raphe-nigral pathways. Science. 1979 Jul 20;205(4403):306-8.

Swadlow HA and Weyand TG. Efferent systems of the rabbit visual cortex: Laminar distribution of the cells of origin, axonal conduction velocities and identification of axonal branches. J. Comp. Neurol. 1981; 203: 799-822.

Swadlow HA. Efferent neurons and suspected interneurons in motor cortex of the awake rabbit: axonal properties, sensory receptive fields, and subthreshold synaptic inputs. J Neurophysiol. 1994 Feb;71(2):437-53.

Urbain N, Deschênes M. Motor cortex gates vibrissal responses in a thalamocortical projection pathway. Neuron. 2007 Nov 21;56(4):714-25.

Veinante P, Deschenes M.: Single-cell study of motor cortex projections to the barrel field in rats. J Comp Neurol. 2003 Sep 8;464(1):98-103.

Welker WI, Johnson JI Jr, Publois BH Jr: Efferent neurons and suspected interneurons in motor cortex of the awake rabbit: axonal properties, sensory receptive fields, and subthreshold synaptic inputs. Some morphological and physiological characteristics of the somatic sensory system in raccoon..Am Zool. 1964 Feb; 136:75-94.

Welker C: Microelectrode delineation of fine grain somatotopic organization of (SmI) cerebral neocortex in albino rat. Brain Res. 1971 Mar 5; 26(2):259-75.

Welker C.: Receptive fields of barrels in the somatosensory neocortex of the rat. J Comp Neurol. 1976 Mar 15; 166(2):173-89.

Welker E, Hoogland PV, Van der Loos H. Organization of feedback and feedforward projections of the barrel cortex: a PHA-L study in the mouse. Exp Brain Res. 1988;73(2):411-35.

Weller RE, Kaas JH. Retinotopic patterns of connections of area 17 with visual areas V-II and MT in macaque monkeys. J Comp Neurol. 1983 Nov 1;220(3):253-79.

White E: Cortical Circuits. New York: Birkhauser; 1989.

White EL, DeAmicis RA. Afferent and efferent projections of the region in mouse SmL cortex which contains the posteromedial barrel subfield. J Comp Neurol. 1977 Oct 15;175(4):455-82.

Woolsey TA, Van der Loos H: The structural organization of layer IV in the somatosensory region (SI) of mouse cerebral cortex. The description of a cortical field composed of discrete cytoarchitectonic units. Brain Research, 17 (1970) 205-42.

Yamashita A, Valkova K, Gonchar Y, Burkhalter A: Rearrangement of synaptic connections with inhibitory neurons in developing mouse visual cortex. J Comp Neurol. 2003 Sept 29; 464 (4): 426-37.